ORIGIN OF AUTOCATALYTIC SETS OF BIOPOLYMERS

THE ORIGIN OF LIFE BY MEANS OF AUTOCATALYTIC SETS OF BIOPOLYMERS

By

MENG WU, B. Sc., M. Sc.

A Thesis Submitted to the School of Graduate Studies

in Partial Fulfilment of the Requirements

for the Degree

Doctor of Science

McMaster University

McMaster University Doctor of Science (2012) Hamilton, Ontario (Physics)

TITLE: The Origin of Life by Means of Autocatalytic Sets of Biopolymers

AUTHOR: Meng Wu, B. Sc., M. Sc.

SUPERVISOR: Dr. Paul G. Higgs

NUMBER OF PAGES: xv, 181

Abstract

A key problem in the origin of life is to understand how an autocatalytic, self-replicating biopolymer system may have originated from a non-living chemical system. This thesis presents mathematical and computational models that address this issue. We consider a reaction system in which monomers (nucleotides) and polymers (RNAs) can be formed by chemical reactions at a slow spontaneous rate, and can also be formed at a high rate by catalysis, if polymer catalysts (ribozymes) are present. The system has two steady states: a 'dead' state with a low concentration of ribozymes and a 'living' state with a high concentration of ribozymes. Using stochastic simulations, we show that if a small number of ribozymes is formed spontaneously, this can drive the system from the dead to the living state. In the well mixed limit, this transition occurs most easily in volumes of intermediate size. In a spatially-extended two-dimensional system with finite diffusion rate, there is an optimal diffusion rate at which the transition to life is very much faster than in the well-mixed case. We therefore argue that the origin of life is a spatially localized stochastic transition. Once life has arisen in one place by a rare stochastic event, the living state spreads deterministically through the rest of the system. We show that similar autocatalytic states can be controlled by nucleotide synthases as well as by polymerase ribozymes, and that the same mechanism can also work with recombinases, if the recombination reaction is not perfectly reversible. Chirality is introduced into the polymerization model by considering simultaneous synthesis and polymerization of left- and right-handed monomers. We show that there is a racemic non-living state and two chiral living states. In this model, the origin of life and the origin of homochirality may occur simultaneously due to the same stochastic transition.

Acknowledgements

I would like to thank my supervisor Dr. Paul Higgs for all his invaluable help to get me familiar to a totally new environment, directions for how to do good research and patient to push me toward the right direction. It is one of my most important experiences in life.

I would like to thank Dr. An-chang Shi, Dr. Jonathon Stone, Dr. Jonathan Dushoff, Dr. Niles Lehman and Dr. Sara I. Walker for their inspiring discussions and suggestions for the research. I would like to thank Sharcnet for providing me scholarship during the year 2008-2009 and computational resources making my research possible.

I would also like to take this opportunity to thank my family for their support. They make my life much more meaningful. And I would like to thank all my friends for accompanying me through the journey of life.

dedicated to Haixia

Table of Contents

List of Figures

Chapter 1

Introduction to Theories and Models for the Origin of Life

1.1 From Non-living to Living

Life as known today is vastly diverse in both forms and niches occupied. Despite huge differences, all modern organisms share some common observable features that are recognized as requirements of life.

- Metabolism - they are bounded chemical systems capable of constructing their components using material and energy from the environment, and capable of breaking down damaged components.
- Homeostasis - they can regulate their internal systems to a stable state.
- Adaptation - they can change according to selective pressure from their environment.
- Reproduction - they can give birth to new individuals like themselves.

These diversities and similarities are among the reasons encouraging people to ask how life came into existence. Even though Darwin's evolution theory shed light on how diverse modern organisms evolved from a simple common ancestor, the exact process of how non-living matter became life remains in the shadow of mystery. It is clear that not all those common observable

features of modern organisms arose at the same time. There may have been many steps along the way from a chemical system that is clearly non-living to a fully-fledged cell having all the features of modern life. It is necessary to determine a plausible starting point and a plausible pathway for this process, and to consider at what intermediate stage the system became sufficiently complex for us to call it life.

1.2 Prebiotic Chemistry

As the sole example available to us, modern life on earth is the only data point that can be used to investigate the origin of life problem. It is known that all forms of life on Earth share the same building blocks such as amino acid, nucleotides and lipids. One possible reason for this is that many of these molecules can be synthesized in space or in the early stages of formation of the solar system. Atoms constituting these building blocks are either widely available, like hydrogen, or have been produced through nuclear reactions in stars and dispersed all over the universe through supernovae, as with carbon, oxygen and nitrogen. These atoms can form simple molecules such as formaldehyde, methanol, dimethyl ether, and hydrogen cyanide, easily in interstellar molecular clouds (Ehrenfreund et. al. 2000). Furthermore, many kinds of amino acid and nucleobases are found in meteorites (Kvenvolden et al. 1970; Martins et. al. 2008), which demonstrates that prebiotic chemistry in the solar system could form

relatively large molecules, and suggests that these molecules may have been available on the early Earth at the time of the origin of life.

In addition to the possibility of molecular synthesis in space, the formation of organic molecules is also possible directly on Earth if there were a reducing atmosphere (Oparin 1924; Haldane 1929). The plausibility of this hypothesis has been proven by the famous Miller-Urey spark discharge experiments (Miller 1953; Oro1961). In these experiments, a heated mixture of hydrogen, ammonia, methane and water was cycled through a spark firing chamber which simulated lighting in the hypothetical primordial atmosphere. Many types of organic molecules including amino acids, sugars, and lipids were found after only two weeks of continuous operation. This has since been challenged on the grounds that the primordial atmosphere was not reducing due to escape of hydrogen that was initially present and the introduction of carbon dioxide and nitrogen by volcanic activities (Abelson 1966; Kasting et al. 2003). However, the composition of the early Earth atmosphere is still under debate (Tian et al. 2005; Russell 2010) and the sysnthesis of organic molecules is still possible to some degree in a neutral atmosphere. It was also demonstrated that the widespread existence of iron and carbonate minerals on primitive earth may make prebiotic formation of amino acid from mixture of carbon dioxide and nitrogen still feasible through spark discharge (Cleaves et al 2008).

Due to their fundamental importance as building blocks of proteins and due to the relative ease with which they can be synthesized, amino acids have

been studied frequently from the point of view of prebiotic synthesis. Higgs and Pudritz (2009) have reviewed the various proposals for sites and mechanisms of abiotic amino acid synthesis, and have found that there is substantial agreement that about 10 of the 20 amino acids found in proteins are likely to have been easy to synthesize by chemical means and to have been relatively common on the early Earth.

It then becomes relevant to consider the possibility of abiotic synthesis of peptides from these amino acids and to ask whether peptide formation could lead to the origin of life. Amino acids can be adsorbed onto certain types of rock surface and condense into polypeptides (Hayakawa and Fox 1967; Paecht-Horowitz et al. 1970; Fox 1980). As they can fold into all kinds of structures that act as catalysts, proteins play critical roles in cells to make many reactions possible. In modern organisms, proteins do not replicate themselves, and rely on nucleic acids as a means of encoding the protein sequence. Nevertheless, some simple autocatalytic systems based on peptides are known experimentally. It has been demonstrated that some peptides with specific amphiphilic sequences (part of the sequence is hydrophilic and part of the sequence is hyrodphobic) can fold into alpha helical structures and catalyze formation of themselves by stacking with two peptide segments through hydrophobic interaction while keeping the ends of these two segments in proximity with each other (Lee et. al. 1996). A similar amphiphilic effect causing the stacking of peptides into beta sheets has been shown to help self replication of certain peptides (Bourbo 2011). However,

without a base pairing mechanism like DNA and RNA, the self replication of proteins can be achieved only for peptides with very specific sequences and secondary structures (Orgel 1992). The fundamental advantage of nucleic acids over proteins in terms of storage and replication of sequence information is one of the main reasons that the RNA World hypothesis is now at the forefront of origins of life research, as we now discuss.

1.3 The RNA World

As stated in the central dogma of molecular biology, information in modern cells is stored in DNA, which is then transcribed to RNA and translated to proteins which catalyze reactions for maintaining and reproducing all component of the cell (Crick 1958). In modern cells, protein synthesis is not possible without DNA and RNA, while without protein, DNA replication and RNA transcription are not possible. On the other hand, DNA and proteins are already very complex molecules with thousands to billions atoms. Hence, a system composed of DNA, RNA and protein is too complex to evolve de novo. There must be something simpler preceding it. As a result of the dual ability of RNA, the RNA World hypothesis was proposed, according to which there was a time when RNA was both the informational polymer and the key catalytic molecule (Gilbert1986; Bartel et al. 1999; Szostak et al. 2001; Joyce 2002; Orgel 2004). The translation mechanism provides the main evidence that RNA preceded proteins. The sequences of proteins are encoded in mRNAs, rRNAs are the main functional

component of the ribosome, and tRNAs enable translation to occur via the codon-anticodon interactions that define the genetic code. Naturally occurring ribozymes are capable of a versatile range of catalytic functions (Doudna et al. 2002). The most important one is ribosomal RNA, and along with several other types of RNAs are considered to be relics of the RNA world (Jeffares et al. 1998). Thus the evidence that RNA-based life once existed and that RNA could have carried out the full range of required functions is persuasive.

To realize all the metabolic activities that would have been required by primitive life in an RNA world, RNA would have had to play many of the catalytic roles played by proteins in modern organisms. The first report of catalytic RNA which is capable of self-splicing (Cech 1981) ignited people's creativity to find all kinds of RNA catalysts, such as a nucleotide synthase which can catalyze synthesis of single RNA nucleotides (Unrau et al. 1998), a template directed RNA ligase which can catalyze ligation of given RNA sequences (Doudna and Szostak 1991; Ekland et al. 1995), and an RNA polymerase which can extend a primer based on any given template (Doudna et al. 1993; Ekland et al. 1996; Johnston et al. 2001; McGinness et al. 2002; Zaher et al. 2007; Vicens 2009). The most recent achievement in this area is an RNA polymerase capable of replicating a template with length up to 95 nucleotides. This is enough to replicate a hammerhead endonuclease ribozyme, but it is still not enough to replicate itself with a length of 185 nucleotides (Wochner et al. 2011). Admittedly, in vitro selection and amplification used in these investigation processes are carried out

with the help of highly efficient laboratory techniques that were not available to the earliest organisms (Wilson et al., 1999; Romero-Lopez et al., 2007). Nevertheless, these artificially synthesized ribozymes have shown the potential of RNA playing the role of catalysts in primitive life.

In a living system in the RNA World, ribozyme synthesis would be autocatalytic. However, if ribozymes were involved in the origin of life, then the first ribozymes must have arisen by spontaneous chemical reactions rather than by reactions catalyzed by other ribozymes. Abiotic synthesis of nucleotides is possible but difficult, as reviewed by Joyce and Orgel (2006), although a new method of abiotic pyrimidine synthesis has recently been proposed (Powner *et al.* 2009). It has also been found that ribose sugars are stabilized by minerals such as borate, which might help to explain how ribose could be selected from a prebiotic mixture of similar sugars (Benner *et al.* 2010).

Another difficulty is that RNA polymerization by nucleotide condensation is an unfavourable reaction in aqueous solution. Progress has also been made in understanding the possible prebiotic mechanisms of RNA polymerization. Mineral catalyzed synthesis of RNA oligomers from activated nucleotides has been known for some time (Sleeper et al., 1979; Ferris *et al.* 1996; Ferris, 2002). Recent work shows that RNA polymerization can be facilitated by cycles of wetting and drying within a matrix of lipid bilayers (Rajamani *et al.* 2008; Olasagasti *et al.* 2011). Thanks to the base pairing ability of RNA, oligonucleotides with length as short as 6 can catalyze formation of their

complementary sequences from nucleotides (Inoue et al 1984). The same base pairing ability makes RNA capable of forming a double helix structure with another RNA strand and acting as information carrier like DNA. It also enables RNA to fold into 3D structure through self-base pairing to be a potential catalyst. RNA polymerization from nucleoside cyclic monophosphates has also been observed (Costanzo *et al.* 2009). It has been shown that the template-directed ligation could greatly increase the chance of producing long polymers, and hence shift the exponentially decaying length distribution of polymers into a distribution with a much fatter tail. (Derr et al. 2012). Although we do not know how well any of these studies match the details of the environmental conditions on the early Earth, these results give support to the idea that some form of prebiotic polymerization of relatively long RNAs could have occurred.

Homochirality remains as yet another problem to the RNA world. Chiral molecules are stereoisomers that are nonsuperposable mirror images of each other like left hand to right hand. Homochirality is the very popular but not well understood phenomenon in biopolymers which are made up by monomer of the same handness (DNA, RNA, protein, sugar). Its peculiarity arose from the fact that monomer made from abiotic reaction will have equal portion of monomers for each handness, while biopolymers all have homochirality. Further detail discussion about chirality please refer to Chapter 5.

It is possible that some other kind of biopolymer with different backbone chemistry might have preceded RNA (Orgel, 2004; Bean et al. 2006), and that

RNA strands may have subsequently been produced as hybrids with the other polymer acting as template. If it were shown that an alternative biopolymer were very much easier to synthesize or very much more stable than RNA in prebiotic conditions, then this might be an attractive way to avoid some of the difficulties of the RNA World. Several alternative polymers seem plausible, such as threose nucleic acid (TNA; Orgel 2000) and peptide nucleic acid (PNA; Nelson et al. 2000). Some of these nucleic acids are not found in nature (xeno-nucleic acid(XNA)), and these have been demonstrated to be able to bind with DNA through the base pairing mechanism, to transfer information back and forth between them and DNA with help of catalysts, and to fold into 3D structures and bind with specific molecules (Pinheiro et al. 2012). However, current experimental work does not seem to demonstrate conclusively that any one of these alternative polymers is a better candidate than RNA in all respects. Therefore, we prefer, on grounds of parsimony to suppose RNAs came first and not to introduce additional hypotheses. Furthermore, from a theoretical point of view, the question of how self-replicating biopolymers arose is the same, whatever the chemical nature of the monomers. In this thesis, when we discuss models for the origin of autocatalytic polymers, monomers will be referred as nucleotides and polymers as RNAs, but the models we will discuss are sufficiently general to apply to any biopolymer system.

The end of the RNA world is presumed to have occurred with the invention of the ribosome and the genetic code, which allowed genetically

encoded proteins to be used as catalysts instead of ribozymes. At some point, DNA synthesis also arose, and DNA took over the role of genetic material. RNA was then left with the reduced set of functions that it performs today. A cell operating by means of DNA, RNA and proteins, in a similar way to current bacteria, would clearly be classed as a living organism by anyone's definition. It is also possible to envisage an RNA-based cell in a late stage of the RNA world that would exhibit all the requirements of life listed in section 1.1, and which would also clearly be counted as a living organism. In an early stage of the RNA world, however, these requirements may not all have arisen simultaneously. For example, one could envisage metabolic reactions and replication in a chemical system that was not divided up into cells, or alternatively, one could imagine a system with protocells and metabolism but lacking information carrying polymers like RNA. When considering these possible intermediate steps between chemistry and modern life, it is not fully clear at which stage a molecular ensemble can be called life. For this reason, we now wish to consider the definition of life more carefully, and this will then be useful possible alternative scenarios for the origin of life.

1.4 Definition of Life

One popular definition of life is the one proposed in the Exobiology program of NASA: it is stated that life is a self-sustained chemical system capable of undergoing Darwinian evolution (Joyce 1994). The self-sustained requirement

reflects the metabolism and homeostasis aspects of life. The requirement for Darwinian evolution implies abilities including reproduction and inheritance, subject to mutation and selection. Only a population of individuals satisfying these two criteria is capable of evolving to different species and adapting to different environmental niches. Another definition of life, emphasises that life is a autopoietic organization, which is "a network of productions of components which (i) participate recursively in the same network of productions of components, and (ii) realize the network of production as a unity in the space in which the components exist" (Varela et. al. 1974). This definition focuses on the aspect of self-maintenance rather than reproduction and evolution. We would agree that organisms such as mules or grandmothers, which are self-maintaining, should be counted as living, even if they cannot reproduce. However, the autopoiesis definition is not very helpful in the context of the origin of life, because it is difficult to see how a self-maintaining entity could have arisen if it were not by a process of evolution and reproduction of a population. Due to the complexity of the life phenomenon, it is very hard to have an all-encompassing definition without any exceptions. After all, the purpose of a definition is to properly describe a problem of real interest, which in this case is how life could originate from a molecular ensemble (Ruiz-Mirazo et al. 2004).

As stated before, a molecular ensemble may not acquire all the features of life simultaneously. It may gain some features first through physical/chemical properties of the ensemble, or by pure chance, and then these features might make

acquisition of other features of life feasible. Due to the importance of these first gained features, they can be used as criteria to differentiate a non-living ensemble from a living ensemble.

Based on differing views about which is the most important feature leading to life, there are different schools of thought about the order in which these features arose during the origin of life. Metabolism first and replicator first are two main camps. As implied by their names, the metabolism first ideas emphasize that the metabolism of a molecular ensemble is the most important and the first feature to arise, while the replicator first ideas insist that it is the origin of self-replicating molecules that is the first step towards modern life. In addition to these, there are other approaches such as the lipid world theory in which metabolism and compartmentalization arose at the same time. In the next few sections, I will consider these alternatives, and I will try to argue that it is the emergence of autocatalytic set of biopolymers that is the crucial step towards life. This argument has features of both metabolism and reproduction, as we shall see.

1.5 Issues Related to the Replicator First View

It is shown in experiments that RNA can catalyze formation of its complementary sequence by condensation of nucleotides through a simple base pairing mechanism (Sulston et al. 1968; Inoue et al. 1984; Visscher et al. 1989; Kanavarioti et al. 1998). It is conceivable that the synthesized complementary sequence may help formation of a new copy of the original sequence, and hence

complete the self-replicating cycle (Cech 1986). Additionally, several other types of molecule have been shown as autocatalytic (Orgel 1992; Lee et al. 1996; Bourbo et al. 2011). Inspired by this possibility, the replicator first theory was proposed, which envisages that beginning with one molecule capable of self replication, a population of such molecules can be obtained. In such a population of naked genes, Darwinian evolution could help invent other features of life to improve individual fitness and lead to proto-cells eventually (Horowitz, 1945; Lifson 1997).

Many criticisms against the replicator first idea are mounted toward the difficulty of prebiotic synthesis and polymerization of nucleotides (Shapiro 2006), although recent progress has been made with chemical synthesis of RNA, as discussed in section 1.3. If polymeric sequences do arise, then the accuracy of replication becomes an issue. Replication is not perfect, even for well-adapted modern enzymes, and presumably for the first replicating molecules, the error rate would have been larger than for modern enzymes. With a given error rate per base pair during replication, there is an upper limit of length beyond which a self-replicating sequence cannot perpetuate its lineage in the population forever, which means there is an upper bound for information complexity to be accumulated and inherited (Eigen 1971). Rajamani et al. have demonstrated that mismatches during non-enzymatic RNA template directed replication could stall inaccurate sequence replication, hence make self-replication of long functional sequence feasible

(Rajamani et al. 2010). Nevertheless, overcoming the error threshold is a key problem for the origin of life and for replicator first theories in particular.

According to the Hypercycle theory, it is possible to get around this error threshold problem by spreading information into multiple self-replicating sequences that help replication of each other in a circular reaction network (Eigen 1977). However, hypercycles have problems associated with dynamic stability and with susceptibility to invasion by parasites, and do not fully solve the error threshold problem. The ability to act as a replicase often requires the molecule folding into a certain structure, while a good template should remain unfolded and easily recognizable; therefore, it is hard to be both a good replicase and a good template. To make things worse, a molecule that remains in an unfolded state as a template for a longer time will have a higher chance to be replicated than one that remains folded as a replicase. This favours the evolution of parasitic molecules that function as better templates and worse replicases, and these parasites eventually cause the hypercycle to break down.

It has been proposed that putting hypercycles into multiple compartments (such as lipid vesicles) that compete against each other can ensure the surviving hypercycle can replicate as a whole (Eigen 1977). It is also found that hypercycles can survive in a spatial system with limited diffusion but no compartments (Boerlijst et al. 1991; Hogeweg 1994; Takeuchi et al. 2009). Another alternative is the stochastic corrector model (Szathmary, 1987), which demonstrates that molecules enclosed in compartments are able to withstand the invasion of parasites. The

problems of error threshold and parasites for the replicator first ideas can be tackled through interactions between replicators, which approach blurs the line between the replicator first idea and metabolism first idea to be discussed in the next section.

1.6 Issues Related to the Metabolism First View

People from the metabolism first school postulated that life started from a collection of molecules carrying out different functions such as energy capture and precursor synthesis, and that these molecules could have catalyzed formation of each other so that the system could reproduce and multiply as a whole (Madison 1953; Hansen 1966; Shapiro 2006) without the need for replication of specific biopolymer sequences. For example, it is found that citric acid cycle lies in the center of metabolism pathways of lives in all domains (Morowitz 2000). It also plays central role in the iron-sulfur world theory, which argues that life arose from iron sulphide related reactions at hydrothermal vents in the deep ocean (Wachtershauser 1988; Wachtershauser 1997; Russell 1997).

Another theory that may be classed as metabolism first is the lipid world model of Segre et al(2000a, 2000b, 2001) in which it is proposed that assemblies of amphiphilic molecules such as lipids can help incorporation of more lipid into the assembly, which allows the assemblies to grow and divide. Such a metabolic system can remain in homeostasis as long as there is enough raw material supply. The reproduction of an assembly can be achieved by incorporation of raw

material, causing it to grow larger and split into two small systems. The two new systems may retain the same kinds of molecules and reactions as the parental system. In this case we would say that the system has compositional inheritance, even though it does not have the usual form of genetic inheritance by means of replicating sequences (Segre et al 2000). As part of my MSc thesis, it has been shown that assemblies controlled by either kinetically favoured catalysis or energetically favoured self-assembly can have compositional inheritance (Wu, Higgs 2008). However, it has been found that information transmitted in compositional inheritance is very limited compared with genetic inheritance, and it is difficult to see how such assemblies can evolve towards more complex system with such limited inheritance.

Closure of the reaction network could impose a challenge for metabolism systems (Hanson 1966; Orgel 1968). Each kind of molecule not available as raw material has to be produced by the system through one or multiple reactions involving more types of molecule that need to be synthesized internally and which may depend on an even larger additional set of molecules and reactions. This would particularly be true for a metabolism made up by many different types of small molecules, which may contain many very different chemical bonds from each other, hence different reactions and precursors may be needed for each kind of molecule. Even if a reaction network has been established, it is difficult to see how it could evolve because every new type of molecule recruited into the system requires a new supporting reaction network to guarantee its perpetual existence in

the network. Hence, if the metabolism network becomes larger, the benefit of inventing the new molecule may be countered by the expense of the new supporting reaction network and the harm caused by disruption of the existing network. Additionally, there are only limited possible types of molecules and reactions in a given small molecular network. After the most stable or efficient combination of these molecules and reactions has been attained, it is not possible for these small molecules to recruit a new molecule type and invent a new reaction on their own.

In summary, we can conceive of a situation in which autocatalytic small molecule ensembles control a metabolic network, however there is no experimental demonstration of this as yet. Furthermore, our definition of life requires a living system to be capable of evolution, and as this would not seem to be possible in a purely small molecule system, such a system would not count as living, in our view.

1.7 Autocatalytic Sets of Biopolymers

Kauffman et al. proposed that autocatalytic sets of polymers built from the same set of monomers can remedy the problem of closure of the reaction network (Kauffman 1986; Kauffman 1993; Giri et al 2012). With increasing length, the number of possible types of polymer with the same length will increase exponentially, while the number of potential reactions between all polymers and number of catalysts for all possible reactions will grow even faster. Hence, if the

probability that a polymer catalyzes any given reaction is fixed, the probability for existence of closed autocatalytic set would converge to one with increasing polymer length. It is also demonstrated that with properly set parameters, a polymer autocatalytic set could emerge from a background polymerization system in which random condensation between polymers and cleavage of polymers happen spontaneously (Farmer et al 1986; Bagley et al 1991). Contrary to small molecules, polymers have practically infinite evolvability. Take RNA for example, with 4 different bases, number of possible RNA sequence with length 90 is about 10^54, which is already larger than number of atoms on earth(10^50). For protein with 20 different amino acids, 10^{91} different sequences are needed to exhaust all possible protein with length 70, while number of atoms in the observable universe is estimated to be 10^{80}. Hence as long as there is a way to produce different long polymers, it is possible that the system could gain new catalysts with higher efficiency for existing reactions or with novel functionality (Szabo et al. 2002; Giri et al. 2012).

Another advantage for an autocatalytic set of polymers is that all polymers share similar types of chemical bonds and the same group of monomers. As long as there is way to synthesize monomers and polymerize them, closure of the reaction network for any polymer is not a problem. Moreover, any newly invented polymer capable of increasing the efficiency of monomer synthesis or polymerization can not only benefit its own synthesis, but also facilitate formation of other new polymers with the potential to be catalysts. Hence, I believe that as a

hybrid between metabolism and replicator, an autocatalytic set of biopolymers can maintain its composition and dynamics through metabolism, and more importantly, recruit practically infinite possible types of new biopolymers for novel functionality much easier. It is the emergence of autocatalytic set of polymers which marks origin of life to our view.

1.8 Theories for Origin of Life in Polymer Systems

Most of the theoretical investigations discussed in the previous section focus on behaviour of a self-sustained system after its establishment. However, it is the emergence of self-sustained polymer system from a background of random polymer formation that a crucial step from non-living to living. Monteiro et al.(1998, 1999) investigated the effect of different parameters on the concentration of long polymers in a system in which polymer is synthesized through random polymerization and spontaneous template directed replication. Wattis and Coveney (1999) added the assumption that polymer can catalyze formation of itself through sequence elongation. Ma et al. argued that if certain long polymers can fold into 3D structure and act as a template directed replicase, ligase or nucleotide synthesase, an autocatalytic set of polymers can emerge (Ma et al. 2006, 2007, 2010). Nowak et al. showed that asymmetric reaction rates for different polymers may lead to selection of autocatalytic polymers, and that depending on choice of parameter value and initial condition, catalytic polymers

can either dominant the system or impose little effect (Nowak et al. 2008; Ohtsuki et al. 2009; Manapat et al. 2010).

It is known that life is a different steady state from non-life even for exactly the same molecules. Hence we think there must be two steady states representing non-life and life respectively, and this is an important aspect of all the models that we will work on in this thesis. Even though highly simplified and abstract, Dyson's model about origin of life is among the earliest mathematically tractable ones which tried to describe the transition from non-living to living steady states (Dyson 1982). He assumes there are catalytic polymers and their component monomers with fixed total number of monomers in a semi-permeable system (island) exchanging monomers with the environment. Monomers can be added, subtracted, or substituted from polymers. He defines active monomer to be the one which happens to be correctly placed as part of catalytic polymer catalyzing formation of other catalytic polymers. He further assumes that the higher fraction of active monomers in an island leads to the higher the probability to recruit new active monomers into the island. With such positive feedback assumption about active (correct) monomer's ability to incorporate more active (correct) monomer into the system, two steady states separated by an unstable state may present: the "disordered state" or "dead state" with few active monomer which can hardly incorporate any more active monomers, and the "ordered state" or "living state" with almost all monomers active. With infinite volume, the system will stay in one of the steady states forever depending on its initial

condition. With finite volume, fluctuation in number of active monomer may bring the system over saddle point to another steady state. Hence, transition from dead to living happened.

1.9 Aims of this Thesis

In this thesis we take the view that the emergence of autocatalytic biopolymers is the most important stepping stone from non-life to life, and that stochastic fluctuations are essential for this to occur. Therefore, we investigate several different models of polymer systems and show that, despite hugely different assumptions and implementations of these models, they share the same feature of bistable living and dead states and that stochastic transitions are crucial in each case.

In Chapter 2, a reaction system for polymerization of RNA monomers is set up that forms the basis of all the subsequent chapters. In this model, polymerization is possible by the addition of an activated monomer to the end of a chain. It is supposed that a small fraction of polymers longer than some minimum length L have the ability to act as polymerase ribozymes.. With such positive feedback as Dyson's model, there are two stable states: a 'dead' state with a very low concentration of ribozymes and a polymerization rate almost equal to the spontaneous rate, and a 'living' state with a high concentration of ribozymes and a high rate of polymerization occurring via ribozyme catalysis. Using this model,

the effect of finite system volume on transition time from dead state to living state can be investigated.

Based on the belief that transition between the non-living state and the living state is important, and inspired by recent experiments about capabilities of ribozymes, in Chapter 3 the basic polymerization model is modified to investigate the effect of different ribozymes such as nucleotide synthases, polymerases and recombinases, on the emergence of autocatalytic biopolymer sets.

For a well mixed system with given concentration of reactant, the larger the system the smaller the fluctuation will be, which will increase the difficulty of the stochastic transition. In reality, due to the limited diffusion speed of molecules, the well mixed assumption will break down quickly when the system size goes beyond the diffusion length. Hence, the exact effect of system size on transition time from dead state to living state with limited diffusion remains an interesting topic to be investigated in Chapter 4.

Inspired by similarity between our self-replicating polymer system model and Sarah I. Walker's chiral polymerization system model, we think that the origin of life problem may have intertwined with origin of homochirality problem, and the stochastic transition of self-replicating polymer system plays a central role to bridge this two problem. Hence the origin of chirality problem is taken as an extension of stochastic transition idea in Chapter 5.

Chapter 2

Origin of Self-Replicating Biopolymers

2.1 Introduction

Life as we know it relies on the existence of self-replicating sets of biopolymers. Modern cells use DNA, RNA and proteins, with DNA acting principally for information storage and proteins acting principally as catalysts. However some much simpler system must have existed at the time of the origin of life. The RNA World hypothesis proposes that early organisms contained self-replicating systems in which RNA was both the informational polymer and the key catalytic molecule (Gilbert, 1986; Bartel and Unrau, 1999; Szostak et al. 2001; Joyce, 2002; Orgel, 2004). In the context of the RNA world, 'replication' means that a functional RNA sequence has the ability to catalyze the synthesis of further copies of the same sequence. There is genetic information stored in the RNA sequence that is passed on when the sequence is replicated. The central questions for the origin of life in an RNA world context are how catalytic RNAs arise in sufficient quantity and how accurate replication of the sequences occurs. However, the origin of replication is not necessarily synonymous with the origin of life. It has sometimes been argued that metabolism preceded replication. Dyson (1999) argued for a dual origin of life in which metabolism and replication arose

separately, with metabolism appearing first. He proposed a simple theoretical model that represents an abstract form of metabolism. Shapiro (2006) emphasized the importance of catalytic cycles involving small molecules that would have been required before synthesis of biopolymers was possible. Kauffman (1993) considered autocatalytic sets of many molecules that, together, can reproduce themselves.

Building on Dyson's (1999) model, Segré *et al.* (2000, 2001) studied 'lipid world' models in which assemblies of amphiphilic molecules such as lipids can grow and divide. Although these assemblies possess no polymers which store information in their sequence, they do store information in the form of the composition of the molecules that they contain, and this compositional information can be passed on if the assemblies divide. We also studied similar models and confirmed that this form of compositional inheritance can occur in the absence of informational polymers (Wu and Higgs, 2008). Nevertheless, compositional inheritance seems very limited in comparison to genetic inheritance based on replication of informational polymers (Szathmary, 2000). It is difficult to see how any living system could have got beyond the most rudimentary level without informational polymers. Historically, it is clear that informational polymers did arise at some point in the early evolution of life, even if something like compositional inheritance or autocatalytic sets of small molecules preceded this. Therefore the origin of self-replicating biopolymers remains as a fundamental question, and this is the issue that we want to address in this chapter.

We will return to the question of whether metabolism preceded replication in the discussion at the end of this chapter.

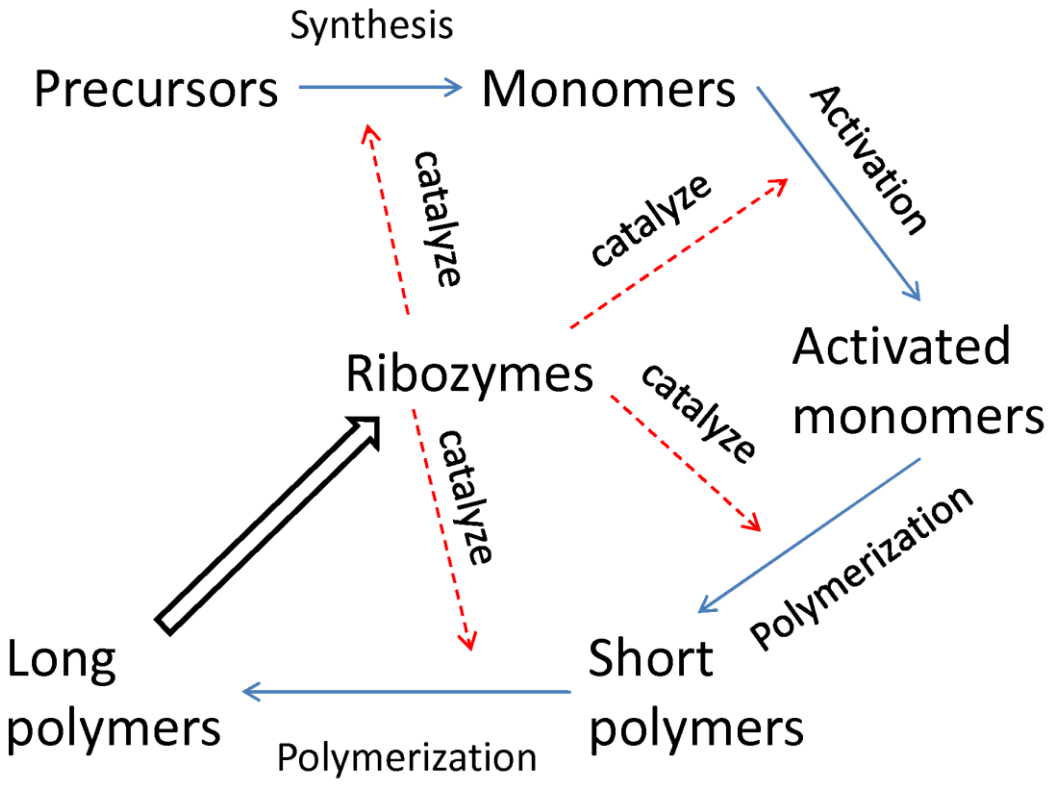

Figure 2.1: Schematic diagram of an autocatalytic RNA polymerization system. We distinguish between long polymers, which have a probability of acting as ribozymes that catalyze the different reactions of the system, and short polymers, which are not long enough to be catalysts.

The central idea of this chapter is shown schematically in Figure 2.1. We suppose that there is some local region in which the chemical reactions that give rise to life can begin to occur. A driving free energy source and a supply of precursor molecules are available, and conditions in the local region are

favourable enough that monomers can be synthesized from these precursors at a non-negligible rate. We suppose that spontaneous polymerization of monomers is unfavourable thermodynamically, but that if the monomer is converted to an activated form, such as a nucleotide triphosphate (as with RNA polymerization in modern cells), or an imidazole (as studied by Ferris *et al.* (1996) and Ferris (2002)), then polymerization can occur by the addition of the activated monomer to the end of a growing strand. Monomers, activated monomers, and polymers are all able to escape from the system into the surrounding world. The net concentration of polymers in the local region is determined by a balance between the rates of formation and escape.

The spontaneous rates of synthesis, activation and polymerization must all be non-negligible, otherwise no polymer synthesis is possible; however, we suppose that all these spontaneous rates are low. This means that the region will contain mostly monomers and short oligomers with very low concentrations of long polymers. We call this state 'dead', because it is an steady state in which polymers are synthesized only at a low rate that occurs spontaneously (*i.e.* non-biologically). Nevertheless, even in this dead state, it is possible for long polymers to form occasionally. These will remain in the region for a certain time before eventually being lost to the outside world. We suppose that a small fraction of these long polymers is able to act as ribozymes that catalyze the polymerization, activation or nucleotide synthesis reactions. The reaction system thus contains autocatalytic feedback. If ribozymes arise spontaneously, they change the reaction

conditions in such a way as to speed up polymerization and to further increase the concentration of ribozymes. In this chapter we will show that, when autocatalytic feedback is present, the system has a second stable state in which long polymers and ribozymes are frequent. We call this state 'living', because polymerization occurs at a much higher rate than the dead state and most polymerization is catalyzed by the ribozymes within the system (*i.e.* biologically), rather than occurring spontaneously.

In this picture, the origin of life (or at least the origin of self-replicating biopolymers) is a transition of the reaction system from the dead to the living state. If it is assumed that the reaction volume is infinite and concentration fluctuations are negligible, the time-dependence of the concentrations of the different molecules can be described by deterministic ordinary differential equations. In this case, if the system begins in the dead state, it will remain stable in the dead state forever. In a finite volume, however, the numbers of long RNA polymers will be small, and stochasticity of chemical reactions will be important; hence fluctuations in concentration of long polymers will be significant. Using stochastic simulations in a finite volume, we will show in this chapter that, if a small number of ribozymes arises by chance, the effect can be large enough to shift the system into the living state. The idea that the origin of life is driven by stochastic fluctuations in a finite volume is also included in the model of Dyson (1999), but this feature seems not to have been followed up by other authors. Here we show that this kind of stochastically-driven transition occurs in a model that is

intended to be a fairly realistic description of RNA polymerization kinetics, and not just in the very abstract model originally considered by Dyson (1999).

2.2 Model Definition

Here we introduce a set of chemical reaction equations describing synthesis of RNA polymers. Our main objective is to look at the distribution of lengths of polymers formed. Therefore, in the first instance, we will ignore the specific sequence of monomers. All nucleotide monomers are denoted as A, and all polymers of n nucleotides are denoted as A_n. In a system with four kinds of nucleotides, there are 4^n possible polymers of length n, and A_n represents the sum of all these. We suppose that the reactions for nucleotide synthesis and polymerization occur in a local region that is separated from the external environment, but which can exchange molecules with the environment. For example, the local region could be the interior of a lipid vesicle, or a cavity in a porous rock, or the surface of a catalytic mineral. The reaction system requires input of high-energy 'food' molecules denoted F_1 and F_2. These molecules are assumed to be available in the environment and to be able to freely enter the local region; hence the concentrations of the food molecules are treated as fixed parameters.

Equation 2.1 represents synthesis of nucleotides from food molecules F_1 with a rate controlled by the synthesis rate constant s. Any waste molecules produced in this process are denoted W_1.

$$F_1 \xrightarrow{s} A + W_1 \qquad (2.1)$$

This synthesis reaction is presumed to be thermodynamically favourable ($\Delta G < 0$). We assume that the reverse reaction is negligible because ΔG would be positive.

Polymerization requires activated nucleotides, denoted *A**. Equation 2.2 represents synthesis of activated nucleotides from food molecules F_2 with a rate controlled by the activation rate constant *a*.

$$F_2 + A \xrightarrow{a} A^* + W_2 \qquad (2.2)$$

Synthesis of A^* from *A* requires free energy input, but since this is coupled to the breakdown of F_2, we suppose that ΔG is negative for the net reaction described by Equation 2.2. We again assume the reverse reaction rate is negligible because ΔG would be positive.

Equation 2.3 describes the growth of a polymer by addition of one activated nucleotide at a rate controlled by the polymerization rate constant *r*.

$$A_n + A^* \xrightarrow{r} A_{n+1} \qquad (2.3)$$

We assume that the rate constant *r* is independent of *n*. Note that A_1 is synonymous with *A*. The forward reaction in Equation 2.3 is thermodynamically favourable because it releases the energy in the activated monomer. Again we neglect the reverse reaction.

In such a polymerization system, if there are template-directed ligation reactions between polymers through a base pairing mechanism, many more long

polymers could be produced than with polymerization reactions alone (Derr *et al*. 2012). Hence, such ligation reactions would increase the probability to produce catalytic long polymers in the system. However, introduction of ligation between all polymers would greatly complicate the analysis and simulations. If our model could work without such beneficial effect, it would work even better with such effect. Hence in all the following analysis the template-directed ligations won't be taken into account.

The build up of nucleotides and polymers in the local region is limited by the escape of these molecules into the surroundings. For simplicity, the rate constant u for escape is assumed to be the same for monomers and polymers of all lengths. This would be true in a flow reactor system (chemostat), for example. In a diffusion-controlled system, we might expect larger molecules to escape more slowly, so u would be a decreasing function of n, and this could be included in a more complex version of the model. It should also be noted that the waste products W_1 and W_2 must also escape from the system, otherwise their concentrations will build up and the reverse reactions in Equations 2.1 and 2.2 will no longer be negligible. However, as long as the waste escapes sufficiently fast, then the rate of escape of the waste is not relevant for the calculation of the concentration of nucleotides and polymers.

Another factor limiting build-up of polymers is the spontaneous breakdown (hydrolysis) of a polymer into two shorter sequences. The polymer could presumably break at any point along its length. Initially, we will neglect this

breakdown reaction because this leads to a substantial simplification in the model and allows the equations to be soluble analytically. This assumption will be reasonable if the main factor limiting polymer concentration is escape of molecules from the system rather than breakdown of molecules within the system.

2.3 Model Analysis

The following differential equations describe the rates of change of concentrations of molecules inside the system. The symbols *A, A_n, etc.* should now be interpreted as the concentrations of the appropriate molecules.

$$\frac{dA}{dt} = sF_1 - aF_2A - rAA^* - uA \tag{2.4}$$

$$\frac{dA_n}{dt} = rA^*(A_{n-1} - A_n) - uA_n \tag{2.5}$$

$$\frac{dA^*}{dt} = aF_2A - rA^*(A + P) - uA^* \tag{2.6}$$

In Equation 2.6, P is the total polymer concentration of all lengths $n \geq 2$.

$$P = \sum_{n=2}^{\infty} A_n \tag{2.7}$$

We are interested in the steady state concentrations when the rates of change are all zero in Equations 2.4-2.6. From Equation 2.5, we know that $A_n/A_{n-1} = z$, where

$$z = \frac{rA^*}{u + rA^*} \ . \tag{2.8}$$

It follows that $A_n = Az^{n-1}$, and hence

$$P = A\sum_{n=2}^{\infty} z^{n-1} = \frac{Az}{1-z} = \frac{r}{u} AA^* \quad . \tag{2.9}$$

Now from Equation 2.4, we can write

$$A^* = \frac{1}{rA}(sF_1 - aF_2 A - uA) \ , \tag{2.10}$$

and from Equations 2.9 and 2.10, we have

$$P = \frac{1}{u}(sF_1 - aF_2 A - uA) \tag{2.11}$$

Finally, substituting 2.10 and 2.11 into 2.6, we obtain a quadratic equation for A for which the relevant root is

$$A = \frac{2asF_1F_2r + usF_1r + aF_2u^2 + u^3 - \sqrt{(2asF_1F_2r + usF_1r + aF_2u^2 + u^3)^2 - 4sa^2F_1F_2^2r(sF_1r + u^2)}}{2a^2F_2^2r}$$

. (2.12)

Having determined A in terms of the parameters u, a, s, r, F_1, and F_2, we can also determine A^* and P from 2.10 and 2.11. The other root of the quadratic equation is not relevant because, if the other root is substituted into 2.10 and 2.11, this gives negative values for A^* and P, which is not physical. In the following section, we will introduce the possibility that long polymers of length $n \geq L$ may act as catalysts of the polymerization reaction. Therefore, at this point, we note that the total concentration of long polymers is

$$P_L = A\sum_{n=L}^{\infty} z^{n-1} = \frac{Az^{L-1}}{1-z} . \tag{2.13}$$

It is also easy to calculate the total concentration of monomers included in polymers, M_P, and the average length of polymers, $\langle n \rangle$:

$$M_P = \sum_{n=2}^{\infty} nA_n = \frac{Az(2-z)}{(1-z)^2}$$

$$< n >= \frac{M_P}{P} = \frac{2-z}{1-z}$$

We are interested in the way the behaviour of the system depends on the polymerization rate. Figure 2.2 shows the effect of varying r over many orders of magnitude while fixing all other parameters with the following values: $F_1 = F_2 = 1$, $a = 1$, $s = 1$, $u = 0.01$. These values are arbitrary but they are sufficient to illustrate the qualitative behaviour of the model. The limiting regimes of small and large r can be easily understood. If r is small, it can be seen that A and A^* are roughly constant, and $A^* >> A$. In Equation 2.4, synthesis term sF_1 is balanced by three terms that reduce A. The most important of these is the term for the activation reaction, aF_2A. If synthesis is balanced only by the activation reaction, then $A \approx sF_1/aF_2$ (this is 1.0 with the parameters chosen). In Equation 2.6, A^* is produced by the activation reaction, and in the small r regime, the most important term limiting A^* is the escape term. Therefore $A^* \approx aF_2A/u \approx sF_1/u$ (this is 100 with the parameters chosen). $A^* >> A$ in this example because we have supposed that most of the A undergoes the activation reaction before it escapes. We know from Equation 2.9 that $P = rAA^*/u$; hence, in this regime, $P \approx r(sF_1)^2/(u^2aF_2)$, which is 10^4r with the parameters chosen. P is small in this regime because r is small, and P is proportional to r, as can be seen from the left side of Figure 2.2. Only very short polymers exist in this regime. The length distribution tails off

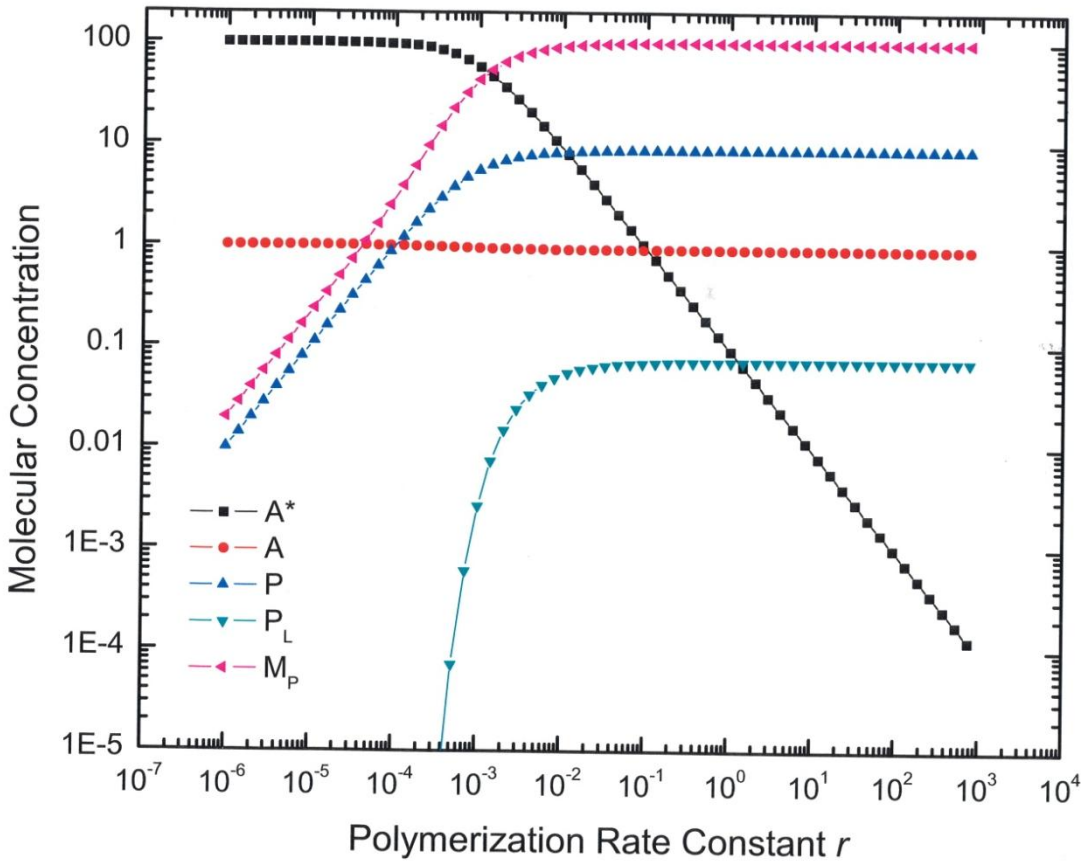

Figure 2.2: Log-Log plot of steady state concentrations of A*, A, P, P_L and M_P vs polymerization rate constant r. Other parameters are fixed as F=1, a=1, s=1, u=0.01, and L=50.

very rapidly because $z << 1$. For very small r, $z \approx rA^*/u \approx rsF_1/u^2$, and the long polymer concentration $P_L \approx Az^{L-1}$. This means that P_L scales as r^{L-1}. Figure 2.2 shows that P_L is extremely small for small r – a value of L = 50 was chosen in this example.

We will now consider the large r regime. It can be seen that A is only very slightly lower for large r than it is for small r. Although the polymerization term

rAA^* in Equation 2.4 is larger when r is larger, it turns out that A^* is small in this regime, so the most important term limiting A is the activation reaction, as it was for small r. Therefore it is still approximately true that $A \approx sF_1/aF_2$. If r is large, then the total polymer concentration P is much larger than A. The most important negative term in Equation 2.6 is rA^*P. Thus $aF_2A \approx rA^*P \approx (rA^*)^2A/u$. Rearranging this, we obtain $A^* \approx \sqrt{uaF_2}/r$, which is $0.1/r$ with these parameters. Thus A^* is small and varies inversely with r when r is large, as can be seen on the right of Figure 2.2. The total polymer concentration is $P \approx sF_1/\sqrt{uaF_2}$. This is independent of r for large r, and is large compared to A, as we assumed above. If r is large, almost all monomers get incorporated into polymers. Since $rA^* \approx \sqrt{uaF_2}$ when r is large, which is a constant, z converges to a constant less than 1 with increasing r. Therefore increasing r even further does not increase the polymer concentration once this limit is reached, and M_P and $\langle n \rangle$ also converge to a constant. When r is large, the distribution An tails off more slowly; hence there is an appreciable concentration of long polymers. P_L reaches a fairly large constant value in this regime, as shown on the right of Figure 2.2.

2.4 Autocatalytic Feedback

We now add the feature that some long polymers have the ability to act as ribozymes. In principle, ribozymes could catalyze the synthesis, activation or the polymerization reactions (as in Figure 2.1), but we will focus on the specific case where only the polymerization reaction is catalyzed, and the rates of synthesis and

activation remain equal to their spontaneous values. We suppose that there is a small spontaneous polymerization rate constant r_0 that exists in absence of long polymers and there is an additional term proportional to P_L, *i.e.* the total polymerization rate is

$$r = r_0 + kP_L \,. \tag{2.14}$$

Here, k is the strength of the catalytic effect of the long polymer ribozymes. It will be useful later to suppose that a small fraction f of long polymers is able to act as a ribozyme and that the catalytic effect of each ribozyme is k_0, so that the net effect is $k = k_0 f$. At this point, however, it does not matter whether there is a very small fraction f, each with a large effect k_0, or a larger fraction, each with a smaller effect. Therefore, we will begin with the single parameter k, rather than two separate parameters, f and k_0.

The dynamical properties of the model with catalytic feedback can be studied using numerical integration of the differential Equations 2.4-2.6 to follow the concentrations as a function of time, and using Equation 2.14 to update r at each time step of the numerical integration. Initially, however, we are interested in the steady state solutions of the model. In the previous section, we calculated the steady state value of P_L for a given value of r. We will denote this as $P_L^{ss}(r)$ from now on. We showed that $P_L^{ss}(r)$ is proportional to r^{L-1} when r is small, and that it tends to a limit when r is large. Therefore $P_L^{ss}(r)$ follows an S-shaped curve as a function of r. This is shown in Figure 2.3a for the same parameter values as in

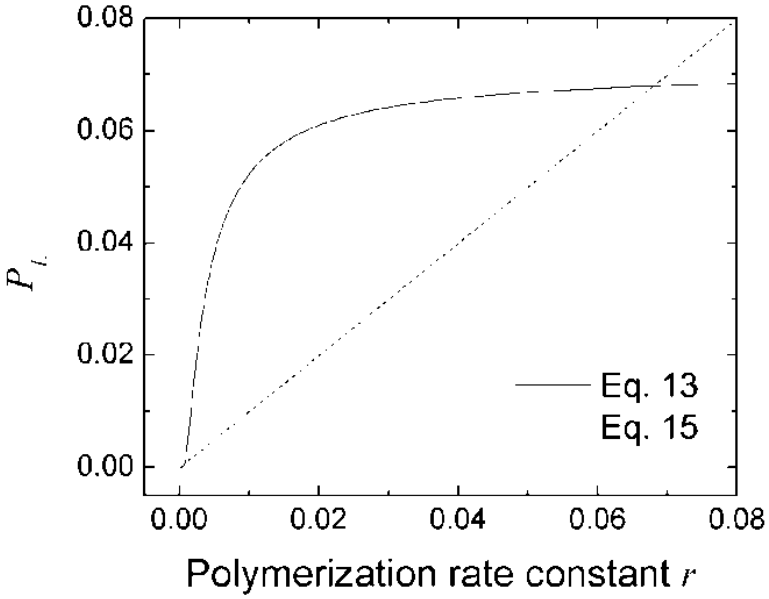

(a)

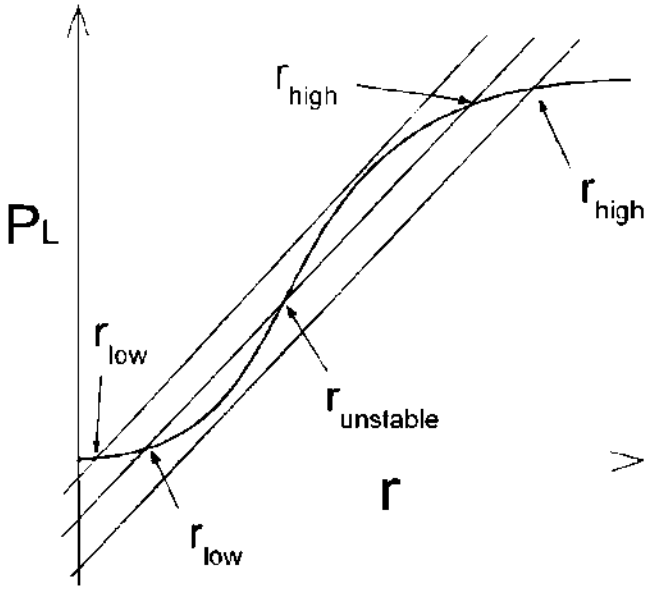

(b)

Figure 2.3: (a) Graphic solution to Eq. 2.13 and Eq. 2.15 when r_0=0.0001, k=1. (b) Schematic diagram illustrating the S-shaped curve and the allowed solutions for r.

Figure 2.2. Unfortunately, the part of the curve for small r is difficult to see when the curve is plotted on a true linear scale. We have therefore redrawn the curve

schematically in Figure 2.3b, in order to emphasize the S shape, which is important for what follows. In Equation 2.14 we introduced catalytic feedback into the system, so that r is no longer an independent variable. Equation 2.14 can be rewritten as $P_L = (r - r_0)/k$, which is a straight line on Figure 2.3. Steady state solutions for r are points where the straight line crosses the S-shaped curve, *i.e.* the solutions for r are the roots of the equation

$$P_L^{ss}(r) = (r - r_0)/k \quad . \tag{2.15}$$

For some values of r_0 and k there are three solutions for r. The middle one, which we denote $r_{unstable}$, is unstable dynamically. The system will move away from this point to one of the two other stable solutions, which we denote r_{low} and r_{high}. We refer to the low and high fixed points as dead and living states, respectively. In the dead state, P_L is extremely small, and r_{low} is very close to r_0, *i.e.* there are too few ribozymes to make much difference to the system. In the living state, P_L is large and $r_{high} >> r_0$, *i.e.* most of the polymerization is due to catalysis by ribozymes rather than the spontaneous reaction. For some values of r_0 and k there is only one root of Equation 2.15. This can be either a low or a high value of r, as shown in Figure 2.3b. In the case where there is only one solution, we will call this a dead state (r_{low}) if the intersection point is below the point of inflection of the S-shaped curve, and we will call it a living state (r_{high}) if the intersection point is above the point of inflection.

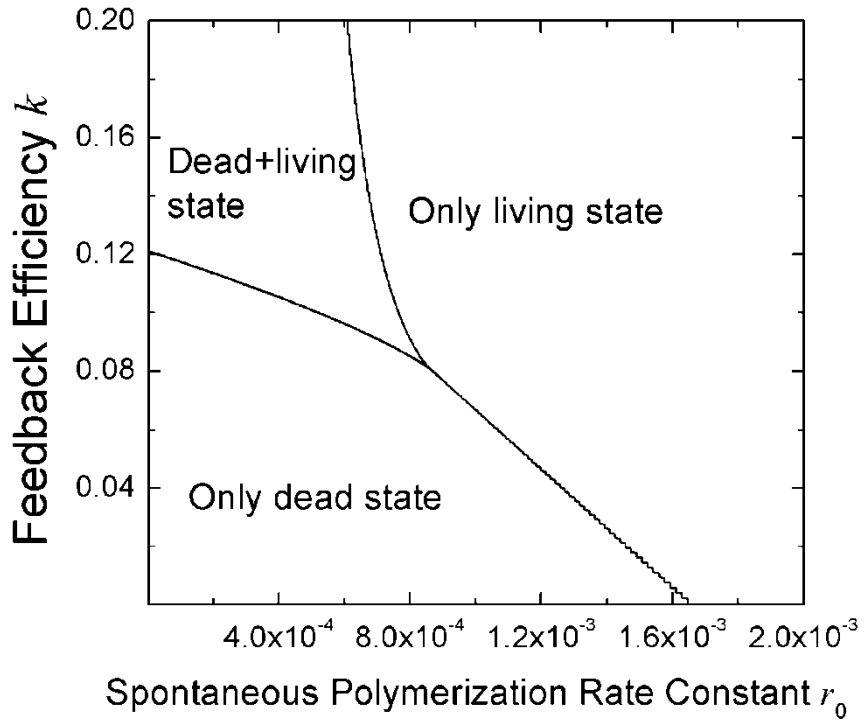

Figure 2.4: Phase diagram of the reaction system as function of feedback efficiency k and spontaneous polymerization rate constant r_0.

Figure 2.4 shows a phase diagram of the model as a function of r_0 and k, showing regions where the living or dead or both states exist. It is clear that if $r_0 = 0$, the dead state always exists because the line in Figure 2.3b intersects the curve at $r_{low} = 0$. The slope of the line is $1/k$. If k is large enough, there will also be a living solution, because the line will also intersect the curve at r_{high}. This corresponds to the top left of the phase diagram. If r_0 increases while keeping k fixed, the line slides down Figure 2.3b until the dead solution disappears. Thus we move into the top right of the phase diagram where only the living state exists. If we return to the case with $r_0 = 0$ where both solutions exist and we gradually

decrease *k*, the slope of the line in Figure 2.3b increases until only the dead state exists. Thus we cross a boundary as we move down into the lower left of the phase diagram. If we begin in the lower left and gradually increase r_0, keeping *k* very small, then there is only one solution which gradually slides up the S-shaped curve. We have drawn a boundary on the phase diagram between the living and dead states at the point where the single intersection point moves across the point of inflection of the curve. However, the system changes smoothly as we cross this boundary – there is no discontinuous change of concentrations. In contrast, the boundaries between the region where both states exist and the two regions where only one state exists are discontinuous because one or other state disappears at these boundaries.

In the real world, the origin of life must be difficult but not impossible. The real world clearly cannot lie in the region where only the dead state exists. The real world cannot lie in the region where only the living state exists, otherwise self-replicating systems would spontaneously emerge very easily and we would not be faced with the puzzling question of the origin of life. We therefore conclude that the real world is in the region where both solutions exist. Suppose that some local region has just come into existence where the conditions are favourable enough that synthesis and activation reactions are possible and that the polymerization reaction can occur spontaneously at some low rate r_0. The system will find itself in the dead state with very low polymer concentration P_L and almost no ribozyme activity. This dead state is dynamically stable for a

system with infinite volume. However, a transition from the dead to the living state can occur in a finite volume. A small number of functional ribozymes will eventually be created, and it may be that a small number in a small volume has a sufficiently large effect to flip the system into the living state. Therefore, in the following section, we consider the dynamics of the reaction system using a stochastic method with finite numbers of molecules in a finite volume.

2.5 An Algorithm for Stochastic Simulation in a Finite Volume

We will briefly discuss methods of stochastic simulation of chemical reaction systems in a general way and then discuss how we implemented a method for the reaction system studied here. In a finite volume, V, let there be $N_i(t)$ molecules of type i at a particular time t, where the index i runs over all possible molecular species in the system. The concentration of type i molecules is $C_i(t) = N_i(t)/V$. Let $R_\mu(t)$ be the rate of reaction μ, where the index μ runs over all possible reactions that could occur among the set of molecules present. $R_\mu(t)$ is a function of the concentrations of the molecules involved in reaction μ. The sum of the rates of all possible reactions that can occur at a given moment is $R_{tot}(t) = \sum_\mu R_\mu(t)$. The simplest algorithm for stochastic simulation is that of Gillespie (1976). In this case, exactly one reaction happens in each time step. The length of time τ before a reaction happens is a random variable chosen from an exponential distribution with mean $1/R_{tot}(t)$. If r_1 is a random variable with a

uniform distribution between 0 and 1, then $\tau = \ln(1/r_1)/R_{tot}(t)$ has the required distribution. One particular reaction μ is then chosen to occur with probability proportional to its rate, *i.e.* the probability that reaction μ is chosen is $R_\mu(t)/R_{tot}(t)$. The number of molecules of each type, $N_i(t)$, is then increased or decreased by the number of molecules produced or consumed by reaction μ, and time is augmented by τ. This algorithm is based on the assumption that no reactions happened in the time interval [t, t+ τ] and that the concentrations of all types of molecules remained the same.

This method treats all reactions in a fully stochastic manner. However, it has the disadvantage of being slow. It is often the case that some molecules have very much higher concentrations than others. Stochasticity is then relevant for the molecules with low concentration, but not for those with high concentration. In Gillespie's algorithm, each time step is very short, because R_{tot} is dominated by the rates of the fast reactions involving the high concentration molecules. It is necessary to carry out a large number of steps in which fast reactions occur before a slow reaction occurs once. A variety of hybrid algorithms have been proposed (Alfonsi 2005, Rudiger 2007, Pahle 2009) that speed up this type of simulation by treating the slow reactions stochastically and the fast reactions with deterministic differential equations. We will use a version of the method referred to as the direct hybrid method by Alfonsi (2005).

We introduce a threshold number N_{min} and define a molecule *i* as rare if $N_i \leq N_{min}$, and common otherwise. We define a reaction μ as rare if at least one of its reactants or products is rare, and common if all reactants and products are common. Rare reactions are treated stochastically. The sum of the rates of all rare reactions in the system is $R_{rare}(t) = \sum_{\mu-rare} R_\mu(t)$. We wish to determine a time step τ in which exactly one rare reaction happens. This time step is much longer than in the Gillespie algorithm because it is not influenced by the rates of the common reactions. In the interval [t, t+ τ], the rates of the rare reactions are not all constant because some of them depend on the concentrations of common molecules, and these concentrations can change due to the occurrence of common reactions during the interval. The time step is determined by finding the value of τ such that

$$\int_t^{t+\tau} R_{rare}(t')dt' = \ln(1/r_1), \qquad (2.16)$$

where r_1 is a uniform random variable between 0 and 1, as before. In order to calculate this integral, the concentrations of all the common molecules need to be followed in time. Deterministic ODEs can be written down that define dC_i/dt for each of the common molecules as a sum of the rates of all the common reactions only. These ODEs can be integrated forward in time using the standard 4th-order Runge-Kutta method with a time step Δt that is small enough that the errors in the concentrations of common molecules are negligible. This is continued over many deterministic time steps until the integral in Equation 2.16

exceeds $\ln(1/r_1)$. The final time step is then shortened by linear interpolation so that Equation 2.16 is valid. At this point we know τ, and we know the values of all concentrations $C_i(t+\tau)$ and rates $R_\mu(t+\tau)$ at time $t+\tau$. One particular rare reaction μ is then chosen to occur with probability $R_\mu(t+\tau)/R_{rare}(t+\tau)$.

To apply this method to the RNA polymerization model, we need to be more specific about which polymers are ribozymes. Polymers shorter than length L are not permitted to be ribozymes. Each polymer of length at least L is given a probability f of being a ribozyme. For $n \geq L$, we define $A_n = A_n^{non} + A_n^{rib}$, where the superscripts 'non' and 'rib' denote non-functional polymers and ribozymes respectively. The stochastic algorithm keeps track of A_n^{non} and A_n^{rib} as two separate kinds of molecules. When each new polymer of length L is generated, it is chosen to be a ribozyme with probability f and non-functional with probability 1-f. For simplicity, we suppose that subsequent addition of nucleotides to a polymer does not influence whether it is a ribozyme or not, *i.e.* if a chain grows to $n > L$ it always remains as either a ribozyme or a non-functional polymer according to what was initially chosen when it was length L. The total concentration of ribozymes is $P_L^{rib} = \sum_{n=L}^{\infty} A_n^{rib}$. Each ribozyme has a catalytic effect k_0; therefore the polymerization rate in the presence of catalytic feedback is $r = r_0 + k_0 P_L^{rib}$. Note that, on average, $P_L^{rib} = fP_L$. Hence, it is approximately true that $r \approx r_0 + k_0 fP_L$. However, ribozymes are rare molecules in this system, and

stochastic fluctuations in the ribozyme concentration are important. Thus, both k_0 and f are relevant parameters in the stochastic simulation, and we cannot replace them by a single parameter $k = k_0 f$, as we did in the deterministic case.

2.6 Results of Stochastic Simulations

This hybrid algorithm was used to simulate the reaction system for RNA polymerization. The nucleotide synthesis reaction was always treated as common. Other reactions were treated as rare or common, as defined by the threshold $N_{min} = 100$. Initially we consider stochastic simulations with no feedback, where $r = r_0$ only. In Figure 2.5, the symbols show the concentrations A_n as a function of n for three different volumes at one typical instant in time after the system has reached a stationary state. There are some missing symbols at the larger lengths in cases where no polymer of that length exists at this particular time. The straight line (on a log scale) shows the steady state concentrations in an infinite system. It can be seen that the stochastic simulations follow the infinite volume result for small n and reach a cutoff where $A_n = 1/V$. For the middle volume shown in the figure, $V = 5 \times 10^6$, and $1/V = 2 \times 10^{-7}$. Several symbols fall at this concentration, meaning that at this point in time there is exactly one molecule of each of these lengths (no symbol is plotted when the number of molecules is zero). For $V = 5 \times 10^6$, the

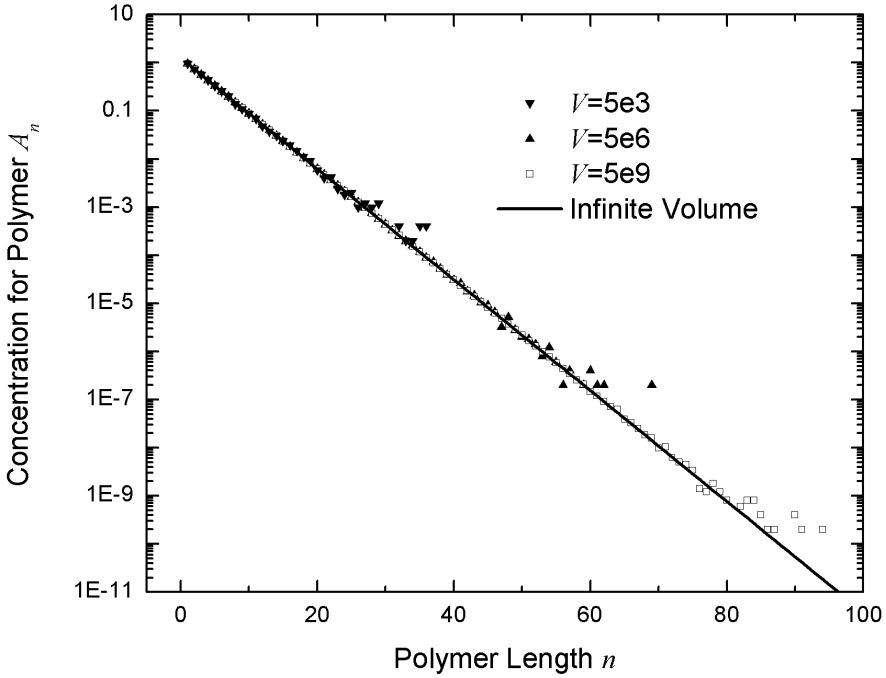

Figure 2.5: Concentrations of polymers as a function of polymer length in stochastic simulations at several different system volumes in comparison to the deterministic solution in an infinite volume.

concentration of A_n falls to $1/V$ when $n \approx 60$. Therefore in a volume of this size, there will only be one or two polymers with length greater than 60, and there are no polymers that are substantially longer than 60.

The finite volume creates an upper limit on the length of polymers that can be produced. If there is a minimum length L required for a polymer to be a ribozyme, then ribozymes will not be produced if the volume is too small. If L = 50, as in these examples, then no ribozymes will be produced for the smallest volume shown in the figure, because the longest chains are considerably shorter than 50. For the middle volume, the distribution extends beyond 50, so some ribozymes will be produced, but the total number of polymers longer than 50 is

very small. Therefore stochastic fluctuations in concentrations of ribozymes will be large. For the largest volume shown, the distribution goes well beyond 50, so the concentration of ribozymes will be essentially the same as in an infinite system and fluctuations will be small.

We now add the feedback term to the stochastic simulations with F=1, s=1, a=1, r_0=4.38× 10^{-4}, u=0.01, k=1, k_0=1000, f=0.001. Chemical reaction rates and k, r_0 are chosen to make sure both living and dead states exist in the system. The simulation begins with only food molecules in a volume with no nucleotides. Monomers and polymers are synthesized and the system moves rapidly to the dead state. For the largest volume shown in Figure 2.6, the system stays in the

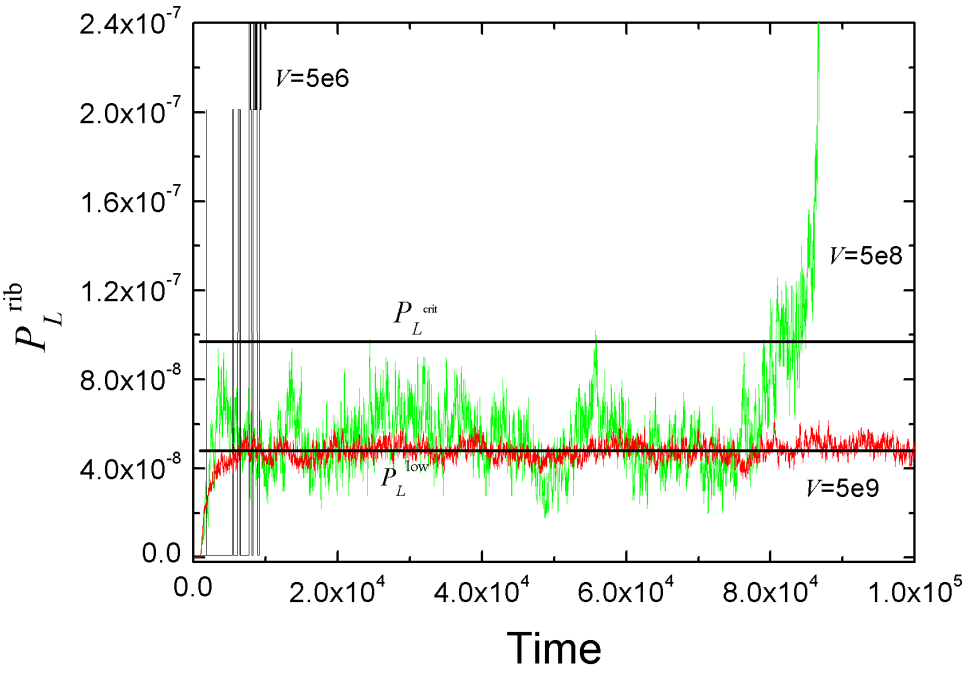

Figure 2.6: Concentrations of catalytic long polymers as function of time in stochastic simulations at different system volumes.

dead state throughout the simulation. The concentration P_L^{low} corresponding to the dead stable state in an infinite system is shown as a horizontal line in the figure. For the intermediate volume, the system remains in the dead state for some time and then goes through a transition to the living state. For the smallest volume, the transition happens very quickly in the example shown. The polymer concentration in the high stable state is orders of magnitude higher than P_L^{low} and is off the scale of the figure. The critical polymer concentration, P_L^{crit}, shown in the figure is the concentration at which $r = r_{unst}$. As can be seen from the intermediate volume example in Figure 2.6, the polymer concentration fluctuates around P_L^{low} until it happens to exceed P_L^{crit}, and then it increases rapidly toward the value in the living state.

In a small volume, concentration fluctuations are larger, and this speeds up the transition. In a small volume, each ribozyme has a large effect, and the chance production of just a few ribozymes is sufficient to cause the transition. When the volume becomes larger, the fluctuations become smaller, and a longer waiting time is required before the transition happens. For a very large volume, the fluctuation is so small that the concentration of ribozymes does not go close to the critical point. Hence the system stays in dead state forever. However, the volume also influences the dynamics in a second way. As we showed in Figure 2.5, if the volume is too small, no long polymers are produced; therefore the transition cannot occur. Figure 2.7 shows the mean time till the transition occurs as a

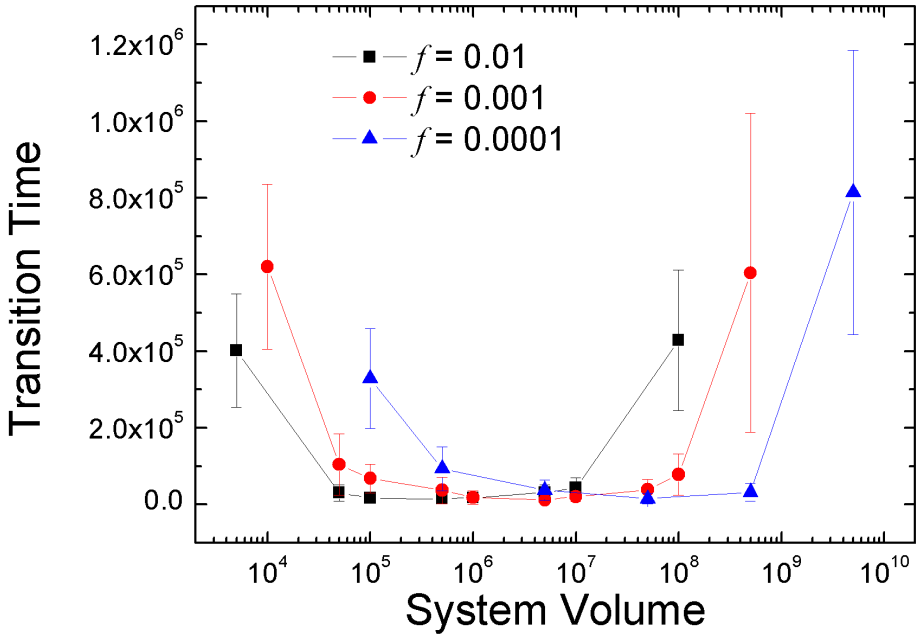

Figure 2.7: Mean transition time from the dead state to the living state and corresponding standard deviation as function of system volume, shown for three different values of the probability *f* that the long polymers are catalytic.

function of the volume. Each point is the average of 10 simulations, and the error bars show the standard deviation of the transition time between these runs. If the volume is made larger or smaller than the range shown, the time increases extremely rapidly and no transition is found to occur within an accessible amount of computer time.

Figure 2.7 also shows the effect of varying the fraction *f* of long polymers that are catalytic. To make all cases comparable, $k=k_0 f$ is kept constant while varying *f*. If *f* is smaller, there are fewer ribozymes but each has a larger effect. Reducing *f* increases the importance of fluctuations in ribozyme concentration; therefore the transition becomes easier in large volumes. However, reducing *f*

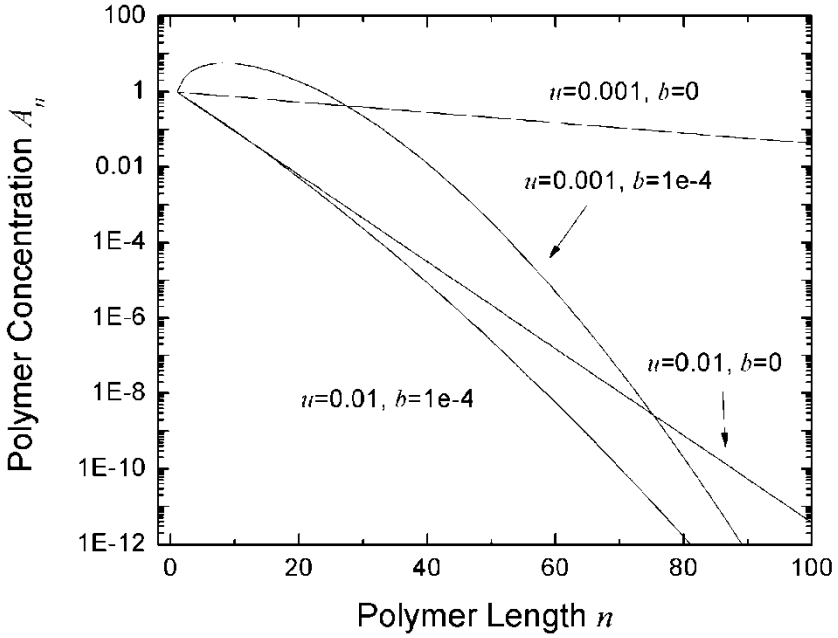

Figure 2.8: Concentration of polymers as function of polymer length with different combination of escape rate *u* and polymer breakdown rate *b*.

means fewer ribozymes; hence a larger volume is required for ribozymes to arise. Therefore, the transition becomes more difficult in smaller volumes. As a result of these two effects, the range over which the transition occurs shifts towards higher volumes when *f* is reduced.

2.7 Effect of Breakdown of Polymers

Up to this point, we supposed that the main factor limiting the accumulation of long polymers was the escape of polymers from the system. We will now introduce the possibility that long polymers can break down into shorter polymers within the system. In this section we show that this additional factor does not qualitatively change the results given above.

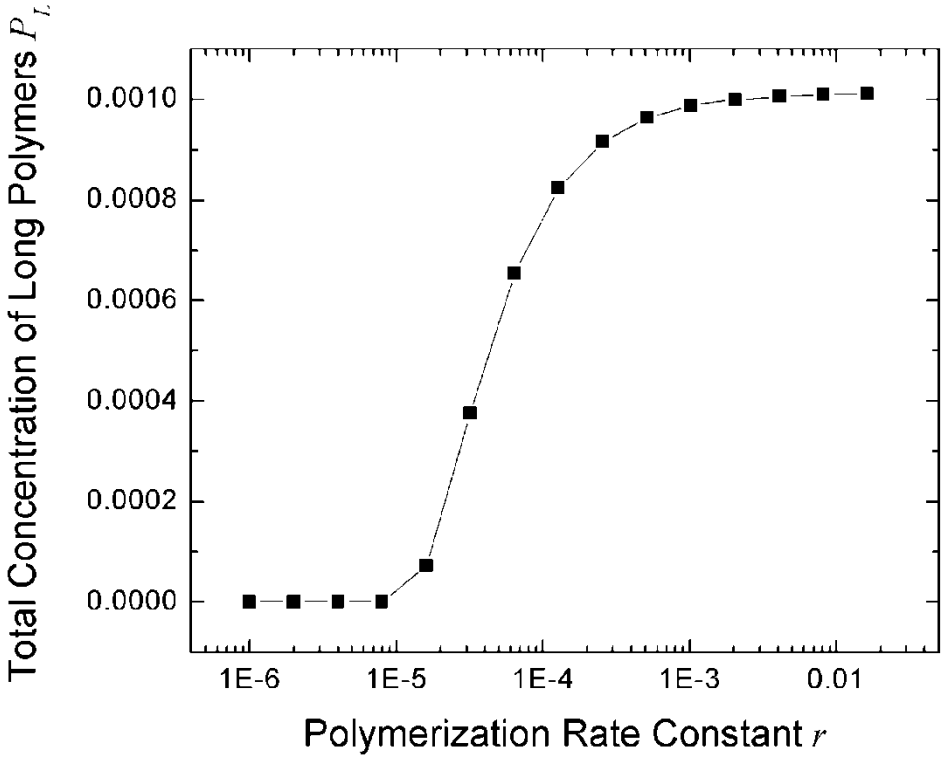

Figure 2.9: Total long polymer concentration P_L in the steady state of the system described by Equations 2.17-2.19 as a function of the polymerization rate constant r.

We suppose that breakage occurs spontaneously at rate b between any pair of monomers. Therefore the total rate of breakdown of a chain of length n is $(n-1)b$. For any chain of length $m > n$, there are two points at which this chain can break down to give a chain of length n. In the special case where $m = 2n$, there is only one place where the break can occur, but two molecules of length n are produced. Adding these terms into Equation 2.4-2.6, we obtain:

$$\frac{dA}{dt} = sF_1 - aF_2A - rAA^* - uA + \sum_{n=2}^{\infty} 2bA_n \tag{2.17}$$

$$\frac{dA_n}{dt} = rA^*(A_{n-1} - A_n) - uA_n - (n-1)bA_n + \sum_{m>n}^{\infty} 2bA_m \qquad (2.18)$$

$$\frac{dA^*}{dt} = aF_2A - rA^*(A+P) - uA^* \qquad (2.19)$$

We did not find an exact expression for the steady state solution of Equations 2.17-2.19, but the steady state concentrations were found numerically by using a standard ODE integration method. The polymer concentration is shown as a function of length in Figure 2.8 for different combinations of escape and break down rates. The two straight lines (exponential decrease) on the figure correspond to cases where $b = 0$. When $b > 0$, the concentration A_n decreases faster than exponentially for large n. When escape is fast, adding a small rate of breakdown leads to a slight decrease in the concentration of longer polymers (example with $u = 0.01$, $b = 0.0001$). When escape is slow, most long polymers are broken down into shorter ones before they escape from the system (example with $u = 0.001$, $b = 0.0001$). This leads to a hump in the concentration distribution at intermediate n. However, the essential qualitative point is that the concentration of long polymers P_L follows an S-shaped curve as a function of r, even when $b > 0$. Figure 2.9 shows P_L as a function of r when the other parameters are fixed at F=1, s=1, a=1, u=0.001, b = 0.0001, k=1. Given that this curve is S-shaped, when autocatalytic feedback is introduced by setting $r = r_0 + kP_L$, there is still a region of parameter space when there is both a living and a dead stable state and it is still possible for concentration fluctuations to drive the system from the dead to the living state.

2.8 Discussion and Conclusions

Here we will summarize the key conclusions we draw from the model presented above and discuss some of the limitations of the model and features that could be added in the future. We began with the observation that life is based on self-replicating sets of biopolymers and we set out to produce a simple model to explain how such sets could arise. The model was designed to describe the steps of polymerization of RNA because there is considerable reason to believe that the first living systems may have been based on RNA or some similar kind of polymer, and because it is known that some RNA sequences have the ability to be ribozymes that can catalyze various steps in RNA synthesis (as discussed in the introduction). It was assumed that only long sequences have the ability to be ribozymes. The key property of the model is that the concentration of long polymers follows an S-shaped curve as a function of the polymerization rate. If long polymers can act as polymerase ribozymes, then there is autocatalytic feedback in the polymerization rate, and the model predicts the existence of two kinds of stable states that we identify with the living and the dead states.

In designing our model, we were aware of the toy model of Dyson (1999), which is also based on the idea of an S-shaped curve and two kinds of stable states. The phase diagram of Dyson's model is qualitatively similar to ours in Figure 2.4. We consider this to be an important feature that is likely to be quite general in chemical reaction systems describing replicating systems and the origin

of life. However, the presentation of Dyson's model seems to us to be overly abstract. It contains no chemical reactions or concentrations of molecules. The living and dead states are distinguished based on high and low fractions of 'active monomers', but the meaning of active is not clear and seems rather arbitrary. If we observed a chemical system described by Dyson's model, it is not obvious how we would tell which monomers were active, and hence how we would decide if the system was dead or alive. In contrast, in our model, there is an easily-observable qualitative difference between the living and the dead states. The concentration of long polymers is very much higher in the living state than the dead, and in the living state, the polymerization reaction occurs chiefly as a result of catalysis by polymers formed within the system, whereas in the dead state, the polymerization reaction occurs principally by the spontaneous reaction, and hence occurs at a much lower rate.

The other key insight of Dyson (1999) is the idea that the transition is caused by stochastic dynamical fluctuations. In our model, these fluctuations are inevitable because of the stochasticity of chemical reactions. Only a small fraction of long polymers is likely to be a functional ribozyme, and so ribozymes are bound to be rare before the transition occurs. This means that stochasticity is bound to be important in the ribozyme concentrations even if the volume is large enough that there is very little fluctuation in the concentration of monomers and short oligomers. Our model shows that the volume of the system is an important parameter and that an intermediate volume is required. If the volume is too small,

ribozymes will never arise. If the volume is too large, the system remains stable in the dead state. The optimal size is big enough such that a few ribozymes will arise with reasonable probability, and small enough such that just a few ribozymes are enough to have a large effect in their local region. We would very much like to estimate how large this optimal volume is! Does it correspond to the volume of a lipid vesicle, or a typical bacterium, or pore in a mineral surface, or a 'warm little pond'? Unfortunately we do not see a way of making a sensible quantitative estimate at present, because the reaction rates are unknown. The concentrations of all the components depend strongly on these rates, and so do the volume and the time scale required for the transition. If some of these parameters could be measured in the laboratory, it would still be difficult to know what the corresponding rates might have been on the early Earth. Thus, reluctantly, we have to leave this as a qualitative argument.

It is clear that the spontaneous rates of polymerization, synthesis and activation are important parameters in our model because these will control the concentrations of polymers in the dead state. If these rates are too low then long polymers will not arise in sufficient frequency to initiate the transition. In particular, if there is no spontaneous polymerization ($r_0 = 0$, and $r = kP_L$), then both the living and the dead state still exist, but the dead state has zero polymer concentration, so there is no way of getting out of the dead state even in a finite volume. It is therefore important that conditions in the local region enable these reactions to occur to some degree, even if the spontaneous rates are low. It is

worth pointing out, however, that once the system shifts to the living state, the spontaneous polymerization rate becomes unimportant because $kP_L >> r_0$. This means that once life originates, it is not restricted to the favourable local region in which it arose. The reaction system could spread to a region where $r_0 = 0$, even though it could not arise in such a region.

We include in our definition of 'spontaneous' any reactions that are catalyzed by substances in the local region that are not part of the reaction system itself. For example, RNA polymerization may be catalyzed by a mineral surface (Ferris, 2002), but the synthesis of RNA polymers does not make more mineral catalyst, so there is no feedback. The mineral catalyzed rate is thus part of r_0, and the presence of the mineral catalyst in the local region may be the reason why r_0 is non zero and why the region is favourable for polymerization reactions to occur in the first place. Rajamani *et al.* (2009) also proposed that lipids might catalyze RNA synthesis. Lipids might exist in the prebiotic environment, in which case such a reaction would be part of the spontaneous rate, as for the mineral catalyst. At some point in the development of life, however, lipids would begin to be synthesized by the organism for construction of cell membranes, in which case the lipids would become part of a larger autocatalytic feedback loop. We note that Ganti (1979) included autocatalytic synthesis of lipids in his model for replication of minimal cells.

In Figure 2.1, we indicated that ribozymes might catalyze the synthesis and activation reactions as well as (or instead of) the polymerization reaction. It is

possible to add autocatalytic feedback to these reaction steps too. We have considered this only very briefly. If feedback is added to the activation rate ($a = a_0 + kP_L$), but r and s are kept constant, then P_L follows an S-shaped curve as a function of a, although P_L decreases with a for very large a (in fact $P_L \sim a^{-1/2}$), rather than saturating to a constant, as it does when r is large in Figures 2.2 and 2.3. It should still be possible for a living state with high polymer concentration to arise in this case in a similar way to when the feedback occurs in r, and it should still be possible for a stochastic transition to occur in to the living state. We therefore expect that feed back in a gives qualitatively similar results to feedback in r. However, if feedback is added to the synthesis rate ($s = s_0 + kP_L$), but a and r are kept constant, then a difficulty arises with the formulation of the model. We assumed, for simplicity, that the food concentration F_1 in Equation 2.4 was constant because it was replaced by diffusion into the local region as fast as it was consumed. If F_1 is constant then P_L increases indefinitely when feedback is added to the synthesis rate, *i.e.* the living state has an infinite polymer concentration. In order to fix this unrealistic behaviour, it would be necessary to make F_1 a variable and to add an additional reaction equation to describe the depletion of F_1 that would occur in the local region if the synthesis rate were very large. In general it would be interesting to consider variations of this model in which all three reactions were catalyzed by three different types of ribozyme, but we have not attempted this.

In this chapter, we have made the gross simplification of ignoring the sequence of the RNA polymers and taking account only of their length. It is clear that the specifics of the sequence and structure are essential in real RNAs. A good deal is known about the structures of ribozymes synthesized in vitro, and we hope to use this information in the future to guide the design of a more detailed model that incorporates specific sequences composed of four types of monomers. Briones *et al.* (2009) have described a scenario in which a series of increasingly efficient ribozymes with longer sequence and more complex structure might arise and eventually give rise to a template-directed RNA polymerase. This scenario makes a lot of sense to us, and is broadly compatible with our model. Our model could be generalized to allow sequences of longer lengths to be better ribozymes, in which case we would expect a series of stochastic transitions giving rise to each new class of more efficient ribozyme. If the model were extended to include details of sequence, it would be necessary to specify which sequences are ribozymes and which sequences are substrates for the ribozymes. For example, sequences folding to a specific secondary structure might be deemed ribozymes. Early ribozymes may have acted only on substrates that had specific sequences or specific structural elements, rather than being general polymerases. Errors in sequence replication would also be an essential quantity, as is emphasized in the quasispecies theory for replicating sequences (Eigen *et al.* 1989). All these issues are interesting and relevant to the origin of the RNA world, but they require a more complex model than the one presented here.

Chapter 3

Comparison of the Roles of Nucleotide Synthesis, Polymerization, and Recombination in the Origin of Autocatalytic Sets of RNAs

3.1 Introduction

In this chapter, we will investigate different catalytic mechanisms which could lead to origin of autocatalytic sets of biopolymers. The reaction scheme that we study in this chapter incorporates three kinds of reaction: synthesis of monomers from precursors, polymerization by sequential addition of monomers, and recombination, as shown in Figure 3.1. We will refer to ribozymes that catalyze these reactions as synthases, polymerases, and recombinases, respectively. In this chapter we present mathematical models of this reaction system and show that these three types of ribozyme can all be autocatalytic, *i.e.* they can increase the rate of their own formation. Before introducing the mathematical models, we will discuss what is known about these ribozymes experimentally.

Polymerases spring immediately to mind when discussing the origin of life because they have the ability to synthesize new RNA strands. In principle, if a polymerase could synthesize another strand of the same length as itself, it could make another copy of itself, and hence be self-replicating. Polymerases that have been studied in the laboratory use a template strand and synthesise a new

complementary strand by sequential addition of complementary monomers. Several polymerases of this kind have been developed (Johnston *et al.* 2001; Lawrence and Bartel, 2005) in by *in vitro* evolution. A recently developed polymerase is able to synthesize strands of up to 95 nt in length (Wochner *et al.* 2011), although the polymerase itself has a length of around 170 nt. These studies provide important support for the concept of the RNA World, even though they still fall short of self-replication. An RNA-based organism would also have to synthesize its own nucleotides from simpler precursor molecules found in the environment. Ribozymes capable of catalyzing uridine nucleotide synthesis from uracil and ribose have also been developed in the laboratory (Unrau and Bartel, 1998).

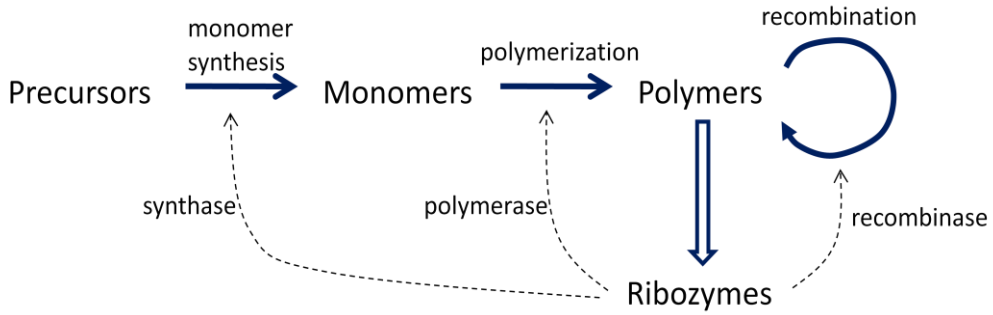

Figure 3.1: Schematic diagram of an autocatalytic RNA system involving monomer synthesis, polymerization and recombination.

We expect that RNA strands must be moderately long in order to have sufficient complexity to function as ribozymes. For example, simple hammerhead ribozymes that catalyze RNA cleavage are of length 40-50 nucleotides (Scott *et al.* 1995), while more complex polymerases are around 170 nucleotides (Wochner

et al. 2011). Random abiotic polymerization will typically give rise to length distributions that decrease exponentially, *i.e.* long polymers will be extremely rare with respect to monomers and short oligomers. Any factors that shift the length distribution towards longer chains are therefore potentially helpful in increasing the likelihood of generation of ribozymes. It has been proposed that recombination reactions can act in this way (Lehman, 2008). The type of recombination that is relevant is non-homologous crossing over between two single strands. Recombination can produce a strand that is substantially longer than either of the input strands, *e.g.* two strands of length n can produce a strand of length $2n$-1 and a single nucleotide. However, the reverse reaction can also occur, *i.e.* long chains can be destroyed by recombination as well as created. In this chapter we investigate the effect of recombination of the length distribution in more detail.

Recombination in RNA has been studied experimentally. Lutay *et al.* (2007) showed that recombination between RNA strands can occur via a cleavage and a subsequent ligation reaction. The cleavage leaves a 2',3'-cyclic phosphate at the end of one of the fragments, which undergoes a ligation reaction with the 5' end of another strand. Hayden and Lehman (2006), Draper *et al.* (2008) and Hayden *et al.* (2008) have studied a recombination system derived from the group I intron of *Azoarcus* sp. BH72, which is one of the smallest known self-splicing introns (Kuo *et al.*, 1999). The *Azoarcus* ribozyme can function as a recombinase by two mechanisms (Draper *et al.* 2008). In the simplest of these, known as *tF2*,

two strands come together due to RNA secondary structure formation, and the ribozyme catalyzes a transesterification reaction betweeen the ends of these strands. A requirement of this reaction is that one of the strands ends with the sequence CAU, which is complementary to the internal guide sequence GUG in the ribozyme. The reaction creates a long sequence with a hairpin loop at the point of connection plus a single nucleotide. It was found that the ribozyme can be broken into four fragments that can self assemble into a *trans* complex that has almost the same structure as the fully connected ribozyme. If the fragments contain the CAU sequence in the required places then they can be linked together by the *tF2* reaction. One copy of the ribozyme can therefore create another copy by linking the four fragments in the *trans* complex, *i.e.* synthesis of the ribozyme is autocatalytic.

The *Azoarcus* recombinase system is somewhat similar to a ligase system studied by Lincoln and Joyce (2009), although the latter case works in two steps. One strand catalyzes the ligation of two fragments to form a complementary sequence. The complementary sequence then catalyzes the ligation of two other fragments that produce the original strand. In both these experiments the formation of the full-length strand from the fragments is autocatalytic, but in both cases it is necessary to supply the correct fragments to keep the reaction going. The fragments themselves are fairly long and would therefore be expected to be rare in an abiotic random polymerization system. Nevertheless, these experiments give proof that autocatalytic systems of RNA can exist. Our aim in this chapter is

to develop a theory of how autocatalytic RNA systems might have emerged initially from within a random polymerization system.

This chapter builds on previous chapter, in which we introduced a model to study the role of polymerase ribozymes in particular. In the current chapter, we consider synthase and recombinase ribozymes in addition to polymerases. We show that in the presence of synthases, there are once again two stable states. The behaviour of the synthase model is very similar to the polymerase case. The recombinase case is somewhat different, because the recombination reaction is inherently reversible. In a general model including fully reversible recombination, we find that there can be no autocatalytic state that is controlled by the recombination reaction. However, we then consider a more specific model of the *Azoarcus* recombinase discussed above, and show that, due to the association of the fragments by RNA secondary structure formation prior to the recombination reaction, the recombination reaction is no longer fully reversible. In this case an autocatalytic state controlled by the recombinase is also possible.

3.2 Basic Model of Polymerization

We start with a basic system of chemical reaction equations that describes the synthesis of biopolymers such as RNAs. We suppose that the reactions for monomer synthesis and polymerization occur in a local region that is separated from the external environment, but which can exchange molecules with the environment. For example, the local region could be the interior of a lipid vesicle,

or a cavity in a porous rock, or the surface of a catalytic mineral. The basic reactions are that precursor molecules, or 'food', *F*, are synthesized into monomers, *A*, and that monomers can polymerize by repeated addition to the end of growing chains.

$$F \xrightarrow{s} A \tag{3.1}$$

$$A_n + A \xrightarrow{r} A_{n+1} \tag{3.2}$$

A denotes any kind of nucleotide monomer, and A_n denotes any chain of length *n* monomers. The model does not keep track of specific sequences of different kinds of monomers. The rate constants for synthesis and polymerization are denoted *s* and *r*, respectively. Initially we treat these as fixed parameters, but later we suppose that these rates are functions of the concentration of biopolymer catalysts. Food molecules enter and exit the system at rate *u*, and there is a fixed concentration F_0 outside the system. Monomers and polymers exit the system at rate *u*, but do not enter the system because the concentration is taken to be negligible outside. The following set of differential equations describes the change of concentrations of F, A and An:

$$\frac{\mathrm{dF}}{\mathrm{dt}} = \mathrm{u}(\mathrm{F}_0 - \mathrm{F}) - \mathrm{sF} \tag{3.3}$$

$$\frac{\mathrm{dA}}{\mathrm{dt}} = \mathrm{sF} - \mathrm{r}(2\mathrm{A} + \mathrm{P})\mathrm{A} - \mathrm{uA} \tag{3.4}$$

$$\frac{\mathrm{dA_n}}{\mathrm{dt}} = \mathrm{rAA_{n-1}} - \mathrm{rAA_n} - \mathrm{uA_n} \tag{3.5}$$

In Equation 3.4, P is the total polymer concentration of all lengths $n \geq 2$.

$$P = \sum_{n=2}^{\infty} A_n \tag{3.6}$$

Solving Equations 3.3-3.5 in the steady state, we find that

$$A_n = Az^{n-1} \tag{3.7}$$

where

$$z = \frac{rA}{rA + u} \tag{3.8}$$

Hence

$$P = A\sum_{n=2}^{\infty} z^{n-1} = \frac{rA^2}{u} \tag{3.9}$$

From Equation 3.3, we have

$$F = \frac{uF_0}{u + s} \tag{3.10}$$

Substituting into Equation 3.4, we have:

$$\frac{r^2A^3}{u} + 2rA^2 + uA = \frac{uF_0 s}{u + s} \tag{3.11}$$

This is a cubic equation for A, for which there is only one real and positive root. Hence, A and all other quantities can be calculated for any given parameters r, s, u, F_0.

3.3 Autocatalytic Feedback in Polymerization

According to Equation 3.7, the polymer length distribution decays exponentially. Unless *z* is very close to 1, the concentration of long polymers will be very small. Nevertheless, long polymers are relevant because we suppose that

only polymers of length greater than or equal to a minimum length L can act as catalysts. The long polymer concentration is

$$P_L = \sum_{n=L}^{\infty} A_n = \frac{Az^{L-1}}{1-z} \tag{3.12}$$

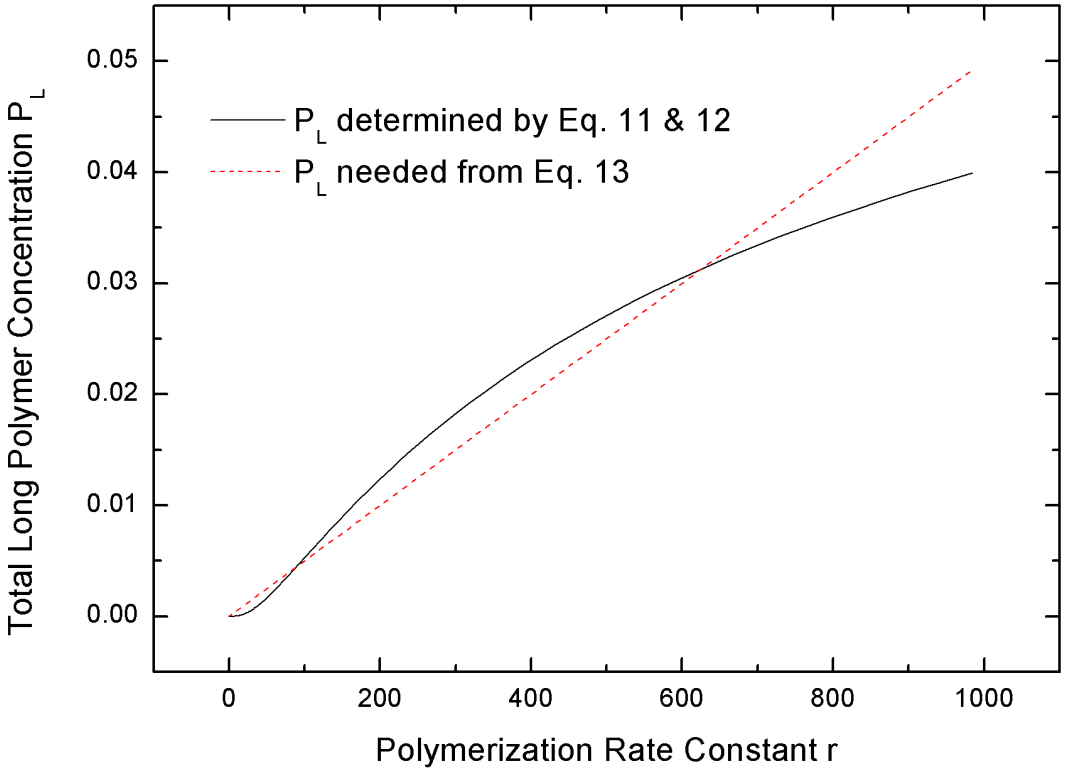

Figure 3.2: Total long polymer concentration P_L as function of polymerization rate constant r. The black solid line is obtained from Equation 3.12 when $u = 1, s = 10, F_0 = 10, L = 50$. The red dash line is obtained from Equation 3.13 when $r_0 = 0.1, k = 20000$

A and z are obtained by numerical solution of Equation 3.11. Figure 3.2 shows P_L as a function of polymerization rate r with fixed values of all the other parameters. This follows an *S*-shaped curve. We now suppose that r can be written as the sum of two components, $r = r_0 + k_r P_L$, where r_0 is a small spontaneous rate (*i.e.* not

driven by biopolymer catalysts) and k_r is the rate constant for the polymerization reaction catalyzed by the long polymers. The catalyzed rate is $k_r P_L$, which is proportional to the long polymer concentration. If a small fraction f of long polymers is a catalyst and the effect per catalyst is k_0, then $k_r = k_0 f$. The relationship between r and P_L can be written as

$$P_L = \frac{r - r_0}{k_r} \tag{3.13}$$

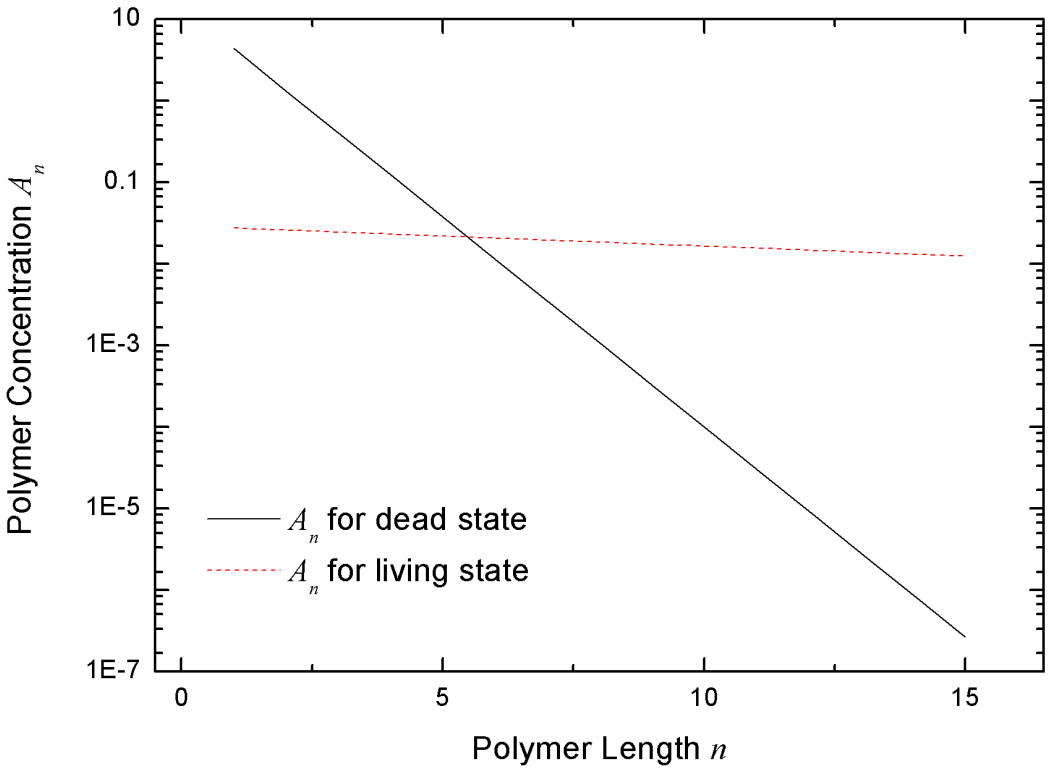

Figure 3.3: Distribution of polymer lengths at the two stable stationary state solutions of the model with feedback in polymerization as in Figure 3.1 . For dead state, $A = 4.3901, z = 0.3051$. For living state, $A = 0.02746,\ z = 0.9450$.

which is a straight line on Figure 3.2. Valid solutions for P_L are where the line intersects the *S*-shaped curve. Depending on the values of r_0 and k_r, the line may

intersect the curve either once or three times. The most interesting region of the parameter space is where the line intersects three times, as in Figure 3.2. In this case, it may be shown that the upper and lower intersection points correspond to stable solutions of the differential equations and the middle intersection point is unstable. Once we know the value of r and P_L at the intersection point, we can determine the values of A and z that correspond to this point from Equations 3.8 and 3.12. Hence, we know the polymer length distribution in the presence of autocatalytic feedback.

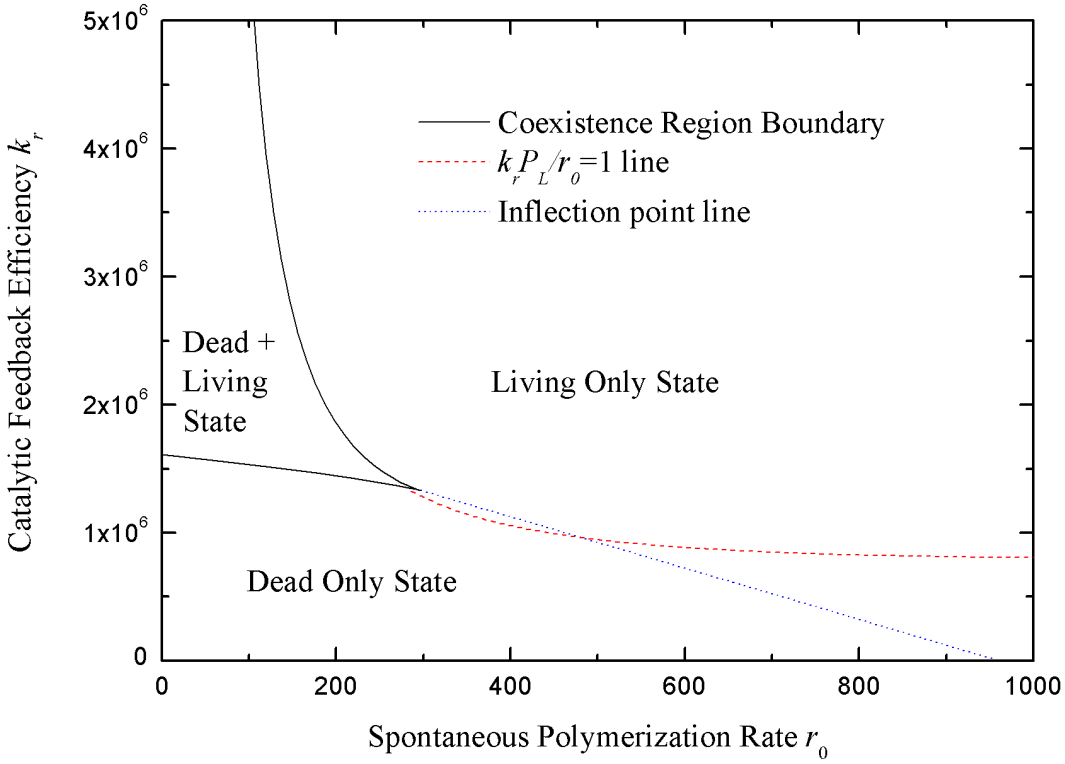

Figure 3.4: Phase diagram of the reaction system as function of feedback efficiency k_r and spontaneous polymerization rate constant r_0, when $u = 1, s = 10, F_0 = 10, L = 50$.

In Figure 3.3, we show the length distribution at the two stable solutions corresponding to the intersection points in Figure 3.2. Both these solutions are exponential distributions (straight lines on the log plot), but the decay rates are different because there are two different values of z. We refer to these solutions as living and dead states. In the dead state, z is much less than 1, and P_L is very small. Hence polymerization is almost entirely controlled by the spontaneous rate, $r \approx r_0$. In the living state, z is only slightly less than 1, and P_L is large. In this case, $k_r P_L >> r_0$, and the total polymerization rate is almost entirely controlled by the catalytic term. The presence of long polymer catalysts leads to a high rate of polymerization of more long polymers. Hence this state is autocatalytic, and that is why we refer to it as the living state.

Figure 3.4 shows the phase diagram of this model in the space of r_0 and k_r, illustrating the region (enclosed by the solid lines) where both living and dead states are stable. Points on the solid boundary lines correspond to points in Figure 3.2 where the line is tangential to the *S*-shaped curve, *i.e.* where the central unstable solution merges with either the upper or the lower stable solution. Outside the solid boundary lines, there is only one solution - either living or dead, but not both. If we move around the outside of Figure 3.4, we move smoothly from a state with very low P_L, which is clearly dead, to a state with very high P_L, which is clearly living. As this change is continuous, it is somewhat arbitrary where to draw the boundary between the regions with only dead and only living solutions. One choice, is to make use of the point of inflection in the *S*-shaped

curve in Figure 3.2. According to this definition, the solution is taken to be living if the intersection point lies above the point of inflection and dead if it lies below. The dotted line in Figure 3.4 shows the boundary between the only-living and only-dead regions of the phase diagram obtained using the point of inflection rule. An alternative choice is to define the solution as living if polymerization occurs predominantly by catalysis ($k_r P_L/r_0 > 1$) and dead if polymerization occurs predominantly by the spontaneous rate ($k_r P_L/r_0 < 1$). The boundary line according to this definition is when $k_r P_L/r_0 = 1$, which is also shown on Figure 3.4. Although the position of the dotted boundary is a matter of definition, the position of the solid boundaries is unambiguous, because the behaviour changes suddenly from a single stable state to two stable states as we cross these boundaries.

The model described here is very similar to that given in previous chapter, but we wish to point out two slight differences. In the previous chapter, we included a step of formation of activated monomers, representing nucleotide triphosphates or imidazoles, as in the experiments of Ferris *et al.* (1996). For simplicity, we have eliminated this step in the present chapter, and we treat monomer synthesis as a single step. The results are very similar to before, and the conclusions do not depend on whether we include the activation step. The second difference to our previous chapter is that we have treated the food molecule concentration F as a variable with its own dynamics given by Equation 3.3, whereas previously we kept F fixed at a constant. This change is necessary in order to consider synthase ribozymes, as we do in the next section. Wu and Higgs

(2009) went on to discuss the stochastic dynamics of the model with polymerase ribozymes. The main result was that, in a finite volume, concentration fluctuations can drive the system from the dead state to the living state, *i.e.* an origin of life can occur in this model. The stochastic dynamics of the model considered here should be very similar to the case in our previous chapter; therefore we will not consider the dynamics further here. In the present chapter, we will proceed to compare the model above, in which feedback is in the polymerization reaction, with models in which feedback occurs by either nucleotide synthesis or recombination.

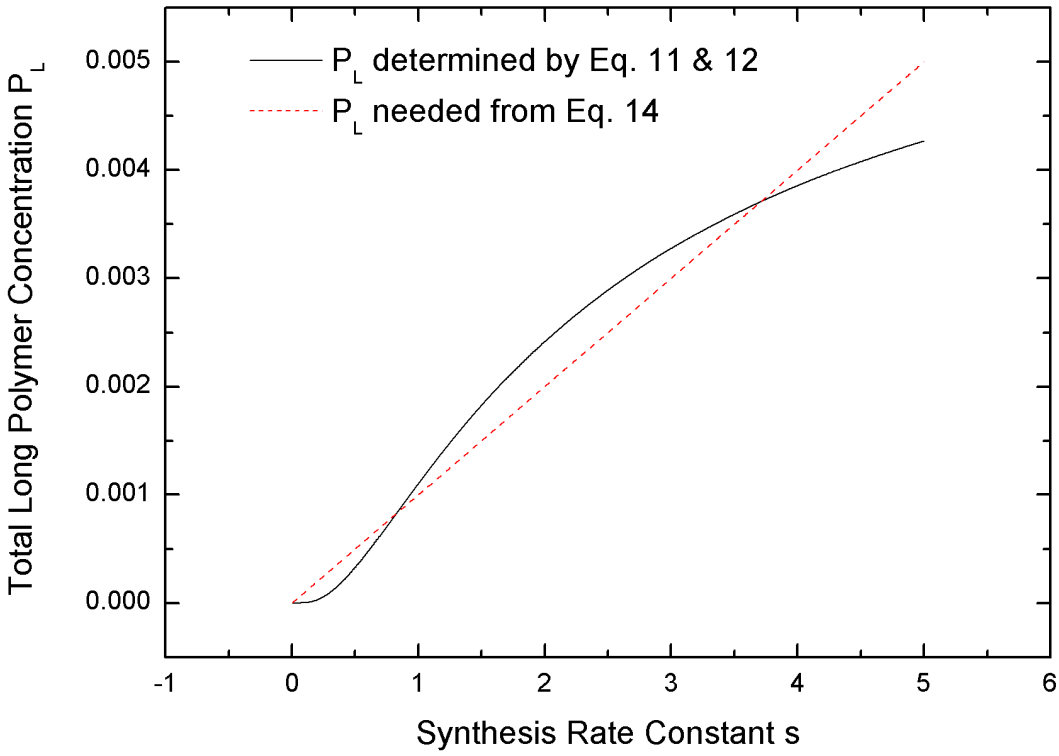

Figure 3.5: Total long polymer concentration P_L as function of monomer synthesis rate. The black solid line is obtained from Equation 3.12 when $u = 1, r = 100, F_0 = 10, L = 50$. The red dash line is obtained from Equation 3.14 when $s_0 = 10^{-6}, k = 1000$

3.4 Autocatalytic Feedback in Nucleotide Synthesis

We now return to the basic model of Equations 3.3-3.5, and we suppose that the polymerization rate, *r*, is simply a constant. However we consider the possibility that long polymers can act as nucleotide synthases, instead of polymerases. Figure 3.5 shows the concentration of long polymers as a function of *s*, when *r* and the other parameters are constant. This is another *S*-shaped curve that is similar to Figure 3.2. We introduce feedback into nucleotide synthesis by setting $s = s_0 + k_s P_L$, where s_0 is a small spontaneous synthesis rate and k_s is the rate constant for synthesis catalyzed by the long polymers. The analysis now proceeds as before. The solutions of the model in the presence of feedback must be where the *S*-shaped curve intersects the line:

$$P_L = \frac{s - s_0}{k_s} \tag{3.14}$$

The phase diagram in the s_0 and k_s parameter space (Figure 3.6) has a similar shape to the previous case in the r_0 and k_r parameter space (Figure 3.4). There is a living state, in which monomer synthesis is controlled by the catalytic rate and ribozyme concentration is high, and a dead state, in which monomer synthesis is controlled by the spontaneous rate and ribozyme concentration is very low. In a finite volume, concentration fluctuations can cause the system to jump from the dead to the living state, as before.

It should be noted that it is important to treat the food concentration *F* as a variable in the case where feedback is in nucleotide synthesis. When *s* is high, *F* is

depleted and becomes much less than F_0, as seen from Equation 3.10. In this case, the rate of food entering the system limits the overall concentration of monomers and polymers and insures that the top part of the *S*-shaped curve in Figure 3.4 flattens out in the limit of large *s*. If the food concentration was treated as a constant, there would be no maximum limit to the rate of nucleotide synthesis, and the concentration of monomers and polymers would grow indefinitely once ribozymes appeared, which would be unrealistic.

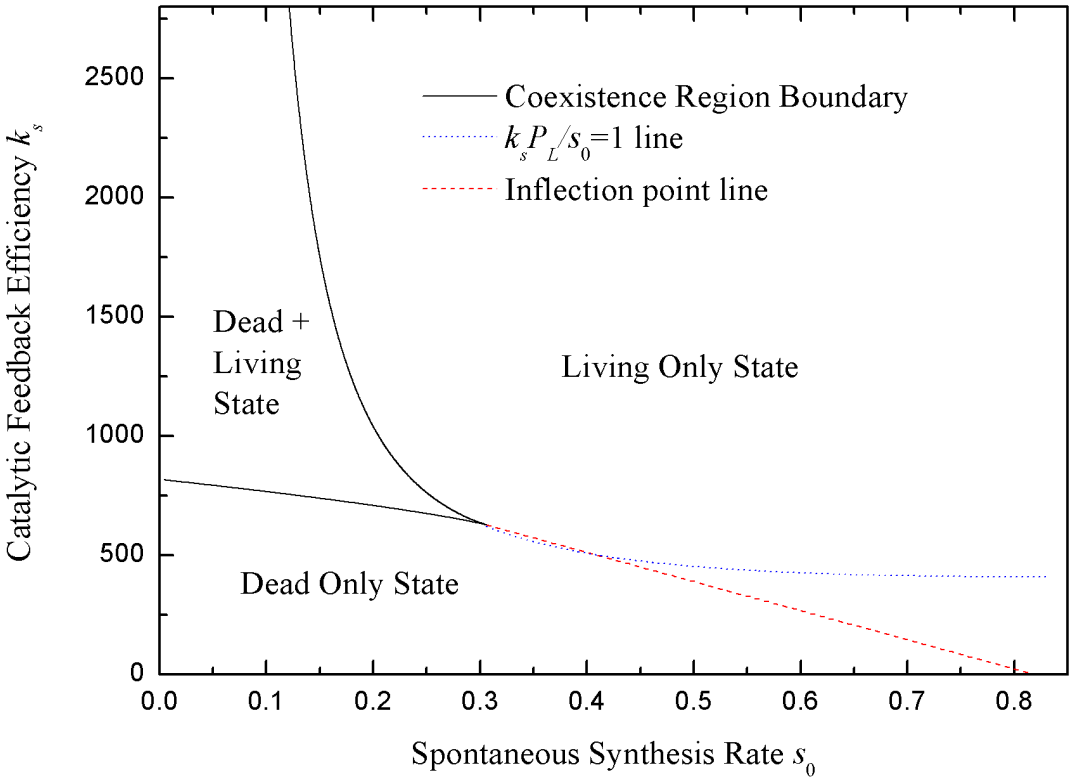

Figure 3.6: Phase diagram of the reaction system as function of feedback efficiency k and spontaneous synthesis rate constant s_0, when $u = 1, r = 100, F_0 = 10, L = 50$.

3.5 Effect of Recombination on the Polymer Length Distribution

According to our argument, the origin of life can only occur if spontaneous reactions are able to generate the first few ribozymes that initiate the autocatalytic feedback. If r_0 and s_0 are both small, then presumably we need to wait very long times for rare fluctuations to occur, as discussed in the dynamical sections of Wu and Higgs (2009). Any factors that increase the likelihood of forming polymers long enough to be ribozymes will increase the probability of the origin of life. It has been proposed that recombination reactions can act in this way (Lehman, 2008). Therefore, we wish to add the possibility of recombination between the polymer chains in our model.

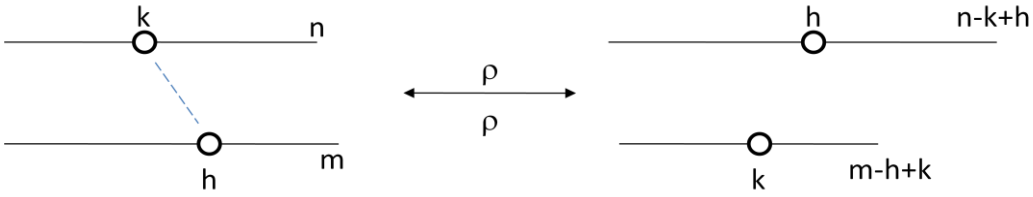

Figure 3.7: A possible random recombination reaction.

Initially we will consider a closed reaction system where the only reactions possible are recombinations of the type shown in Figure 3.7, where a chain of length n reacts with a chain of length m to produce chains of length n-k+h and m-h+k. We suppose that the rate constant for both forward and backward reactions is ρ. These rates are should be equal because the same kind of chemical bond is being made and broken in each case. We suppose that $1 \leq k \leq n$, so there are n places where a chain of length n can recombine.

In a closed system with only recombination, the total number of monomers is fixed, but the length distribution can change. The rate of change of polymer concentration for any given *n* is

$$\frac{dA_n}{dt} = -\lambda_n + \mu_n \tag{3.15}$$

where λ_n and μ_n are the total rates of destruction and creation of chains of length *n*. From Figure 3.7, we have

$$\lambda_n = 2\rho \sum_{m=1}^{\infty} \sum_{k=1}^{n} \sum_{h=1}^{m} A_n A_m = 2\rho n A_n \sum_{m=1}^{\infty} m\, A_m \tag{3.16}$$

and

$$\mu_n = 2\rho \sum_{m=1}^{\infty} \sum_{k=1}^{n} \sum_{h=1}^{m} A_{n-k+h} A_{m-h+k} \tag{3.17}$$

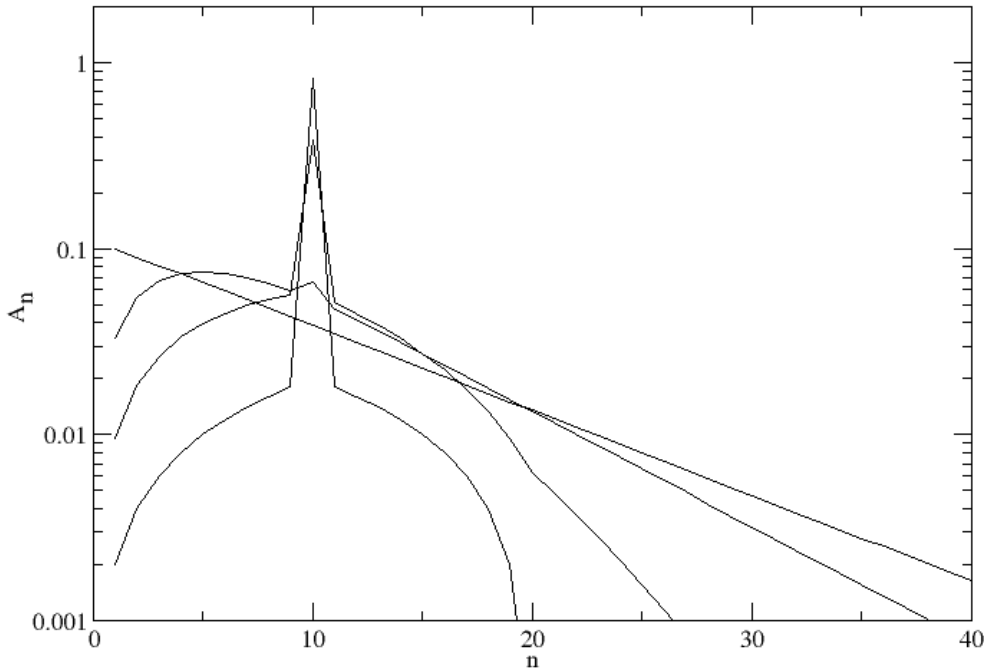

Figure 3.8: The effect of recombination on the polymer length distribution in a closed system. Beginning with only chains of length 10, the distribution is shown at three finite times and also in the long time limit, where it converges to an exponential with mean length 10.

Figure 3.8 shows a simulation of the distribution following Equation 3.15, beginning from the case where all chains are length n = 10. Recombination causes this distribution to broaden and eventually tend to an exponential distribution of the form $A_n = Az^{n-1}$. In order to see that the exponential distribution is stationary, consider the pair of reactions in Figure 3.7. The forward and backward rates are equal if the distribution is exponential:

$$\rho A_n A_m = \rho A_{n-k+h} A_{m-h+k} = \rho A^2 z^{n+m-2} \tag{3.18}$$

It also follows that the total rates of creation and destruction of chains are equal if the distribution is exponential:

$$\lambda_n = \mu_n = \frac{2\rho A^2 n z^{n-1}}{(1-z)^2} \tag{3.19}$$

The mean length from the exponential distribution is 1/(1-z). As the mean length was 10 initially, and as recombination does not change the mean length, it must be the case that z = 0.9 in this example. However, from Equations 3.18 and 3.19, we see that *any* exponential distribution, irrespective of z, will be stable under recombination. The value of z is determined by the initial conditions and not by the recombination rate ρ.

We now consider the effect of adding recombination to our polymerization reaction system. Equation 3.3 stays the same, and Equations 3.4 and 3.5 are modified to

$$\frac{dA}{dt} = sF - r(2A + P)A - uA - \lambda_1 + \mu_1 \tag{3.20}$$

$$\frac{dA_n}{dt} = rAA_{n-1} - rAA_n - uA_n - \lambda_n + \mu_n \tag{3.21}$$

In absence of recombination, the stationary distribution is exponential, with a value of A and z determined from Equations 3.8 and 3.11. As $\lambda_n = \mu_n$ for *any* exponential distribution, it follows that the stationary distribution of Equations 3.20 and 3.21 is unchanged by the presence of the recombination terms, *i.e.* the polymer length distribution depends on s and r as before, but it does not depend on ρ. If ribozymes arise in this system that catalyze recombination, we might try to introduce feedback in the recombination rate by writing $\rho = \rho_0 + k_\rho P_L$, as we did before for s and r. However, this will make no difference to the length distribution. The presence of recombinases does not increase the rate of forming more recombinases. Therefore, if recombination is completely reversible, there cannot be an autocatalytic state that is initiated by recombinases.

3.6 A Non-Reversible Recombinase

In the introduction we already discussed the experiments on the *Azoarcus* ribozyme that have demonstrated that autocatalysis can arise in a recombinase system (Hayden and Lehman, 2006; Draper *et al.* 2008; Hayden *et al.* 2008). This might seem to contradict the result of the previous section; however, there is really no contradiction because in the experimental system recombination is not fully reversible. Figure 3.9 shows a schematic diagram of a non-reversible

recombination reaction that is intended to model the case of the *Azoarcus* ribozyme. Two distinct RNA strands, X_1 and X_2, which we will call building blocks, associate together by formation of RNA secondary structure to form a complex, *B*. This brings the ends of the strands into close proximity. Recombination then occurs between the end of one strand and the penultimate nucleotide of the other strand, resulting in a longer strand and a single nucleotide. The longer strand is denoted *C* for 'catalyst'. It is a recombinase that specifically catalyzes the recombination of X_1 and X_2. In other words, the formation of *C* is autocatalytic. In the experiment, there are four building block strands and three recombination reactions needed to create the catalyst, but in the following model we will consider only two building blocks, as this is sufficient to illustrate the point.

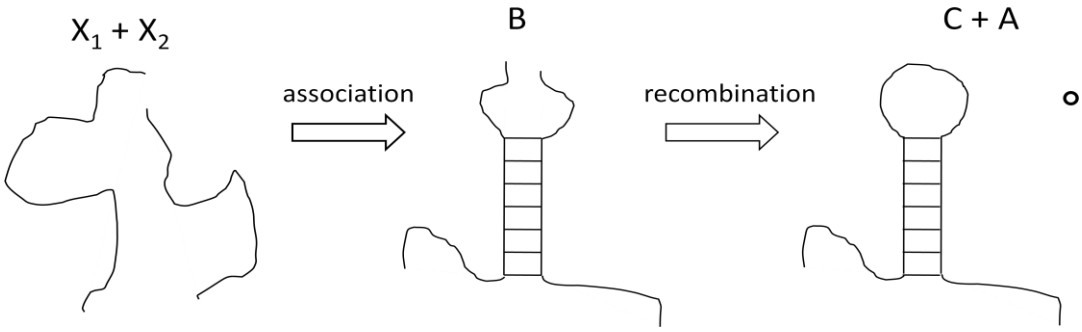

Figure 3.9: Schematic diagram of association between two RNA strands followed by a recombination reaction giving rise to a longer strand and a single nucleotide.

We want to know whether this autocatalytic reaction can emerge from within our random polymerization system considered above. Suppose that both building blocks are of length *m*, and the catalyst is of length 2*m*-1. Suppose that a

fraction *x* of random sequences of length *m* is suitable to be each of the building blocks. The rate of formation of each building block by random polymerization is therefore *x* times the rate of synthesis of chains of length *m*. It follows that a fraction x^2 of sequences of length 2*m*-1 are catalysts, and the rate of synthesis of the catalyst by random polymerization is x^2 times the rate of synthesis of chains of length 2*m*-1. Initially, we ignore the complex formation, and treat the formation of *C* as a single reversible reaction:

$$X_1 + X_2 \underset{\rho}{\overset{\rho}{\rightleftarrows}} C + A \tag{3.22}$$

Adding this to our random polymerization system gives

$$\frac{dX}{dt} = rA(xA_{m-1} - X) - uX - \rho(X^2 - AC) \tag{3.23}$$

$$\frac{dC}{dt} = rA(x^2A_{2m-2} - C) - uC + \rho(X^2 - AC) \tag{3.24}$$

Both X_1 and X_2 have the same concentration, denoted *X*, so we only need one equation for these two. We suppose that the chain length distribution is unaffected by the small fraction *x* that form the building blocks, so the monomer and polymer concentrations are still given by Equations 3.7 and 3.11. From 3.23 and 3.24, it can be seen that if the recombination rate is zero, *X* and *C* tend to steady state concentrations X_0 and C_0, given by

$$X_0 = \frac{rAxA_{m-1}}{rA + u} = xA_m \tag{3.25}$$

$$C_0 = \frac{rAx^2A_{2m-2}}{rA + u} = x^2A_{2m-1} \tag{3.26}$$

In this state, $X^2 = AC$, and the presence of the reversible recombination reaction does not make any difference to the frequency of C.

In order for the recombination reaction to be a useful way to generate the longer sequence, it is necessary to make it non-reversible, which can be done by adding the complex formation step into the model.

$$X_1 + X_2 \xrightarrow{v} B \underset{\rho}{\overset{\alpha\rho}{\rightleftarrows}} C + A \tag{3.27}$$

The rate constant for formation of the complex is v and this is taken to be irreversible because the secondary structure is strong, *i.e.* the backward rate is assumed to be negligible with respect to u, so that the complex is lost from the system before it disassociates. In the complex, the two ends that undergo recombination are close together. The forward recombination reaction is essentially a monomolecular reaction, whereas the reverse reaction is bimolecular. Although the reaction itself is reversible, the rates are no longer equal. Let α be the effective concentration of chain ends close to the bond at which recombination occurs, so the forward recombination rate is $\rho\alpha B$. It is possible that $\alpha > A$, in which case recombination can also be biased towards the creation of longer chains. The dynamical equations become

$$\frac{dX}{dt} = rA(xA_{m-1} - X) - uX - vX^2 \tag{3.28}$$

$$\frac{dB}{dt} = vX^2 - rAB - uB - \rho(\alpha B - AC) \tag{3.29}$$

$$\frac{dC}{dt} = rA(x^2A_{2m-2} - C) - uC + \rho(\alpha B - AC) \tag{3.30}$$

Here it is assumed that the complex escapes from the system at the same rate *u* as the polymers. In the steady state, Equation 3.28 can be written as

$$\omega X^2 + X - X_0 = 0 \tag{3.31}$$

where $\omega = v/(rA+u)$. Hence,

$$X = \frac{-1 + \sqrt{1 + 4\omega X_0}}{2\omega} \tag{3.32}$$

By summing Equation 3.28-3.30 in the steady state, we obtain

$$X + B + C = X_0 + C_0 \tag{3.33}$$

The simplest way to introduce autocatalytic feedback into the model is to suppose that the recombination rate is proportional to the catalyst concentration: $\rho = kC$. It would also be possible to add a small spontaneous rate ρ_0 of recombination in absence of *C*, in the same way as we included s_0 and r_0 in previous sections of this chapter. However, *C* is already formed by random polymerization at a small rate, and this is sufficient to get the autocatalytic system started; therefore the addition of ρ_0 is not essential and we will leave it out. Substituting $\rho = kC$ into Equation 3.30 and using 3.33 to eliminate *B*, we obtain the following quadratic equation for *C*:

$$k(\alpha + A)C^2 + C\big(rA + u - k\alpha(X_0 + C_0 - X)\big) - rAx^2A_{2m-2} = 0 \tag{3.34}$$

This has a single positive root for *C*. Thus *X*, *B* and *C* are all obtained explicitly. These are shown as a function of *k* in Figure 3.10. The parameters for the random polymerization reaction system are $F_0 = 10$, $s = 10$, $r = 5$, and $u = 1$, in which case $A = 0.587$ and $z = 0.746$. We also chose building block length $m = 25$, and a

fraction $x = 0.01$. The stationary concentrations are $X_0 = 5.1 \times 10^{-6}$ and $C_0 = 4.5 \times 10^{-11}$. The concentrations and reaction rates are in arbitrary units, and their values are unimportant. All that matters is that, as the catalyst is much longer than the building blocks, C_0 is very much less than X_0. The limits C_0 and X_0 are shown as dashed lines in Figure 3.10.

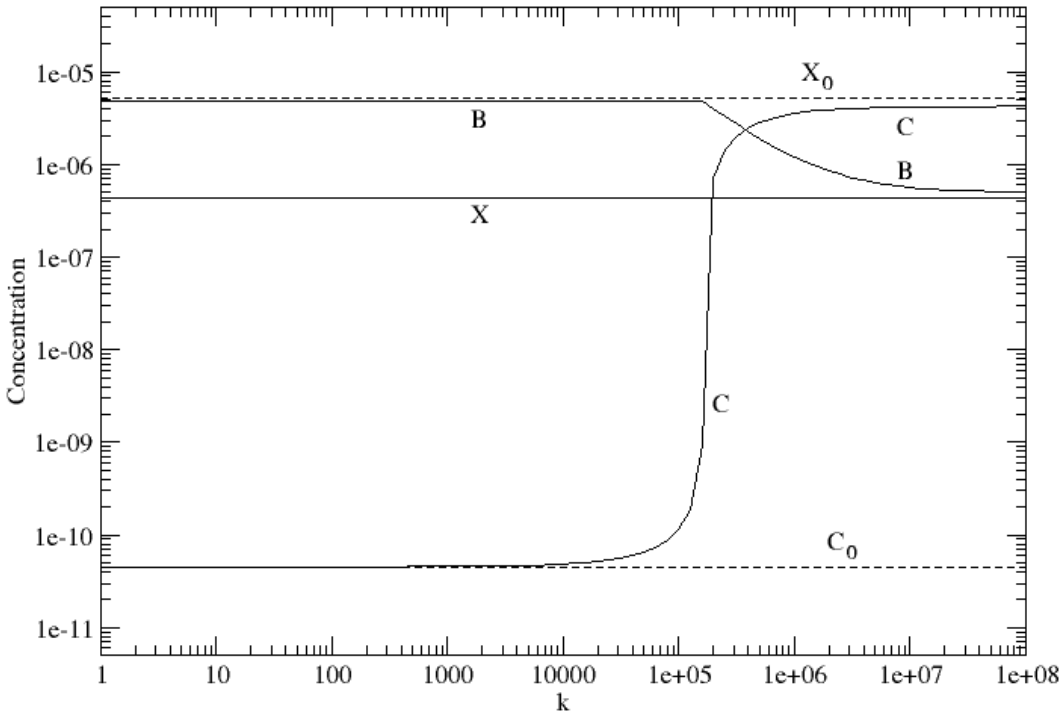

Figure 3.10: The non-reversible recombinase model in the case where only C is a catalyst. Parameters are $F_0 = 10$, $s = 10$, $r = 5$, $u = 1$, $v = 10^8$, $x = 0.01$, $\alpha = 5$ and $m = 25$.

We now consider formation of the complex B. If X is close to X_0, the ratio of the rates of formation and removal of B is ωX_0. From Equation 3.32, if ωX_0 is small, $X \approx X_0$. In order for complex formation to make a difference, v must be large enough so that $\omega X_0 >> 1$. This means that the complex has time to form

before the building blocks escape the system or are destroyed by further random polymerization. In this example, we chose $v = 10^8$, which gives $\omega X_0 = 131$. For these parameters, X falls substantially below X_0 because most of the building blocks are converted to the complex. Note that X depends on v, but it does not depend on the recombination reaction; therefore X is a horizontal line on Figure 3.10. If k is small, then the recombination reaction is negligible. Thus B is close to the limiting value of X_0 and C is close to C_0. If k is sufficiently large, the recombination reaction becomes significant. Most of the complex is converted to C, so C approaches X_0 and B decreases. It can be seen that there is a rather rapid switch between the regime where $C \approx C_0$ and the regime where $C \approx X_0$. The value of k required for recombination to switch between regimes is roughly where the formation rate of the catalyst, $\rho\alpha B$, is equal to the removal rate, $(rA+u)C$. This gives $\rho\alpha B \approx kC\alpha X_0 \approx (rA+u)C$, or $k \approx (rA+u)/\alpha X_0$. In this example $\alpha = 5$, and the predicted value of the switch is $k \approx 1.5 \times 10^5$, which is close to what is seen from the exact solution in the graph. Once again, the numbers are arbitrary, but the point is that the required k value is of order $1/X_0$. Thus if the building block concentration is low, then only a very efficient catalyst with very high k will have a noticeable effect.

Let us summarize the argument of this section so far. If the complex formation step is included in the reaction system, the recombination reaction is no longer exactly reversible. In this case it is possible for a recombinase C to arise that catalyzes its own formation. The high C regime in Figure 3.10 could be

classed as a living state because it is autocatalytic. The rate of formation of the catalyst in this regime is almost entirely determined by the catalyzed reaction and not by the spontaneous rate of random polymerization. However, if the building blocks are moderately large, the concentration of the building blocks produced by random polymerization, X_0, is fairly low. For this reason, this system has two important limitations. Firstly, the catalyst does not make more of its own building blocks. The best that it can do is to convert all the existing supply of building blocks to more catalyst. Thus C can never rise higher than X_0. Secondly, only catalysts with very high k can reach the autocatalytic regime if X_0 is low. Such catalysts are presumably rare.

We will now introduce one further feature that is also a property of the *Azoarcus* experimental system. It was found that the complex B was also a catalyst of roughly equal efficiency to the fully-formed long strand C (Hayden *et al.* 2008). This is presumably because the structure of B is almost the same as that of C except for the hairpin loop formed where the building blocks are connected. Therefore, we will consider the case where the recombination rate is proportional to the sum of these concentrations: $\rho = k(B+C)$. Using Equation 3.33, this means that $\rho = k(X_0 + C_0 - X)$, and X is already known from Equation 3.32. Substituting this value of ρ into Equation 3.30 gives the steady state solution for C:

$$C = \frac{rA + u + (\alpha + A)k(X_0 + C_0 - X)}{rAx^2A_{2m-2} + \alpha k(X_0 + C_0 - X)^2} \tag{3.35}$$

Figure 3.11 shows the concentrations of *X*, *B* and *C* as a function of *k* in the case where both *B* and *C* are catalysts. This differs from Figure 3.10 in that *C* can be several orders of magnitude higher than C_0 even when *k* is low because a substantial amount of *C* is formed by *B* acting as a catalyst. When *k* is large, most of *B* is converted to *C*. The situation is then similar to Figure 3.10, and *C* approaches X_0. Thus if *B* is also a catalyst, this gets round the limitation that the system only works with very high *k*, but it does not avoid the limitation that the maximum concentration of catalyst is equal to the building block concentration.

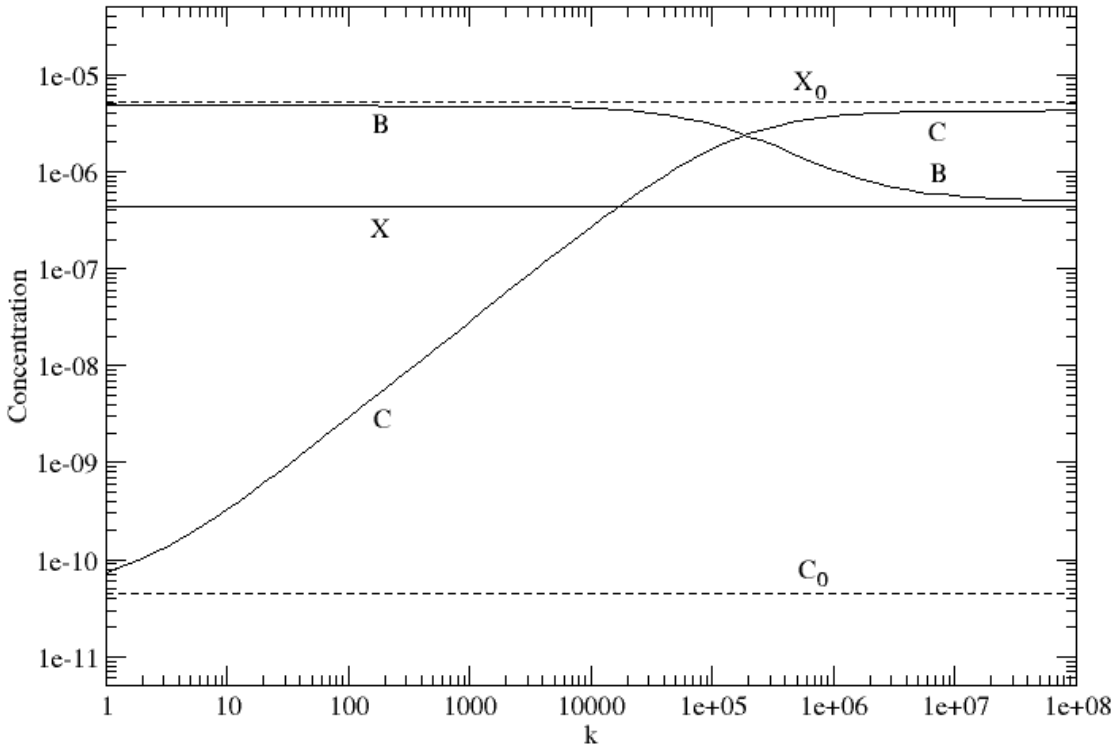

Figure 3.11: The non-reversible recombinase model in the case where both *B* and *C* are catalysts. Parameters are as in Figure 3.10.

3.7 Discussion

A key feature of our model in the case when feedback occurs in either polymerization or nucleotide synthesis is the S-shaped curve of the long polymer concentration as a function of the reaction rate (shown in Figures 3.2 and 3.5). From this curve it is clear that the phase diagram has regions where there is only one stable solution, and regions where there are two stable solutions separated by an unstable solution. The S-shaped curve and the two kinds of stable state seem to be rather general features, as they are found to occur in our original model in previous chapter, in two cases in this chapter, and in Dyson's model. This suggests that they may also apply in real-world chemical systems that are evidently much more complicated than any of the models that we can study theoretically. This is important because the idea of the origin of life as a stochastic transition follows directly from the S-shaped curve. The intermediate unstable state acts as a barrier between the dead and the living states. We have shown by stochastic simulations in chapter 2 that concentration fluctuations can drive the system across the barrier and lead to an origin of life. Although we have not carried out stochastic simulations with the case of the nucleotide synthase ribozymes discussed here, the structure of these models is the same, so we expect that the same phenomena will occur in the stochastic dynamics.

Although the relevance of recombination reactions to ribozyme synthesis had been proposed previously, our research makes it clear that recombination is only a useful feature if it is not fully reversible and if it is biased towards

synthesis of longer chains. In the case we considered, the reaction occurred after the association of the strands to form a complex. This brought the strands into close proximity and increased the forward reaction rate relative to the backward rate. The complex formation step itself was also assumed to be non-reversible. The free energy of RNA structure formation is large compared to the thermal energy kT; therefore the rate of disassociation of the strands is likely to be very slow. For this reason, we did not include the possibility that the strands might disassociate without undergoing recombination (*i.e.* $B \rightarrow X_1 + X_2$). Addition of a small rate of disassociation would not qualitatively change the conclusions. In the case considered, secondary structure formed before recombination, but it is also possible that secondary structure formed after recombination could create a bias towards the formation of longer strands. If a strand folds into a stable secondary structure, a substantial fraction of the nucleotides are in double stranded conformations that are less likely to interact with other strands than the single stranded regions. Shorter strands have lower folding free energies and are more likely to be in unfolded configurations than longer strands; therefore they should potentially be more likely to recombine. If a long strand forms and subsequently folds to a stable structure, this might slow the reverse reaction. Secondary structure formation is also relevant in the ligase system of Lincoln and Joyce (2009). In this case the building blocks interact with the catalyst strand rather than with each other. This is useful in that it brings the building blocks close together, however it means that after the reaction, the newly synthesized strand is strongly

associated with the catalyst strand. For further catalytic steps it is necessary to separate these strands, which might be difficult. In the recombinase case, this problem does not arise because base pairing between the catalyst and the building blocks occurs only at the three-nucleotide guide sequence, rather than along the whole length of the catalyst.

An important feature of the *Azoarcus* recombinase system (Hayden *et al.* 2008) is that the trans complex is a catalyst even if the building block strands are not linked covalently. This makes it much more likely that the ribozyme will arise in a random polymerization system, because it is only necessary to synthesize strands of the length of the building blocks rather than the length of the full ribozyme. This property could also be true of any other kind of ribozyme. For example, if there were a trans complex that could act as a polymerase, this would make the origin of an autocatalytic state controlled by the polymerase much easier. In this case it would not matter very much whether there was an additional recombinase or ligase that linked the building blocks of the polymerase covalently. The system could continue to function with only trans complexes as catalysts.

Chapter 4

Investigation of Spatially Localized Stochastic Transitions

4.1 Introduction

In the previous chapters, it has been argued that origin of life is the emergence of autocatalytic set of biopolymers from background reactions through stochastic fluctuations. In chapter 2, it was shown that for a well mixed finite system with a given concentration of reactant, the larger the system, the smaller the fluctuation will be, which will make it harder for a stochastic transition to occur, even if there are long polymers in the system. As shown as the right branch of the U-shaped transition time as function of system size curve in Figure 2.7 from Chapter 2, with increasing system size, the transition time goes to infinity very fast. In reality, molecules have finite diffusion speed. For a given diffusion coefficient, when the system size is smaller than the diffusion length, the system is still well mixed. And the stochastic fluctuation will decrease with an increasing system size just like a homogenous system. Eventually, diffusion can no longer maintain the system to be well mixed if its size keeps increasing. Hence, the well mixed assumption would inevitably break down when a system becomes sufficiently large.

Several experimental studies have illustrated the importance of spatial localization for RNA synthesis. It has been demonstrated that nucleotides can be absorbed on to mineral surface and condense into polynucleotide with help from proper type of mineral (Ferris 1996; Kawamura 1999; Ertem 2004). It has also been shown that vesicles can enrich nucleotide inside themselves to make the polymerization process more energetically favourable (Rajamani 2008). Hence it is conceivable that emergence of autocatalytic polymer system may occur locally on a rock surface or inside a vesicle.

Spatial localization is also an important part of several theoretical models. Ma et al.(2007, 2010) have shown that an autocatalytic polymer system can emerge from a pool of nucleotides with random polymerization using a stochastic simulation on a 2D square lattice. For an established self-replicating polymer system, it has been shown that limited diffusion may help localize catalysts together while prevent the rapid spreading of parasites that would tend to overrun the system if it were well mixed (Boerlijst et al. 1991; Boerlijst et al. 1995; Szabo et al. 2002). Takeuchi et al (2009) compared effect of compartments and limited diffusion for self-replicating polymer systems, showing that both compartments and limited diffusion can mitigate destructive effect of parasites on the system. However, they are different in long term evolutionary dynamics. When confined in compartments, it may be advantageous for parasites to evolve to be more harmful or less harmful depending on the frequency of compartment division.

While for limited diffusion case, it is always advantageous for parasite evolving towards high affinity with replicase to trail the travelling waves of replicase.

Inspired by these studies, an investigation of that way that a stochastic transition from a non-living to a living state can occur in a finite system with limited diffusion has been carried out in this chapter.

4.2 A Generic Phase Diagram for Replicating Molecules

Essential features of the RNA polymerization models that we studied in previous chapters are that the phase diagram contains a region where both living and dead states are stable for the same parameters and that a transition from the dead to the living state can occur due to stochastic fluctuations. In this chapter, we will begin by considering a simplified generic model of replicators that has these same essential features. This will allow us to investigate the effect of the spatial distribution of replicators on the stochastic transition that leads to the origin of life.

We consider a single type of replicating molecule whose concentration is ϕ. Replicators can appear at rate s, representing a slow rate of spontaneous synthesis by random polymerization (as in the more detailed chemical reaction systems for RNA that we considered previously). This process is independent of the replicator concentration. Existing replicators may be copied with a rate constant r, representing a process of non-living template-directed synthesis. This

process is proportional to the current replication concentration, ϕ. Replicators may also act as polymerases that catalyze replication by using another replicator as a template. The rate constant for this catalytic process is k and this process is proportional to the square of the current concentration, ϕ^2. The increase in replicator concentration is limited by finite resources. The simplest way to model this is to assume a finite carrying capacity of the system, corresponding to a concentration $\phi = 1$, and to multiply all the growth rates by a factor $(1-\phi)$. Finally, replicators die (or are destroyed or removed from the system) at a rate u. The deterministic dynamical equation for ϕ is:

$$\frac{d\phi}{dt} = \left(s + r\phi + k\phi^2\right)(1-\phi) - u\phi \qquad (4.1)$$

In many models of population dynamics in evolution and ecology, the linear growth term, $r\phi$, is natural, and the spontaneous term, s, and nonlinear term, $k\phi^2$, are not considered. However, when considering the origin of life, the spontaneous term is essential for generation of the initial replicators, and the nonlinear term is essential in order to give the possibility of two stable states. The linear term is less important; therefore we will first consider the case where $r = 0$. The stationary states are the roots of this cubic equation. If s is small and k is fairly large, there are two stable states, ϕ_1 and ϕ_2, separated by an unstable state ϕ_3. The lower stable state is a dead state, controlled by the balance between spontaneous generation and death: $\phi_1 \sim s/u$. The upper stable state is a living state controlled by the catalytic term k. If k is large, the concentration will approach the

carrying capacity, $\phi_2 \sim 1$. It is easy to obtain phase diagram for existence of dead and living state as in Figure 4.1. If k is too small, only the dead state exists, and if k is too large only the living state exists. If the linear growth term r, is non-zero, the positions of the phase boundaries move, but shape of the diagram is qualitatively unchanged. The phase diagram looks surprisingly similar to phase diagram in previous chapters (see Figs 2.4, 3.4 and 3.6). We therefore argue that this kind of phase diagram is a generic feature of replicator models for the origin of life, and that the single equation (4.1) is the simplest possible dynamical equation that has this phase diagram.

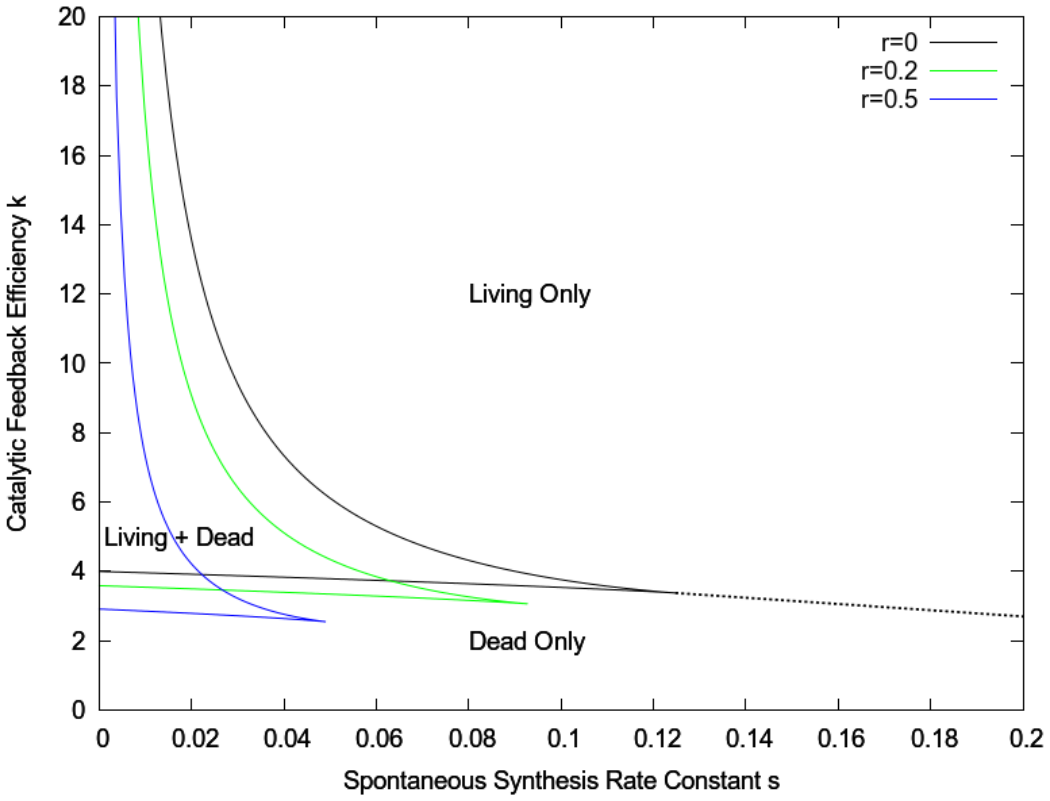

Figure 4.1: Phase diagram for existence of dead and living states as function of catalytic feedback efficiency k and spontaneous synthesis rate constant s with u=1

If we were interested in the stochastic dynamics of replicators in a finite well-mixed system, it would be possible to do stochastic simulations of Equation 4.1 using the Gillespie algorithm, as we did for the RNA models in Section 2.5. However, our purpose in introducing this simplified equation was because we wished to include spatial concentration fluctuations. Therefore we will proceed to define a spatial lattice model, which we call the Two's Company Model, that is a spatial version of Equation 4.1 and that allows spatial concentration fluctuations to be model in a very simple way.

4.3 The Two's Company Model

We consider a 2D square lattice of L x L sites. The number of molecules on any one site may be n = 0, 1, 2 or 3 only. The carrying capacity of the whole lattice is therefore $3L^2$. If there are N molecules on the lattice, the mean concentration relative to the carrying capacity is $\phi = N/(3L^2)$. There are 3-n vacancies on a site with n molecules. Vacancies are treated as resources, and the rates of spontaneous, linear, and replicative growth are all proportional to the number of vacancies. The rate of adding a molecule by the spontaneous reaction is defined as s times the number of resources, *i.e.* s(3-n). The rate of adding a molecule by the linear growth process is defined as r/2 times the number of molecules times the number of resources, *i.e.* $rn(3-n)/2$. This is equal to r when n = 1 or 2, and zero otherwise. The rate of catalytic replication is defined as $k/2$ times the number of ways of picking a replicator-template pair times the number

of resources, *i.e.* $n(n-1)(3-n)k/2$. This is k when n = 2 and zero otherwise. The replication process in the model can only occur when n = 2, "two's company, three's a crowd"; hence the name 'Two's Company'.

The stochastic dynamics of the Two's Company Model are simulated using the Gillespie algorithm. Three types of elementary reaction are possible: birth of one molecule on one site, death of one molecule on one site, and hopping of one molecule to a neighbouring site. Combining the three birth processes above, we obtain a_n, the total birth rate of sequences on a site with n sequences:

$$\begin{aligned} a_0 &= 3s \\ a_1 &= 2s + r \\ a_2 &= s + r + k \end{aligned} \qquad (4.2)$$

The death rate of a molecule on a site with n molecules is un (i.e. u per molecule). Hopping of molecules between sites is implemented as follows. Each molecule attempts to hop at rate h. A destination site is chosen for the molecule. In the case of local hopping rules, the destination is chosen at random from the 8 neighbouring sites of the original site. In the case of global hopping rules, the destination site is chosen at random from all the other sites on the lattice. The molecule hops successfully to the destination site if it finds a vacancy there, *i.e.* the hop is successful with probability 1-n/3, and unsuccessful with probability n/3, where n is the number of molecules already on the destination site. If the hop is unsuccessful, the molecule remains on its original site.

The local hopping rules simulate local molecular diffusion, which is an important part of this model. The global hopping rules are intended as a

comparison that helps to illustrate the importance of local hopping. It can be seen that the probabilities of birth and death of molecules depend only on the number of molecules on the site in question, whereas the probability of hopping of a molecule depends on the number of molecules on surrounding sites. The introduction of local hopping rules means that correlations exist between the numbers of molecules on neighbouring sites. However, if h is sufficiently large, the system reaches a well-mixed limit where molecules are randomly positioned over the whole lattice and there is no remaining correlation between neighbouring sites. In the case of global hopping, there is no correlation between sites, even when h is small. In a subsequent section we will discuss the mean field approximation, which is a way of obtaining an approximate solution to a lattice model by neglecting correlations between sites. The mean field method is exact for the global hopping dynamics but it is only an approximation for the model with local hopping dynamics. When h is very large, both global and local hopping models reach the same well-mixed limit. Before proceeding to the simulations, we will demonstrate that the well mixed limit of the lattice model corresponds to the generic replicator model in Equation 4.1

Let P_n be the fraction of sites that have n molecules. The rate of change of N due to birth and death processes is

$$\frac{dN}{dt} = L^2\left(a_0 P_0 + (a_1 - u)P_1 + (a_2 - 2u)P_2 - 3uP_3\right) \tag{4.3}$$

Hence

$$\frac{d\phi}{dt} = \frac{1}{3}\left(a_0 P_0 + (a_1 - u)P_1 + (a_2 - 2u)P_2 - 3uP_3\right). \quad (4.4)$$

Note that these equations do not depend on the hopping rate because the hopping process does not change the total number of molecules. However, the P_n probabilities do depend on h. If both N and L are large and h is large enough to be in the well-mixed limit, where molecules are randomly distributed between lattice sites, P_n has a binomial distribution:

$$P_n = \phi^n (1-\phi)^{3-n} \frac{3!}{n!(3-n)!} \quad (4.5)$$

Substitution of these probabilities into Equation 4.4 gives Equation 4.1. Thus, the lattice model reduces to the desired continuum model if there is rapid mixing of molecules.

4.4 Results for the Two's Company Model

Since a lot of chemical details of prebiotic environment, such as concentrations and reaction rate constants, are unknown, all parameters will be scaled with respect to escape rate u, which is set to be 1. The other parameters are set to be s=0.02, r=0, k=9, h=24, which is expected to be in the region of the phase diagram where both living and dead states exist (see Fig. 4.1). The concentration in the dead state should be close to the stable solution ϕ_1 of Equation 4.1. In order to initiate the stochastic simulation in the dead state, each

lattice site is seeded with molecular numbers sampled from a binomial distribution with average as the dead state concentration ϕ_I .

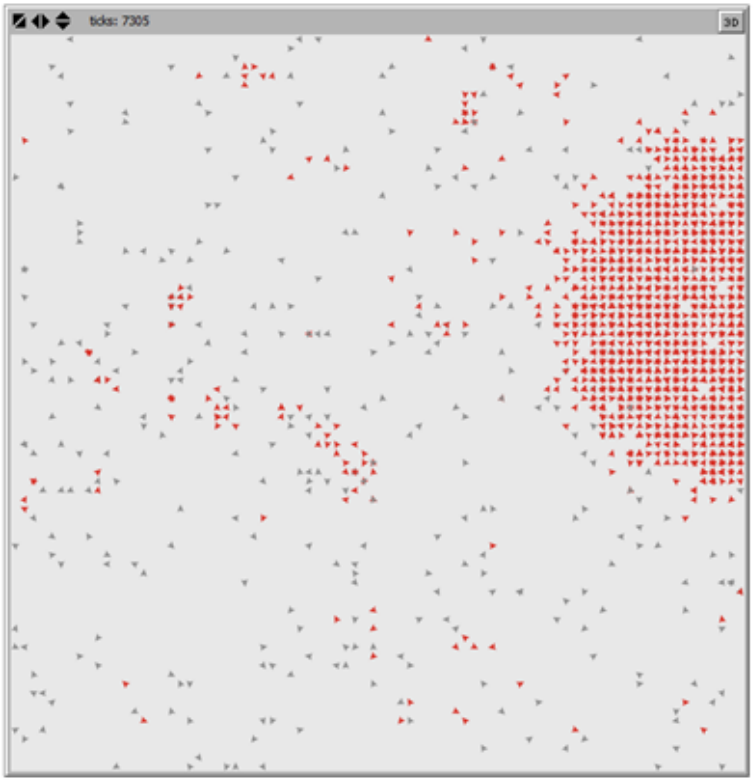

Figure 4.2: Snapshot of a system shortly after the transition to life. The non-living state is characterized by a low density of replicators created by spontaneous synthesis (coloured grey). The living state is a dense patch of replicators that have been synthesized catalytically (red). Once it is big enough to be stable, the living patch spreads deterministically across the lattice.

The spatial stochastic algorithm as described above was used to follow the dynamics of the system until a stochastic transition occurred to the living state. A snapshot of a system shortly after the transition to life is shown in Figure 4.2. It is shown that in dead state most molecules are synthesized spontaneously (colored grey), while in living state most molecules are synthesized by the catalyzed

replication (colored red). With limited diffusion, transition to living state happens locally first and then spread out to the whole system. The concentration in the living state should be close to the solution ϕ_2 of Equation 4.1. The simulations were stopped when the global concentration became close to ϕ_2. In order to insure that the system was stable in the living state, ϕ was averaged over a sliding time interval of width 20, which is 20 times of average time before molecule escapes from the system. The simulation was stopped when the sliding average density reached 90% of ϕ_2. At this point, the time interval from start to stop is taken as the system transition time of one trial. The average system transition time, $T_{sys,}$ was obtained from 1000 trials.

When the local hopping rule is used, it is expected that the transition will happen at one place then spread out to the whole system, hence we may write $T_{sys} = T_{reg} + T_{spread}$, where T_{reg} is the time until a local transition occurs in any one region, and T_{spread} is the time for the living state to spread from one region across the rest of the lattice. To investigate these two aspects, it is necessary to record the regional transition time. For this reason, the system was divided into multiple regions of size 10 x 10 lattice sites. The concentration was calculated within each region and averaged over a time window in the same way as the global concentration. T_{reg} was defined as the point at which the sliding window concentration of any one region reaches 90% of ϕ_2.

Figure 4.3 shows the average T_{sys} as h is varied with a fixed system size. The main figure shows a small lattice with $L = 10$. For large h the measured times

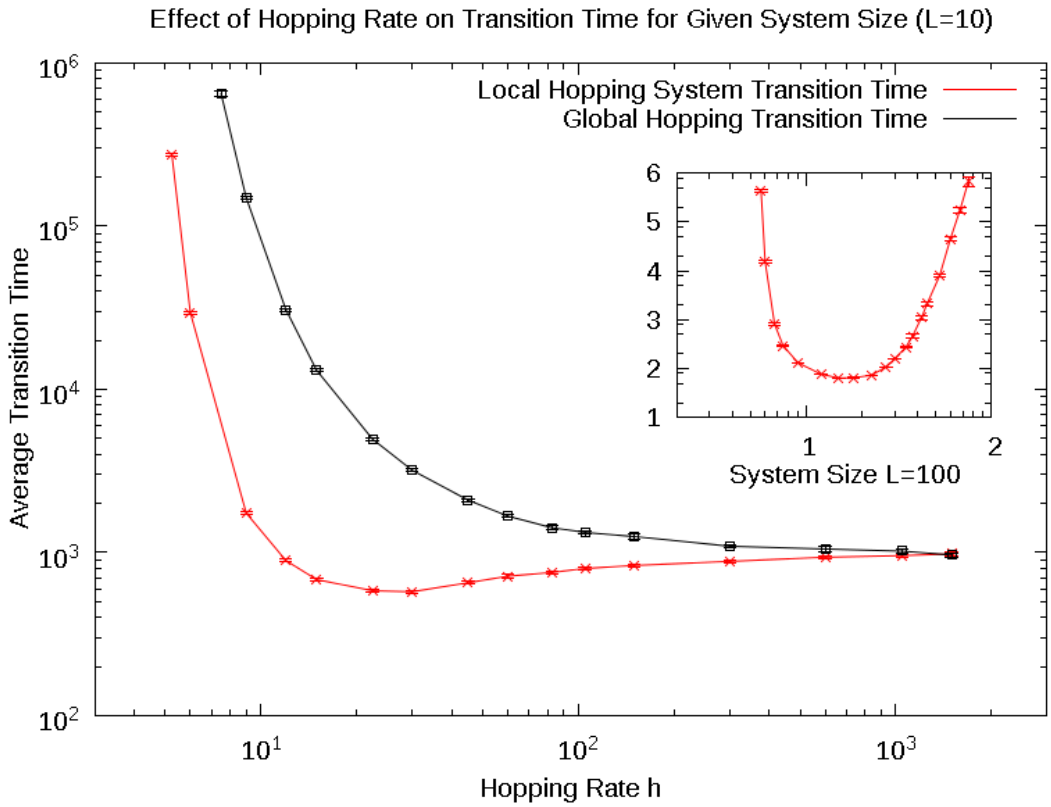

Figure 4.3: Effect of hopping rate on transition time for fixed system size (L=10 for the main plot, L=100 for the inset) with other parameters set as: s=0.02, r=0, k=9

for local and global hopping converge, showing that the system is well mixed. For smaller h, the transition time with local hopping is always shorter than that with global hopping. This shows that the local concentration fluctuations that arise in the local hopping model make the transition much easier. It can be seen that if h is very small, the transition time becomes very long, both for local and global hopping. It should be remembered that the spontaneous generation rate s is very small, so the concentration of molecules in the dead state is very small. For the catalytic process to occur, it requires two molecules on the same site. If h is too

small, molecules do not encounter one another frequently. Furthermore, if molecules do encounter one another and a replication occurs, there will now be three molecules on one site, which blocks further growth. It is necessary for one of these molecules to hop away before a second replication can occur; hence, h should not be too small. It can be seen that, for the local hopping rules, there is an optimum diffusion rate at which the transition is fastest. This effect is not very strong in the small lattice (L = 10), but is very pronounced in the larger lattice (L = 100) shown in the inset to Fig. 4.3. The transition time decreases by several orders of magnitude in the middle of the range of h. It is not possible to show the transition time for the global hopping case for the larger lattice size because it is too long to measure in the simulation with these parameters. In summary, Fig. 4.3 shows that local diffusion is essential in order to allow the transition to life to occur at a reasonable rate in large systems, and when diffusion is local, there is an optimal intermediate rate of diffusion.

Figure 4.4 shows the variation of transition time with system size when the hopping rate is kept fixed. For the global hopping case (black curve) it is only possible to do these simulations for fairly small lattice sizes, because the transition time increases very rapidly with L. For the local hopping case, it is possible to carry out simulations over a much wider range of L, and it can be seen that the transition time actually decreases with L, if L is sufficiently large. To understand this, it is useful to calculate how far a molecule diffuses in its lifetime. When the death rate is u and the hopping rate is h, any one molecule should have hopped h/u

times on average in its lifetime. The typical distance, x, moved in this time by diffusion is $x^2 \sim l^2 h/u$. As both the lattice size l and the death rate are set to 1, the diffusion length is $x \sim h^{1/2}$. This is approximate because some hops are diagonal (distance $\sqrt{2}l$) and not all hops are successful, depending on the density. Nevertheless the scaling with $h^{1/2}$ should apply.

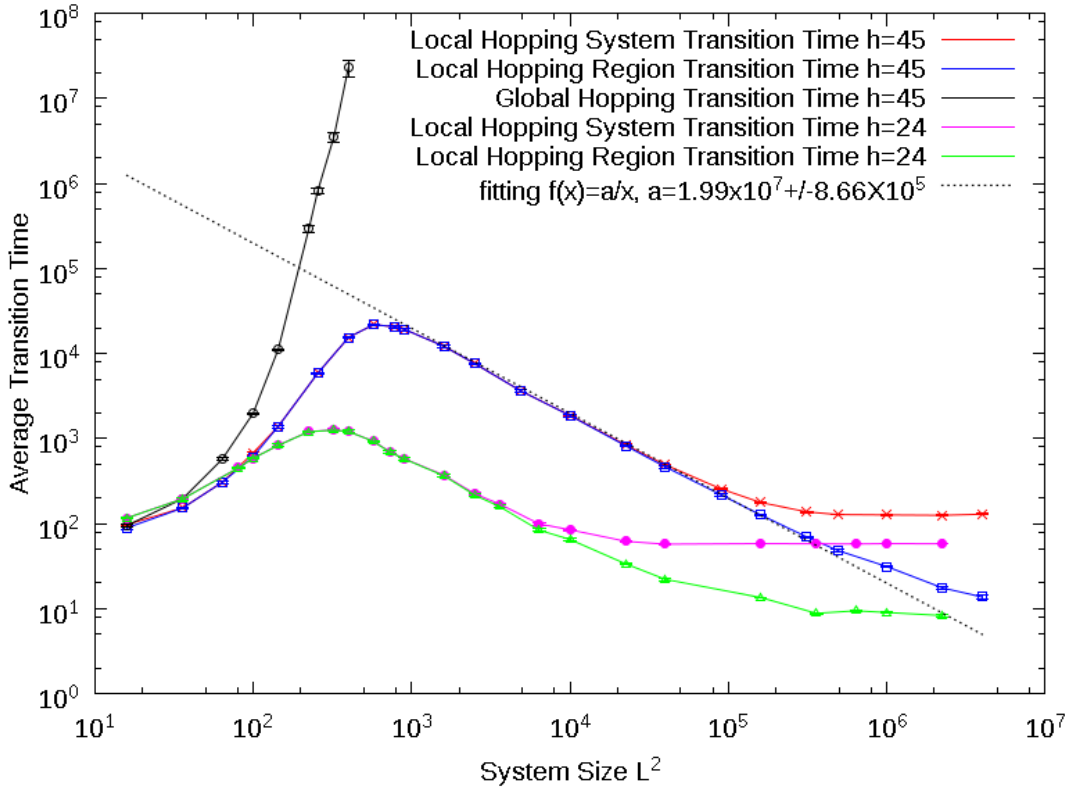

Figure 4.4: Average transition time from dead state to living state as function of system size with parameters set as: s=0.02, r=0, k=9, u=1

As shown in left part of Figure 4.4, when system is small (L<x), the system is more or less well mixed. Hence the transition will happen globally across the whole system at the same time. When system size is larger than diffusion length (L>x), the system is no longer homogenous. The transition will

happen at a local region first, then it will spread out to the whole system. The number of independent local regions should be L^2/x^2. The average time taken for the transition to occur in any one of these regions should vary inversely with the number of regions, *i.e.* $T_{reg} \sim 1/L^2$. If the system is not extremely large, spreading time of living state across the whole system, T_{spread} is still small compared with the time taken for the transition to occur, T_{reg}. In this case the time taken for the whole system to go through the transition is close to T_{reg}. It can be seen that there is an intermediate range of L in Figure 4.4, where T_{reg} and T_{sys} are very close to one another and where both scale as $1/L^2$, as expected from this argument. Comparison of the results with h = 24 and h = 45 shows that when diffusion length is smaller, the transition from homogenous system to heterogeneous system happens for a smaller system size.

If the system size is extremely large, there comes a point where T_{spread} is comparable to T_{reg}, and the curves for T_{sys} and T_{reg} separate in Fig. 4.4. At this point it is possible for the transition to life to occur in another region independently before the living state from the first transition has spread across the lattice. Beyond this point, T_{reg} continues to decrease, but T_{sys} reaches a constant value, which is what we expect if there are multiple origins happening in the system.

4.5 Mean Field Approximation

A useful way to understand the effects of the limited diffusion rate in this model is to calculate the mean field solution for the model. In section 4.2 we

considered the probabilities P_n that there are n molecules on a site. These probabilities tend to the binomial limit when h is large. In this section we consider more carefully what happens for smaller h. We now consider the hopping process. Let there be n molecules on the site and m molecules on the neighbouring site with which the exchange is made. Let q_{nm} be the conditional probability that there are m particles on the neighbour, given that there are n on the first site. Thus the rate that n increases by 1 due to a molecule arriving from a neighbouring site is

$$p_n^+ = h(q_{n1} + 2q_{n2} + 3q_{n3})(1 - \frac{n}{3}) = 3(1 - \frac{n}{3})h\phi_n \quad , \tag{4.6}$$

where $\phi_n = (q_{n1} + 2q_{n2} + 3q_{n3})/3$ is the mean density on neighbours of sites that have n particles. Note that there are 8 neighbours from which a molecule could come, but only 1/8 of the hops from any one neighbour move to the site in question. Therefore these two factors of 8 cancel out.

The rate at which n decreases by 1 due to a molecule leaving the site is

$$p_n^- = hn((1 - \frac{1}{3})q_{n1} + (1 - \frac{2}{3})q_{n2} + (1-1)q_{n3}) = hn(1 - \phi_n)\,, \tag{4.7}$$

We may now write a set of equations for the rates of change of P_n that include birth, death and hopping.

$$\begin{aligned}
\frac{dP_0}{dt} &= -a_0P_0 + uP_1 + p_1^-P_1 - p_0^+P_0 \\
\frac{dP_1}{dt} &= a_0P_0 - a_1P_1 + u(2P_2 - P_1) + p_2^-P_2 - p_1^+P_1 - p_1^-P_1 + p_0^+P_0 \\
\frac{dP_2}{dt} &= a_1P_1 - a_2P_2 + u(3P_3 - 2P_2) + p_3^-P_3 - p_2^+P_2 - p_2^-P_2 + p_1^+P_1
\end{aligned} \tag{4.8}$$

$$\frac{dP_3}{dt} = a_2 P_2 - 3uP_3 - p_3^- P_3 + p_2^+ P_2$$

As it stands, this set of equations is not closed, because the hopping rates depend on the conditional probabilities q_{nm}, which are affected by correlations in the numbers of molecules on neighbouring sites. A standard way of approximating the solution to lattice models is to make a mean field approximation which ignores these correlations. In this case we assume that $q_{nm} = P_m$, in which case:

$$\phi_n = \phi = \frac{1}{3}P_1 + \frac{2}{3}P_2 + P_3 \qquad (4.9)$$

Substituting Equations 4.2 and 4.9 into 4.8, we get the following equations

$$\begin{aligned}
\frac{dP_0}{dt} &= -3sP_0 + uP_1 + h((1-\phi)P_1 - 3\phi P_0) \\
\frac{dP_1}{dt} &= 3sP_0 - (2s+r)P_1 + u(2P_2 - P_1) + h(2(1-\phi)P_2 - 2\phi P_1 - (1-\phi)P_1 + 3\phi P_0) \qquad (4.10) \\
\frac{dP_2}{dt} &= (2s+r)P_1 - (s+r+k)P_2 + u(3P_3 - 2P_2) + h(3(1-\phi)P_3 - \phi P_2 - 2(1-\phi)P_2 + 2\phi P_1) \\
\frac{dP_3}{dt} &= (s+r+k)P_2 - 3uP_3 + h(-3(1-\phi)P_3 + \phi P_2)
\end{aligned}$$

We expect that the mean field approximation will be fairly good for the local hopping model if h is large, because correlations will disappear in this limit. We also note that for the global hopping model, the mean field approximation should be exact, even for small h.

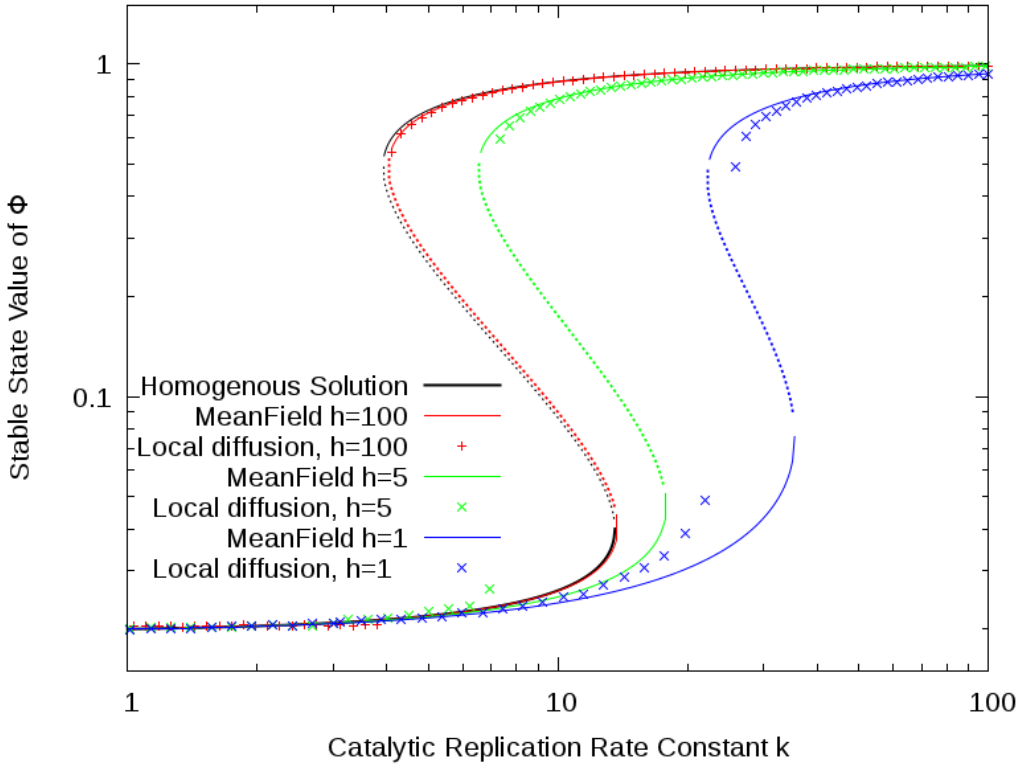

Figure 4.5: Comparison of stable state solution between local diffusion model, mean field theory and homogenous model as function of replication rate *k*, Other parameters are set as: *s*=0.02, *r*=0, *u*=1, *L*=100.

In Figure 4.5, we compare the solutions of the mean field equations with dynamical simulations. The black curve is the homogeneous solution from the roots of the cubic Equation 4.1. This is the well mixed limit of the spatial model. The solid black lines illustrate the stable living and dead states and the dashed line is the unstable intermediate state. The solid red, green and blue lines show the stable solutions of the mean field equations with three values of *h*. For large *h*, the mean field solution is close to the well-mixed limit, as expected. The symbols show average concentrations of molecules obtained from simulations of the lattice

model with local hopping. For the living state, the mean field theory gives a fairly good approximation to the result with local hopping, even for the smaller values of h. This is because the density is quite high across the whole lattice in the living state and correlations between neighbouring sites are quite weak. On the other hand, there are large deviations for mean field theory from local hopping model in dead state when it is close to the bistable region, which shows that there are important local spatial correlations in this case.

Figure 4.5 illustrates that reduction in the local diffusion rate has both positive and negative effects on the replication process. As h is reduced, the concentration of the living state is reduced because there is more local interference between fully occupied sites in the growth process. Also the minimum value of k required for the living state to be stable increases as h decreases. Thus, rapid diffusion is favourable for the living state, if the living state is already established. However, we have already seen in Fig. 4.3 that high diffusion rates cause the system to be well mixed, in which case the transition time is extremely long. It is therefore important to have a diffusion rate that is not too large in order for the transition to the living state to occur at an appreciable rate in the first place.

4.6 Polymerization Model on Surface

The Two's Company model is the simplest model that can be used to study the stochastic transition to life in a spatially distributed system, however, we wish to show that the same behaviour occurs in other models. We will now return to

the model of RNA polymerization used in Chapter 2 in order to study the effects of diffusion and spatial concentration fluctuations in a more realistic model. For detail model description please refer to Chapter 2 section 2 and 3.

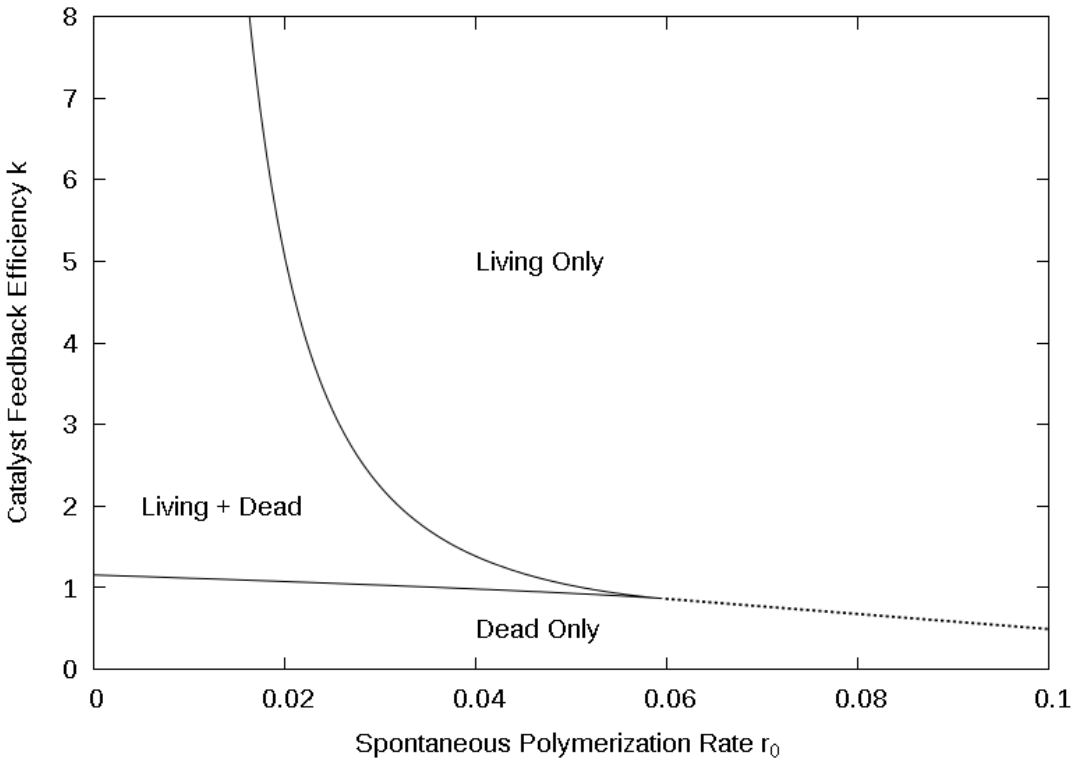

Figure 4.6: Phase diagram for existence of dead and living states as function of catalyst feedback efficiency k and spontaneous polymerization rate r_0 with other parameter set as: m=5, s=10, a=10, u=1, f=1

With the same method used in Chapter 2, phase diagram can be obtained for existence of dead and living states as function of catalyst feedback efficiency k and spontaneous polymerization rate r_0 in a well mixed system as in Figure 4.6, which looks surprisingly similar to Figure 4.1. As described in Chapter 2, we think that the transition process from dead to living can only happen when there are dead state and living state for a given set of parameters. Otherwise, the system will stay dead forever, or start from an already living state. Hence the system

should have the parameter combination with which both living and dead states exist. We already investigated the effect of system size on transition time for a well mixed system. In the following section we will focus on dynamics of this system with limited diffusion on a surface.

As in the Two's company model, the simulation is carried out on 2D square lattice composed of $L \times L$ lattices with lattice size as 1. The reactions of monomer synthesis, activation, and polymerization all occur locally on individual lattice sites. The rates of these reactions are determined from the numbers of molecules of each type on each site. These rates are input to stochastic simulations using the Gillespie algorithm, as described in Section 2.5 The hopping rate h is chosen to be fast enough to ensure smooth concentration fluctuation among neighbouring lattice sites, but slow enough so that differences in concentration can arise across the whole lattice. It is supposed that monomers and polymers all have the same hopping rate. All other parameters are set to make sure the system has both living state and dead state. Since the activated monomer is the most abundant type of molecule in the dead state, and its dead state value differs a lot from living state value, the change in concentration of activated monomers is averaged over a sliding time interval (as with the Two's Company model), and this is used to define the time of transition.

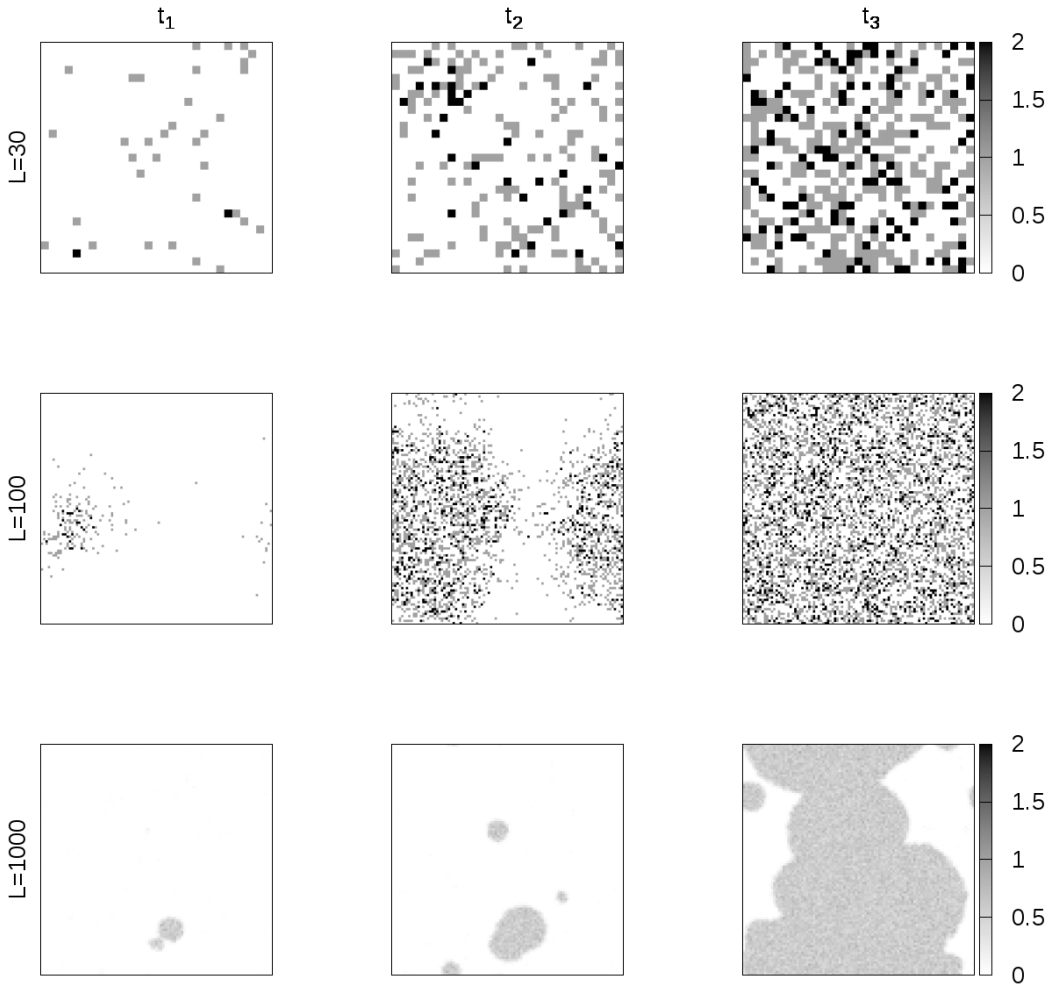

Figure 4.7: Snapshot of catalytic polymer concentration at the beginning(t_0), during(t_2), after(t_3) transition from dead state to living state for different system size (L=30, 100, 1000) with local hopping model. Parameters are set as: m=5, s=10, a=10, r_0=0.02, k=2, u=1, h=50, f=1

4.7 Results for the Polymerization Model

Figure 4.7 shows snapshots of the distribution of catalytic polymers across the lattice. Three time points are chosen in order to illustrate the way the catalyst concentration increases over time. As shown in first row of Figure 4.7, when system is small (L=30), the system is more or less well mixed. Hence the

transition happens across the whole system at the same time. When system is larger (L=100), the system is no longer homogenous. The transition happens at a local region first, then it spreads out to the whole system as shown in second row of Figure 4.7. When the system is very large (L=1000), the time it takes to spread across the whole system is longer than the average local transition time. Hence there will be multiple origins happening in the system as shown in third row of Figure 4.7.

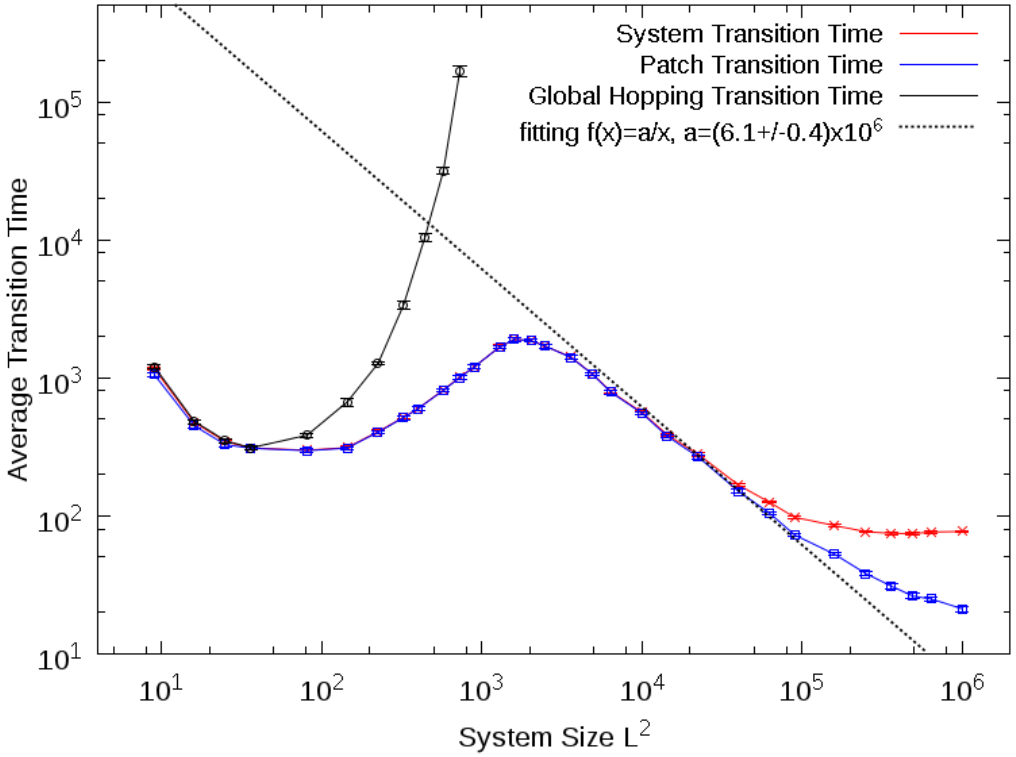

Figure 4.8: Average transition time from dead state to living state as function of system size with parameters set as: m=5, s=10, a=10, r_0=0.02, k=2, u=1, h=50, f=1

More insight can be gained by looking at average transition time as function of system size with local and global hopping models as shown in Figure

4.8. For global hopping, the transition time follows a U-shaped curve, for the same reasons as described in Chapter 2 (see Fig. 2.7). If the system is too small there are too few polymers long enough to be catalysts, and if the system is too big, the concentrations are too small in the global case to allow the stochastic transition to occur.

When the lattice is very small, the time for the transition with local hopping is close to that with global hopping, but when the lattice size is larger, the transition is much faster with local hopping. The transition time follows the same shape curve for this model as for the Two's Company model in Fig 4.4. There is an intermediate range where the transition time scales as $1/L^2$ and where $T_{sys} = T_{reg}$, and there is a range for large lattice size where multiple origins can occur and where $T_{sys} > T_{reg}$.

4.8 Discussion and Conclusion

Despite hugely different detail settings, the Two's company model exhibits surprisingly similar behaviour as the RNA polymerization model from Chapter 2 in both phase diagram as shown in Figure 4.1 and Figure 4.6, and dependence of transition time as function of system size as shown in Figure 4.4 and Figure 4.8. In our view, their behavioural similarity lies in their features of nonlinear feedback and limited resources. In the case of the Two's company model, the catalyzed replication rate of the molecule depends nonlinearly on the concentration of the molecule, and limited resources are modelled by the rule that

there can be only 3 molecules on the same site. In the case of the RNA polymerization model, there is a nonlinear dependence of the ribozyme concentration on the polymerization rate, and there is only limited supply of food molecule from environment. With nonlinear feedback and limited resources, it is feasible for coexistence of a dead state, in which nonlinear feedback is not important, and a living state, in which nonlinear feedback dominant the system. Hence it is reasonable to have similar phase diagram.

As both models have a bistable parameter range, these two models exhibit essentially the same stochastic transition arising as a result of concentration fluctuations. When the system is well mixed, fluctuation will decrease with increasing system size due to increasing number of molecules in the system. With limited diffusion, the system is no longer well mixed and breaks down into many weakly interacting regions whose size is determined by diffusion effect. Due to the fact that lattice sites separated by distance longer than diffusion length are more or less independent from each other, there are multiple transition trials happening at the same time in the system. Given the fixed diffusion length, the larger the system, the more such independent transition trials will be in the system.

Both models illustrate that multiple origins of life will occur if the system is large enough. As far as we know, however, all current life on Earth is descended from a single origin. The size of the Earth is very much larger than the diffusion length of a molecule, which means the origin of life happens in a

heterogeneous system. However, it is likely that origin of life is a very rare event taking hundreds of millions of years to happen, and once it happens it will spread across the whole world in a very short time leaving no space for a second origin of life. In other words, it is likely that the real world falls in the intermediate part of Fig. 4.8, where the transition time varies like $1/L^2$ and there is a single origin. On the other hand, it is not impossible that the origin of life takes a comparable time to happen as spreading of life, in which case there would be multiple origins of life. This scenario can still be compatible with current view of single tree of life if there were competition between different forms of life and only one remained, or if there were symbiosis and merging of features that derived from different origins. Discrimination between these two scenarios requires further information about types, concentration, distribution of prebiotic molecule ensemble and relevant reaction rate constant leading to life.

Chapter 5

Autocatalytic Replication and Homochirality in Biopolymers: Is Homochirality a Requirement of Life or a Result of it?

5.1 Introduction

Symmetry is a fundamental aspect of nature, and many important problems in science depend on understanding the reasons for the presence or absence of symmetry.An important symmetry that is broken in nature is that between the optical isomers (enantiomers) of amino acids in living systems. Naturally occurring proteins are composed of L-form amino acids, whereas DNA and RNA contain D-form ribose and deoxyribose. Understanding how this situation arose is a long standing issue in the field of the origin of life (Bonner, 1991;1995).

The key concept is asymmetric autocatalysis:molecules of one enantiomer must selectively catalyze the formation of further molecules of the same enantiomer. In the presence of asymmetric autocatalysis, the racemic mixture (equal concentrations of the two enantiomers) can sometimes be unstable. Any slight asymmetry in concentration of the two enantiomers that may exist initially can be amplified, giving rise to a system with a large excess of one enantiomer over the other. A simple theoretical model illustrating the principle of asymmetric autocatalysis was given by Frank (1953), and this has given rise to a large number

of more complex models that will be discussed in more detail below. Experimental examples are much harder to come by. The Soai reaction (Soai *et al.*, 1995; 2001) is the reaction of 5-pyrimidyl alkanol with diisopropyl zinc. This is a well-documented case of a small-molecule chemical system that shows that a large enantiomeric excess (ee) can arise by asymmetric autocatalysis.Although this demonstrates the principle that a homochiral system of small molecules could arise spontaneously, the specific chemical components of the Soai reaction are not directly relevant to prebiotic chemistry. No-one has yet found an experimental system involving amino acids, sugars or nucleotides, in which an ee spontaneously arises by autocatalysis, and it would appear that these small biomolecules cannot themselves carry out asymmetric autocatalytic synthesis.

There is an important distinction between small molecules, like amino acids and sugars, and biopolymers, like proteins and nucleic acids. The observation of homochirality of biopolymers in living organisms tells us that asymmetric autocatalytic systems of large biopolymers can maintain high ee. Biochemistry in living organisms relies on specific recognition between biopolymer catalysts and their substrates (either small molecules or other biopolymers). The enzymes or ribozymes in a living system are built from amino acids or nucleotides of a definite handedness, and they would not react with the molecules of the opposite enantiomer. Furthermore, pathways of synthesis of chiral molecules from non-chiral precursors are also controlled by enzymes of one enantiomer, and these can catalyze synthesis of monomers of the same enantiomer

in an asymmetric way. Thus, the maintenance of homochirality in a living system appears straightforward because of the high efficiency and specificity of biopolymer catalysts, whereas the origin of homochirality in a non-living system of small molecules is less easy to understand.

An important part of this puzzle is the observation that amino acids with a relatively high ee ofup to 15% have been observed in carbonaceous chondrite meteorites (Cronin and Pizzarello, 1997; Pizzarello *et al.* 2003; Pizzarello *et al.* 2008; Glavin and Dworkin, 2009). As these molecules are presumed to be a product of non-living chemistry, it must either be the case that the amino acids are synthesized by asymmetric autocatalysis involving small molecules, or that they are synthesized by a non-autocatalytic process that is asymmetric for some other reason. Among non-autocatalytic sources for an initial asymmetry, one plausible mechanism involves the influence of circularly polarized light. It has been shown that irradiation with circularly polarized light leads to asymmetric photolysis of the two enantiomers, and ees of a few percent have been created by this means (Balavoine *et al.* 1974; Bonner 1991 and references therein; Bonner and Bean, 2000).For the Soai reaction, it has been shown that circularly polarized light can provide an initial ee which is subsequently amplified by autocatalysis (Soai *et al.* 2001; Kawasaki, 2004). Furthermore, circularly polarized light has been observed in regions of star and planet formation (Bailey *et al.* 1998; Bailey, 2001; Fukue *et al.* 2010). Any chiral bias in the chemistry of the protoplanetary disk arising from asymmetric photolysis by circularly polarized light would be passed on to

asteroids and planetesimals that are the parent bodies of meteorites. The direction of the circular polarization depends on the way light from a nearby star is reflected from dust grains in the solar system. Although the orientation could be of either sign, it is likely to be constant over any one solar system, and hence it could provide a planet-wide bias. Another electromagnetic effect that might cause an initial asymmetry is the interaction of spin isomers with large magnetic fields (Popa *et al.* 2009).

Enantiomorphic crystals of materials such as quartz and sodium chlorate might also provide a possible source of chiral asymmetry. Single grains of these crystals are optically active. The surfaces of such crystals could potentially act as chiral catalysts for organic reactions. Once again, with the Soai reaction, it has been shown that an initial ee induced by chiral sodium chlorate crystals can be amplified by autocatalysis (Sato *et al.* 2004). However, the sign of the effect would vary between crystals, and there is no net bias favouring one enantiomorph over the whole surface of the Earth (Klabunovskii, 2001). Despite this lack of a global biasing mechanism, mineral and/or clay surfaces might provide a platform for asymmetric synthesis of biopolymers (Hazen *et al.* 2001, Joshi *et al.* 2011) and thus contribute to an initial local asymmetry that could be amplified by autocatalysis.

It is also possible that crystallization of chiral organic molecules themselves can be important. When a solution of chiral molecules is in equilibrium with chiral crystals, the ee of the molecules in the solution can be

higher than that in the crystals (Klussmann *et al.* 2006). This could provide another means for amplification of the ee, although this mechanism does not amplify the ee unstably from an initial small perturbation, as would be the case with asymmetric autocatalysis. Another crystallization mechanism that does amplify to a high excess from a small perturbation is given by Viedma (2007) and Noorduin *et al.* (2008). Here, an almost racemic solution of a chiral molecule is in equilibrium with chiral crystals of the two enantiomers. Breakup of the crystals is induced mechanically, and there is a tendency for large crystals to grow at the expense of smaller ones. Racemization of the molecules occurs in solution. The combination of crystal growth, dissolution and racemization leads to almost complete homochirality.

In any sample of a finite volume with a finite number of molecules, a small random difference in the concentrations of the two enantiomers would arise by chance. If an external bias is to be relevant, it must be larger than this random statistical bias. It has been pointed out that the parity violation of the weak nuclear interaction makes a very slight difference in the thermodynamic properties of the two enantiomers. However, as argued by Bonner (2000), this effect would be much too small to give the observed enantiomeric excesses of up to 15% in the meteorite samples, unless an autocatalytic process was able to amplify the excess. If an autocatalytic process was indeed occurring, then a small random bias could be amplified in any case, and so a tiny bias arising from parity violation would not be a key aspect of the problem.

It should be borne in mind that current observations of the ee in meteorites are based on rather few samples. There is still insufficient information to say what fraction of carbonaceous meteorites contain molecules with significant ee, and why certain molecules have a higher ee than others in the same sample. Also, the more general question of the relevance of the delivery of extraterrestrial organic material to Earth is still not resolved (Whittet, 1996; Pasek and Lauretta, 2008). The quantity of organic molecules arriving from outside may have been small compared to what was already on Earth, or chemical reactions (including racemization) may have occurred on Earth after arrival of the material from outside. In either of these cases, the ee on Earth at the time of the origin of life would not be the same as that observed in the meteorites. Furthermore, observations of chirality in meteorites have focussed on amino acids, whereas in the context of the RNA World hypothesis, it would be nucleotides that would be more relevant at the time of the origin of life. Unfortunately, we have no data on the extent of the ee that may have existed in nucleotides prebiotically. Encouragingly, however, it has been shown that sugars synthesized in the presence of chiral amino acids may have an ee transferred to them (Pizzarello and Weber, 2004& 2010; Weber and Pizzarello, 2006). Hein *et al.*(2011) have also shown that RNA precursor molecules can be enriched to high levels of ee from racemic starting materials provided that amino acids enantiomers with a small initial bias are present in the reaction mixture. These two experiments suggest mechanisms by which chirality may have arisen in the backbone of nucleic acids.

If we accept that the ees of a few percent observed for amino acids in meteorites are indicative of the degree of chiral bias that existed in the monomers from which the first living biopolymers were composed, then there is still the question of how to get from a few percent to the essentially 100% homochiral state observed in life. It seems likely that it is the autocatalytic properties of the biopolymers that create the amplification that leads to a highly biased state. An example of a chirally selective peptide replicator has been studied by Saghatelian *et al.* (2001). Also in an RNA-world scenario, polymerization of nucleotides is likely to be chirally selective, whether this is by a non-enzymatic, template-directed mechanism (Bolli *et al.* 1997), or due to the action of a polymerase ribozyme that catalyzes primer extension (Johnston *et al.* 2001).

At this point, the chirality problem links to our previous work on the origin of autocatalytic biopolymers (Wu and Higgs, 2009; 2011). We considered a prebiotic chemical reaction system in which monomers (such as nucleotides) and polymers (such as RNAs) could be synthesized. Our aim was to consider how catalytic biopolymers (ribozymes) could arise in this system. We supposed that only polymers longer than some minimum length, m, could be sufficiently complex to be ribozymes. In absence of ribozymes, the steady state concentration ofRNAs decreases rapidly with length. However, if a small number of ribozymes arises by random chemical synthesis, this can cause the system to switch to a living state in which nucleotide synthesis and/or polymerization is autocatalytic. In the living state, the concentration of RNAs decreases much more slowly with

length, and the total concentration of ribozymes is large. Our previous work considered the origin of life but not the origin of homochirality, and we considered only one kind of monomer. Thus, we implicitly assumed that homochirality arose before the origin of life and that a supply of homochiral monomers was present from which the first autocatalytic biopolymers could be formed. If so, the origin of homochirality and the origin of life are separate problems. Previous theories for origin of chirality (see the following section) typically assume that this is the case, and do not deal with the origin of life. However, the discussion above suggests that the two problems may be at least partially linked. This leads us to consider a range of possible scenarios linking the origin of homochirality and the origin of life. These are summarized in Figure 5.1.

Boxes 1(a-d) in Figure 5.1 consider the states of chirality that could have existed before the origin of life, and boxes 2(a-d) in Figure 5.1 consider the states of chirality that could have arisen when life originated. In 1(a), it is supposed that an asymmetric autocatalysis process arises that incorporates the monomers themselves. As this is autocatalytic, it has the potential to create a high ee, so that when biopolymer catalysts arise (state 2(a)), they are formed from a completely homochiral supply of monomers. In this scenario, the problem of homochirality is fully solved at the small-molecule stage, prior to the origin of life. On the other hand, if the small molecule system only creates a moderate ee, biopolymer catalysts will arise within a partially biased mixture of monomers of the two enantiomers. As the biopolymers are likely to be more efficient chiral catalysts,

the ee will be amplified when life arises (state 2(b)). Thus, the origin of homochirality is partially before the origin of life, and the process is completed at the time of the origin of life.

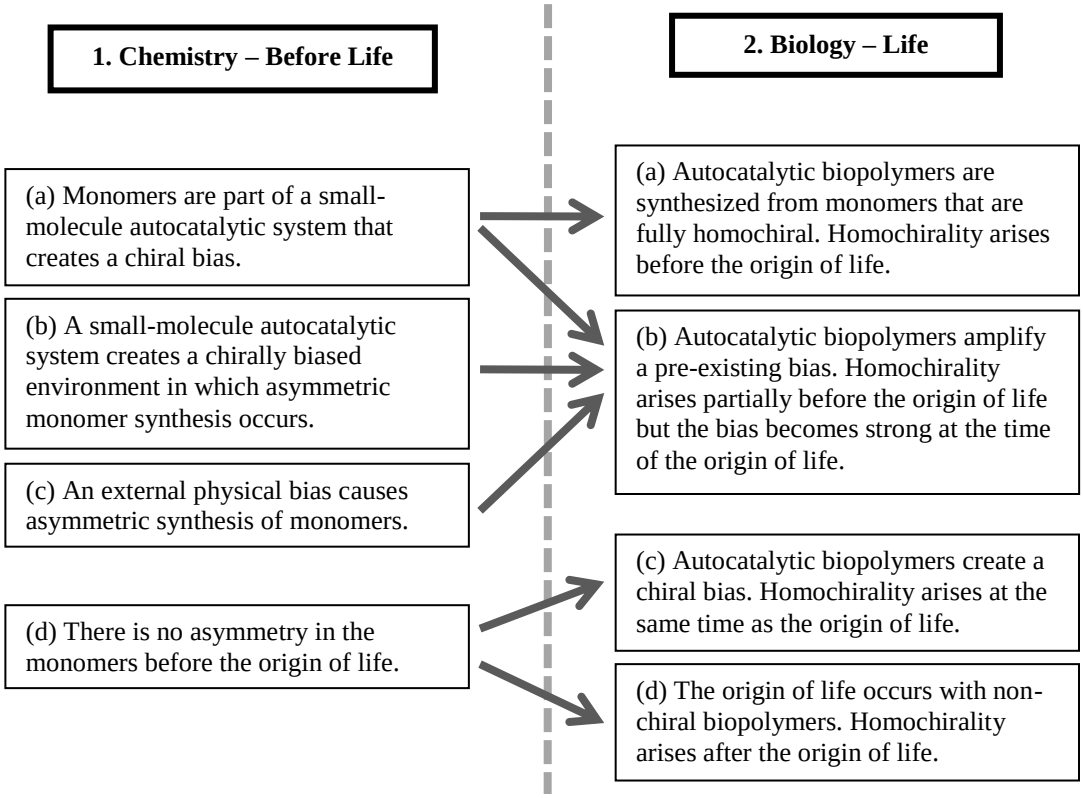

Figure 5.1: Scenarios relating the origin of chirality to the origin of life.

In 1(b), it is supposed that a system of asymmetric autocatalysis arises with small molecules (such as the Soai reaction), but the monomers are not part of this. In this situation, monomer synthesis may be asymmetric because it occurs in a chirally biased environment, *i.e.* chirality may be transferred from the autocatalytic small molecule to the monomer. This relieves the monomer from the dual responsibility of having to act as a chiral autocatalyst when present as a

monomer as well as a functional component of a biopolymer catalyst when it is polymerized. For example, ribonucleotides can do the latter, but not the former, as far as we know.

In 1(c), we suppose that some physical influence, such as asymmetric photolysis or the presence of chiral crystals, causes monomer synthesis to be asymmetric. In both 1(b) and 1(c), monomer synthesis is not autocatalytic; therefore it seems likely that these states would only be partially chirally biased. These states would thus lead on to 2(b), in which full homochirality arises only when life arises.

In 1(d), it is supposed that there is no ee at the monomer level. This would be the case if the extraterrestrial supply of chiral molecules is too small to influence the overall chirality on Earth, or if any chirality that does exist in the prebiotic mixture is not transferred to monomers from which the biopolymer catalysts are composed. In this case, the biopolymers arise from a racemic mixture, and it is the origin of the autocatalytic process of biopolymer synthesis that creates the instability that leads to an asymmetric state (2(c)). Homochirality thus arises at the same time as the origin of life in this case.

In principle, state 1(d) could also lead to a state 2(d) in which life arises without chirality. In 2(d), there could be biopolymers composed either of achiral monomers or of racemic mixtures of chiral monomers. Both of these seem unlikely, but we have included this case as it is at least a logical possibility. In this scenario, life would arise before homochirality. Homochiral biopolymers would

take over from achiral or racemic biopolymers at some point after the origin of life. Bonner (1991; 1995) reviewed some early proposals of this kind, which he termed biotic theories, because life would be required for the origin of homochirality. However, he effectively rejected these in favour of abiotic theories, in which chirality is required for the origin of life. The scenarios we show in Figure 5.1, are an updated and more detailed version of the distinction between abiotic and biotic theories made by Bonner. Whilst we have difficulty in imagining a living system of achiral or racemic biopolymers, as in 2(d), we think that it is quite likely that the problem of the origin of homochirality is at least partly biological, as in 2(b), and we would argue that the possibility of simultaneous origin of life and homochirality, as in 2(c), should at least be considered seriously. The principal aim of this chapter is to develop a theory with which to investigate cases 2(b) and 2(c).

In the discussion of Figure 5.1, we adopted the viewpoint that the origin of life means the origin of an autocatalytic system of information-carrying biopolymers, such as RNAs. However, if one takes a metabolism-first viewpoint, then it is possible that an autocatalytic system of small molecules may have existed before the origin of biopolymers (Shapiro, 2006) or that compositional inheritance may have existed before information-carrying biopolymers, as in the lipid-world theories (Segre *et al.* 2000; Wu & Higgs, 2008). From this viewpoint, states 1(a-d) might already be classed as living, and states 1(a-d) and 2(a-d) would represent the situations before and after the origin of biopolymers, rather than

before and after the origin of life *per se*. For concreteness in the rest of the chapter, however, we will stick to our original viewpoint, and we will describe a system as livingonly if there are autocatalytic biopolymer catalysts present.

5.2 Previous Autocatalytic Theories

Before presenting the model used in this chapter, it is useful to discuss the models for asymmetric autocatalysis that have been proposed previously, beginning with the simple case studied by Frank (1953). In Frank's model, *L* and *D* monomers are autocatalysts for their own synthesis, and they also inhibit one another by the formation of *LD* dimers that are non-reactive. This cross-inhibition is important because if a slight excess of one enantiomer arises, formation of the *LD* dimer is a greater penalty for the rarer enantiomer, and this amplifies the ee and makes the symmetric state unstable. Variations of this model have been considered in which *LL* and *DD* homodimers form in addition to *LD* heterodimers, and in which dimer formation is reversible (Ribo and Hochberg, 2008; Hochberg, 2009), and the conditions for the instability of the symmetric case have been worked out in detail.

Models have also been studied in which the monomers are not directly autocatalytic, but the homodimers (*LL* and *DD*) are catalysts for synthesis of monomers of the same enantiomer (Blackmond, 2004; Islas *et al.* 2005). Hence there is still asymmetric autocatalysis of monomer synthesis via the effect of the dimers. If dimers are the catalysts, then cross inhibition is less important. For

example if heterodimers and homodimers form at the same rate, there is no instability in models with monomer catalysts, whereas there is still an instability when dimers are catalysts. For this reason, Blackmond (2004) argued that dimer catalysts were essential to interpret the Soai reaction. However, Islas *et al.* (2005) found that the results of the Soai reaction were still consistent with monomer catalysis. A slightly different mechanism that works at the dimer level is the epimerization model of Plasson *et al.* (2004;2007) in which *LD* dimers are converted to *LL* or *DD*, which creates an instability without requiring autocatalysis in monomer synthesis.

A next step toward modelling chiral asymmetry in biopolymers is to allow *L* and *D* monomers to make polymers of all lengths and to assume that only long polymers are catalysts. In the model of Sandars (2003), homochiral poymers, L_n and D_n, can grow from both ends, but cross-inhibition occurs of a monomer of the opposite type is added, such that L_nD and D_nL can no longer grow from the blocked end. We will use m to denote the length of the polymer catalyst. Homochiral polymers, L_m and D_m, are assumed to be catalysts for synthesis of monomers of their own type. Saito and Hyuga (2005) described a polymerization model in which only pure homochiral polymers can form and cross reactions do not occur, although only the dimer catalyst case (m = 2) was considered in detail. Brandenburg *et al.* (2005a; 2005b) extended the Sandars (2003) model and considered a case where dissociation of polymers into smaller sequences was permitted as well as polymer growth. Gleiser and Walker (2008) considered a

variant that explicitly included monomer synthesis, treated polymers of all lengths as catalysts, and avoided putting in a maximum length of polymers. All of these models share the implicit assumption that homochirality must arise prior to the origin of life.

We have previously considered models for the origin of autocatalytic biopolymers such as ribozymes (Wu and Higgs, 2009; 2011). The ingredients of our models are similar to those for the polymer models of chirality, although we were interested in the origin of life rather than the origin of homochirality. We considered monomers of a single type, as would be the case if a non-living process generated fully homochiral monomers prior to the origin of life. Our models consider monomer synthesis and polymerization reactions. Both of these are presumed to occur at a small spontaneous rate in absence of ribozymes and at a much higher rate when they are catalyzed by ribozymes. An important feature of our models is that there is a clear distinction between states that are living and dead. In the dead state, reactions proceed at the spontaneous rate and the concentration of ribozymes is negligible. In the living state, the reactions proceed at high rates that are controlled by the ribozymes. The living/dead distinction is not present in previous models for chirality. Therefore, the aim of this chapter is to study a model in which transitions between racemic and homochiral states can be studied alongside transitions from non-living to living states.

Another feature of our ribozyme models is that an autocatalytic set can be created either by polymerase ribozymes that increase the polymerization rate or

by nucleotide synthetase ribozymes that increase the rate of monomer synthesis (Wu and Higgs, 2011). Previous models for origin of homochirality have focussed principally on catalysis of monomer synthesis. In contrast, other papers dealing with the pre-life to life transition (Ohtsuki and Nowak, 2009; Manapat *et al*. 2010) have dealt with catalysis of polymerization, but ignored the chirality issue.

5.3 A model describing both the origin of homochirality and the origin of life

Here we propose a system of chemical reaction equations that describes the synthesis of monomers of two possible enantiomers, which we denote L and D, from a non-chiral precursor (or 'food') molecule, F. We consider a reactor system with a fixed external concentration, F_0, of precursor, and a constant rate of entry uF_0 of precursor molecules. Molecules of all types exit the system at the same rate u. The monomers are synthesized from F with rate constants s_L and s_D, which are not necessarily equal.

$$F \xrightarrow{s_L} L$$

$$F \xrightarrow{s_D} D$$

Monomers can polymerize by addition to the end of growing chains. L_n and D_n denote homochiral polymers of length n. Mixed polymers, with at least one monomer of each kind, are denoted M_n. Addition of a monomer of the wrong type to a homochiral polymer creates a mixed polymer. Addition of a monomer of either type to a mixed polymer creates a longer mixed polymer.

$$L_n + L \xrightarrow{r} L_{n+1}$$

$$D_n + D \xrightarrow{r} D_{n+1}$$

$$L_n + D \xrightarrow{r} M_{n+1}$$

$$D_n + L \xrightarrow{r} M_{n+1}$$

$$M_n + L \xrightarrow{r} M_{n+1}$$

$$M_n + D \xrightarrow{r} M_{n+1}$$

We assume that the rate constant for polymerization, *r*, is equal to the spontaneous rate r_0, which is a constant parameter. However, the synthesis rates are not constant because they depend on the catalyst concentration. The total concentrations of homochiral sequences of at least length *m* are

$$C_L = \sum_{n=m}^{\infty} L_n \ , \quad C_D = \sum_{n=m}^{\infty} D_n \ . \tag{5.1}$$

We suppose that some fraction of these homochiral polymers can be catalysts. The synthesis rates are the sum of a spontaneous term and a term proportional to $C_L$and C_D:

$$s_L = s_0(1-\varepsilon) + kC_L, \qquad s_D = s_0(1+\varepsilon) + kC_D. \tag{5.2}$$

The parameter ε controls the degree of chiral bias in the chemical system prior to life. If ε = 1, the chemical system is completely homochiral, and only one type of monomer is synthesized. If ε = 0, the chemical system is racemic prior to the origin of life. We have set the bias to be in favour of *D* in Equation 5.2, because *D* riboses arise in nucleotides, but the model is clearly equivalent if the bias goes the other way. The total rate of spontaneous synthesis of the two types of monomer is

$2s_0$. The parameter *k* controls the strength of the catalytic effect. The following set of ordinary differential equations (ODEs) can be used to describe the system.

$$\frac{dF}{dt} = u(F_0 - F) - \big(2s_0 + k(C_L + C_D)\big)F \tag{5.3}$$

$$\frac{dL}{dt} = (s_0(1-\varepsilon) + kC_L)F - r_0(2L + 2D + P_L + P_D + M)L - uL \tag{5.4}$$

$$\frac{dD}{dt} = (s_0(1+\varepsilon) + kC_D)F - r_0(2L + 2D + P_L + P_D + M)D - uD \tag{5.5}$$

$$\frac{dL_n}{dt} = r_0 L_{n-1} L - r_0(L + D)L_n - uL_n \tag{5.6}$$

$$\frac{dD_n}{dt} = r_0 D_{n-1} D - r_0(L + D)D_n - uD_n \tag{5.7}$$

$$\frac{dC_L}{dt} = r_0 L_{m-1} L - r_0 C_L D - uC_L \tag{5.8}$$

$$\frac{dC_D}{dt} = r_0 D_{m-1} D - r_0 C_D L - uC_D \tag{5.9}$$

$$\frac{dM}{dt} = r_0(2LD + LP_D + DP_L) - uM \tag{5.10}$$

Where

$$P_L = \sum_{n=2}^{\infty} L_n, \quad P_D = \sum_{n=2}^{\infty} D_n \ , \ M = \sum_{n=2}^{\infty} M_n \tag{5.11}$$

Note that Equations 5.8 and 5.9 are collective equations for homochiral polymers of at least length *m*,hence Equations 5.6 and 5.7 are needed only for $n < m$. Therefore, the total number of independent equations is $2m + 2$.

Note that, unlike previous models (Sandars, 2003; Brandenburg *et al.* 2005; Gleiser and Walker, 2008), we assume that mixed polymers can continue to

grow and are not inhibited by a single monomer of the opposite sign. We do this for simplicity, but also because it is a conservative assumption. The effects of enantiomeric cross-inhibition are readily apparent in template-directed polymerization (Joyce *et al*, 1984), however it is less clear if this is the case in the absence of a chiral template such as a homochiral polymer or mineral surface. We will show that homochiral living states arise in this model despite the wastage of monomers in non-functional mixed polymers. If cross-inhibition of polymer growth were treated more explicitly in the model, this would lead to an additional favouring of homochiral living states, because there would be fewer mixed polymers.

Inclusion of the loss term (proportional to $-u$) in all equations means that polymers escape from the system and do not accumulate indefinitely. The equilibrium concentration inside the system is controlled by a balance between the supply of precursors and the loss rate.

5.4 Numerical methods

Two methods were utilized to find the stationary solutions for the concentrations. The first approach was to integrate Equations 5.3-5.10 numerically using a method appropriate for stiff systems of ODEs (Bader and Deuflhard, 1983) until convergence was reached. The second method was to use the NSolve function from Mathematica which is based on solving the eigen system of the right hand side of the equations (Lichtblau, 2000). This method can

find all the fixed points for the ODE system, including both stable and unstable solutions. The stability of the fixed points was determined by analyzing the eigenvalues of the Jacobian matrix of the ODE. For the small *m* case (*m*=5) that we consider in detail in this chapter, both methods were practical, and we checked that the same results were obtained both ways. For the large *m* case (*m*= 25), we used only the first method, because it was much faster, although it can find only stable solutions and it requires some prior knowledge of which solutions to expect.

5.5 Fully Homochiral Monomer Synthesis (ε = 1)

Firstly, we consider scenario 1(a)-2(a) in Figure 5.1, where the monomer system is fully chiral prior to the origin of life. This means that ε = 1, and there is only one type of monomer produced, which is *D* with the sign convention used here. The system can be simplified to following equation set:

$$\frac{dF}{dt} = u(F_0 - F) - (2s_0 + kC_D)F \tag{5.12}$$

$$\frac{dD}{dt} = (2s_0 + kC_D)F - r_0(2D + P_D)D - uD \tag{5.13}$$

$$\frac{dD_n}{dt} = r_0 D_{n-1} D - r_0 D_n D - uD_n \tag{5.14}$$

$$\frac{dC_D}{dt} = r_0 D_{m-1} D - uC_D \tag{5.15}$$

This model is equivalent to the model for the origin of self-replicating biopolymers that we studied previously in chapter 3. We consider this case

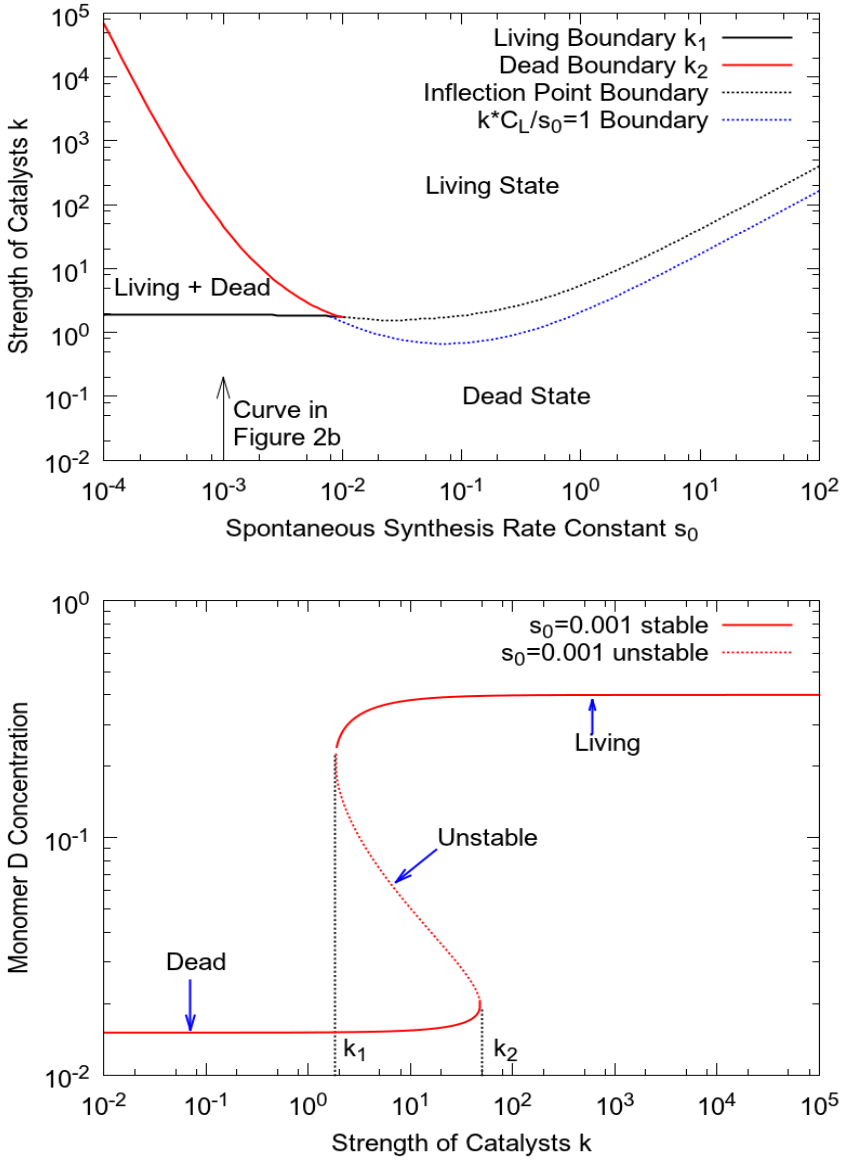

Figure 5.2: (a) Phase diagram for the case $\varepsilon = 1$, where monomer synthesis is fully homochiral for chemical or physical reasons prior to the origin of life. This corresponds to scenario 1(a)-2(a) in Figure 5.1. In the s_0-k plane there are regions where both living and dead states exist and regions where only one or other state exists. Both living and dead states are fully homochiral. The other parameters fixed as follows: $m = 5,\ r = 10, u = 1,\ F_0 = 10$.
(b) Monomer concentration as a function of $k$with s_0 fixed, moving along the vertical line indicated by the arrow in (a). Between the values k_1 and k_2, the living and dead states are both stable and there is an unstable state between them. Outside of this range of k, only one stable state exists.

briefly here, in order to compare with the case of $\varepsilon < 1$, where both monomer types are relevant. For the numerical examples in this chapter, we set $u = 1$. This sets a timescale to which other reaction rates can be compared. We assume $r_0 = 10$ and $F_0 = 10$, unless specified otherwise. The two most important rate parameters are the spontaneous monomer synthesis rate s_0 and the catalytic efficiency k , and we consider the effect of varying these parameters in detail. The choice of the minimum catalyst length, m, is also important. We intend that the catalysts should represent ribozymes that are long enough to have a well-defined structure and function. For reasons of computational speed and practicality of finding the numerical solutions, we keep m fairly small, and consider the case of $m = 5$ in detail. At the end of the chapter, we compare this with a case of longer ribozymes ($m = 25$) and with the special case of dimer catalysts ($m = 2$).

Figure 5.2a shows the phase diagram of the system in terms of k and s_0. Figure 5.2b shows the monomer concentration as k is increased, moving vertically along the line indicated by the arrow in Figure 5.2a. In the range $k_1 < k < k_2$, two stable states exist with an unstable state between them. Within this range, the concentrations in Equations 5.12-5.15 converge to one or other of the two stable solutions, depending on the starting conditions. Outside this range, only one stable state exists. The ratio kC_D/s_0 measures the relative rate of catalyzed to spontaneous monomer synthesis. We call the lower stable state 'dead' because the concentration of ribozymes is very small and the catalytic effect of the ribozymes

is negligible compared to the spontaneous synthesis rate, *i.e.* $kC_D/s_0 << 1$. We call the upper stable state 'living' because it is autocatalytic. The concentration of ribozymes is high, and the monomer synthesis rate is dominated by the ribozymes, not the spontaneous rate, *i.e.* $kC_D/s_0 >> 1$.

For larger values of s_0 the two boundaries, k_1 and k_2, meet and there is only one stable solution for the system in which the monomer concentration increases smoothly with k. In this case, the boundary between the dead state and living states is not clear cut, but we used two ways to define an approximate boundary. The blue dotted line is the point where the ratio $kC_D/s_0 = 1$, *i.e.* where the catalytic effect of the ribozymes becomes equal to the spontaneous rate (see also Figure 5.3).The black dotted line is the point where the monomer concentration increases most rapidly with k (*i.e.* the point of inflection of the monomer concentration as a function of k). This is a simple way of separating high and low concentration regions.

Further details of models that consider monomers of a single chirality are given by Wu and Higgs (2009; 2011) and Ohtsuki and Nowak (2009). All these models show regions where both living and dead states are stable, and they have a phase diagram similar to that in Figure 5.2.

5.6 Symmetric Synthesis of Monomers *L* and *D* (ε = 0)

We now consider the scenario 1(d)-2(c) in Figure 5.1, where there is no chiral bias in the chemical system prior to the origin of life ($\varepsilon = 0$), and

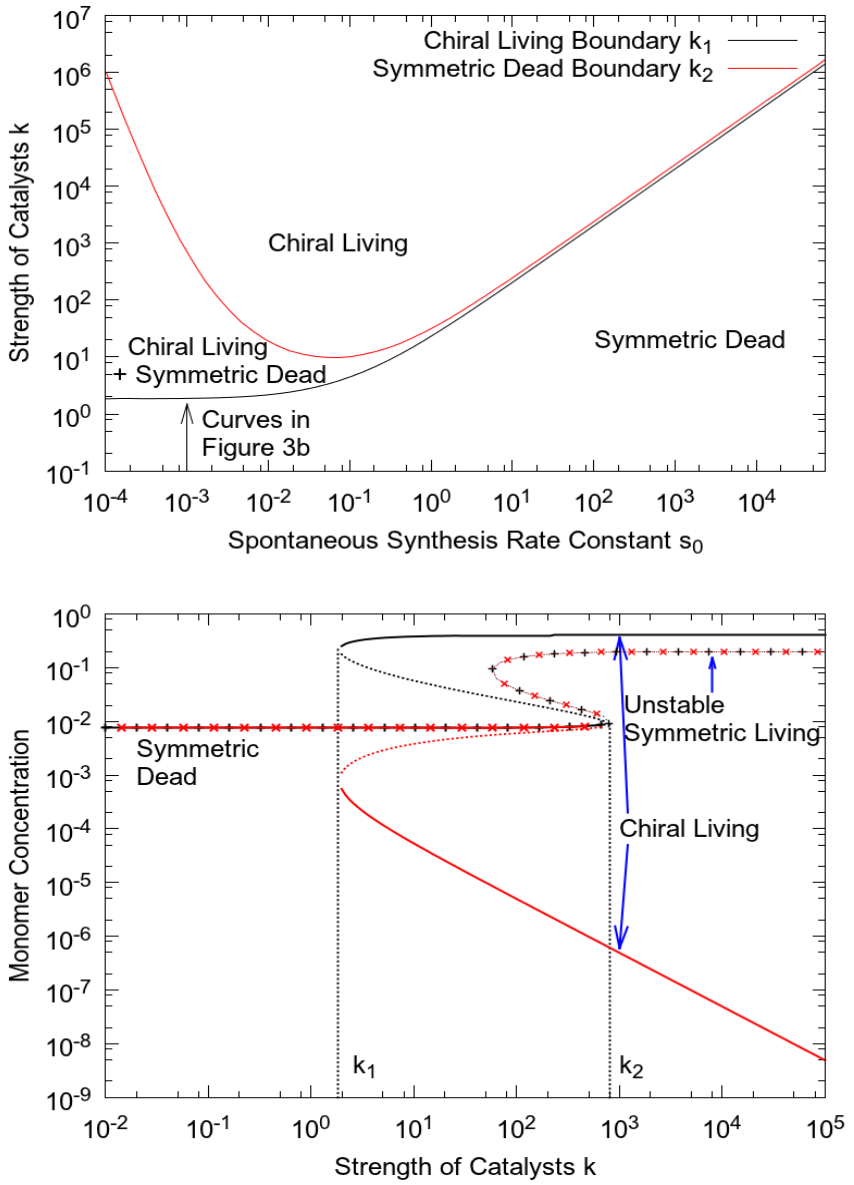

Figure 5.3: Phase diagram for the case $\varepsilon = 0$, where monomer synthesis is symmetric prior to the origin of life. This corresponds to scenario 1(d)-2(c) in Figure 5.1. There are two equivalent living states with a strong chiral asymmetry in one direction or the other. The dead state is symmetric. There is a significant portion of the phase diagram where both living and dead states exist. The other parameters fixed as follows: $m = 5,\ r = 10, u = 1,\ F_0 = 10$.
(b) Monomer concentration as a function of k with s_0 fixed, moving along the vertical line indicated by the arrow in (a). Solid lines indicate stable states and dotted lines indicate unstable states. Red and black symbols label the symmetric states. The symmetric dead state is stable up to k_2. The branch corresponding to the symmetric living state is shown, but this is always unstable. For $k > k_1$, the red and black solid lines show the chiral living state, in which one of the monomers has a high concentration and the other one has a low concentration compared to the dead state.

homochirality arises at the same time as the origin of life. The phase diagram for this case is shown in Figure 5.3a, and the solutions for the monomer concentrations as a function of k with $s_0 = 0.001$ are shown in Figure 5.3b.

For $k < k_1$, there is only one stable state, which is a symmetric dead state, *i.e.* L and D monomer concentrations are equal, the ribozyme concentration is negligible, and the monomer synthesis rate is virtually equal to the spontaneous rate. For $k_1 < k < k_2$, there are two chiral living states in addition to the symmetric dead state. For $k > k_2$, only the chiral living states exist. The chiral states with L dominant and D dominant are equivalent to one another, and either monomer could become dominant by chance. In the chiral states, the concentration of the dominant enantiomer (black curve in Figure 5.3b) is much higher than that of the rare enantiomer (red curve), so the enantiomeric excess is virtually 100%. For example, at $k_1 = 1.97$ (close to k_1), the two concentrations are 0.295 and 0.00055, which corresponds to an ee of 99.6%. The ee becomes even larger as k increases.

The chiral states are classed as living, because the concentration of ribozymes of the dominant enantiomer is high, and synthesis of the dominant monomer is predominantly autocatalytic, *i.e.* if D is the dominant monomer, $kC_D/s_0 >> 1$. Figure 5.3b also shows a symmetric living branch. This corresponds to a situation in which both C_L and C_D are large and there is no ee in either the monomers or polymers. However, the symmetric living solution is always unstable, so it does not appear in the phase diagram. This is intuitive, because the living state is autocatalytic by definition and the autocatalysis is asymmetric,

because only homochiral polymers are catalysts. We know from the many previous models of chirality that the symmetric state is unstable in situations of strong asymmetric autocatalysis. This model therefore illustrates the 1(d)-2(c) scenario, where life and homochirality arise together and it is not possible to have one without the other.

There are some other features of the living and dead states that are worth noting. In the dead state, the precursor concentration, F, is virtually equal to the concentration,F_0, in the surrounding medium (F_0= 10 in this example). Monomer synthesis is occurring at a slow spontaneous rate that does not significantly deplete F. In contrast, in the chiral living state, monomer synthesis is occurring at a fast rate that is catalyzed by the ribozymes. This causes a significant depletion of the precursor such that F is approximately inversely proportional to the catalytic efficiency k. This explains why the monomer concentrations do not increase indefinitely, even when k continues to increase. In the dead state, the concentrations of the two homochiral polymers are equal, $P_L = P_D$, and both are less than M. Random polymerization leads to a majority of mixed polymers, as we would expect. In the chiral living state, the concentration of homochiral polymers of the dominant monomer is much larger than M, whereas it is much less than M for the rare monomer. Thus, in the living state, most polymers are homochiral. The rare monomer has a very low concentration and does not significantly impede polymerization of the dominant monomer, even though we have assumed a worst

case scenario, where the rates of addition of the two monomers are independent of the previous polymer sequence.

5.7 Asymmetric Synthesis of Monomers L and D ($0 < \varepsilon < 1$)

We now consider the situation where monomer synthesis is partially biased and where full homochirality arises with the origin of biopolymer catalysts (scenario 1(b) or 1(c) followed by 2(b)). For the numerical example, we will set $\varepsilon = 0.5$, and keep all other parameters as in the previous section. The phase diagram for this case is shown in Figure 5.4a, and Figures 5.4b shows the monomer concentrations as a function of *k* for a vertical section through the phase diagram. Regions I - V label parts of parameter space where different combinations of solutions are stable.

In this case, the dead state is 'prebiased', meaning that there is an enantiomeric excess of the monomer whose chemical synthesis rate is higher. A prebiased state would arise if for example, circularly polarized UV radiation biased one enantiomer over another, or if meteorites seeded the prebiotic Earth with a slight asymmetry of organic precursor molecules as discussed in the introduction. It can be shown from Equations 5.3-5.10 that if the catalytic terms kC_L and kC_D in the synthesis rates are negligible compared to s_0, then the enantiomeric excess of the monomers is equal to the excess in the synthesis rate, *i.e.* $(D-L)/(D+L) = \varepsilon$, and $D/L = (1+\varepsilon)/(1-\varepsilon)$. In this example with $\varepsilon = 0.5$, D/L is approximately 3 over the whole range for which the prebiased dead state is stable.

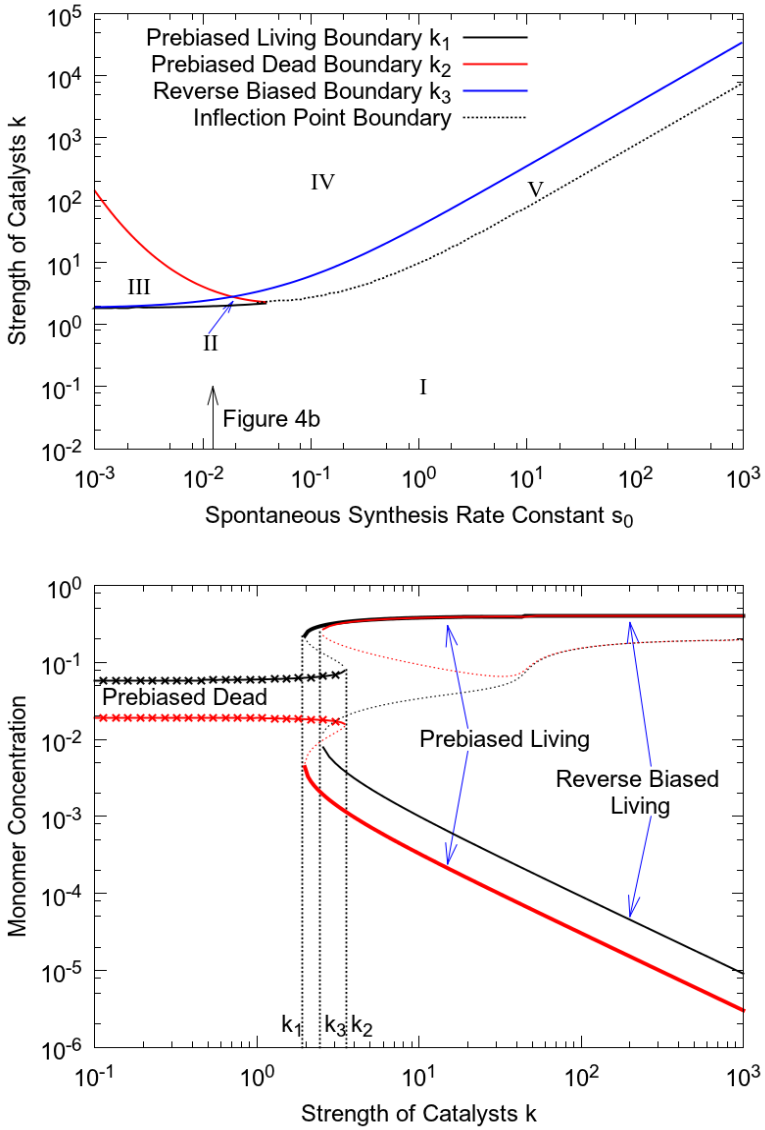

Figure 5.4: (a) Phase diagram for the case $\varepsilon = 0.5$, where monomer synthesis is partially biased for chemical or physical reasons prior to the origin of life. This corresponds to scenario 1(c)-2(b) in Figure 5.1.The stable states are as follows. Region I: Prebiased dead; Region II: Prebiased dead and Prebiased Living; Region III: Prebiased dead; Prebiased Living and Reverse-Biased Living; Region IV: Prebiased Living and Reverse-Biased Living; Region V: Prebiased Living. The other parameters are fixed as follows: $m = 5, r = 10, u = 1, F_0 = 10$.

(b) Monomer concentration as a function of k with s_0 fixed, moving along the vertical line indicated by the arrow in (a). Solid lines indicate stable states and dotted lines indicate unstable states. Red and black symbols label the prebiased dead state, in which one monomer (black) has a slightly higher concentration than the other (red). This state is stable up to k_2.For $k > k_1$,the prebiased living state is stable, in which the black monomer has a much higher concentration than the red. For $k > k_3$,the reverse-biased living state is stable, in which the red monomer has a much higher concentration than the black.

For $k > k_1$, a prebiased living state becomes stable. This is an autocatalytic state in which there is a high concentration of catalysts of the dominant monomer, and the dominant monomer is the same as that favoured by the chemical synthesis. The enantiomeric excess is close to 100% in this case ($D>>L$) because the dominant monomer is synthesized catalytically and the rare monomer is only synthesized at the spontaneous rate. For $k > k_3$ a reversed-biased living state becomes stable in which the dominant monomer is the one whose chemical synthesis rate is lower (L in this example). The synthesis rate of L is dominated by the catalytic term kC_L, which is much larger than the spontaneous rate of synthesis of D, even though bias in the spontaneous rates favours D. For $k > k_2$, the dead state becomes unstable. The example of $\varepsilon = 0.5$ shown here is quite a large bias. This was done in order to make the difference between the prebiased and reverse-biased states clear in the figures. If a smaller ε chosen, the difference in concentrations between the prebiased and reversed biased states is smaller.

5.8 Dynamical considerations and the effect of changing *m*

In the previous sections we have considered only the stability of the stationary solutions of the differential equations, and we have not considered the dynamics of how those solutions are reached. We have argued previously (Wu and Higgs, 2009) that the origin of life probably occurred in a region of parameter space where both living and dead states are stable. If the only solution were a dead state, we would not be here, and if the only solution were a living state, we

would have rapid spontaneous emergence of life all the time. In reality, the origin of life seems to be difficult but not impossible. We have argued that the origin of life requires a transition from a dead to a living state that occurs due to stochastic fluctuations of concentrations in a finite volume. We demonstrated that this can occur in stochastic dynamical simulations in a model with only one kind of monomer (Wu and Higgs, 2009), similar to the $\varepsilon = 1$ case in this chapter. An infinite deterministic system will remain stable in a dead state forever. In a finite volume, with finite numbers of molecules, concentration fluctuations become significant, and these can cause the system to jump from a dead to a living state.

In the stochastic case, it is necessary to consider the meaning of the catalysis rate k more carefully. If we suppose that all homochiral polymers of length at least m are catalysts, then C_D (or C_L) is the concentration of catalysts and k is the catalytic effect of each catalyst. If we are thinking of a chemical mechanism of catalysis that works with small molecules, then this seems reasonable. For example, if the mechanism is simple enough that dimers are catalysts ($m = 2$), then it seems reasonable to suppose that *all* dimers are catalysts. However, in our previous papers (Wu and Higgs, 2009; 2011) we were thinking of biological catalysts, *i.e.* the catalysts were ribozymes. In this case, m must be reasonably large, and only a small fraction of sequences of this length will function as ribozymes. If a fraction f of polymers are ribozymes, and the effect of each ribozyme is k_0 then the net effect of the catalysts is $k_0 f C_D$. For deterministic solutions of the differential equations, we can write $k = k_0 f$; hence, it makes no

difference whether we have a large fraction of weak catalysts or a tiny fraction of very effective catalysts. For the stochastic case, these situations are different, *i.e.* both f and k_0 are relevant separately. This has been investigated in our original model (Wu and Higgs, 2009). We have not yet studied the stochastic dynamics of the chiral model. However, it is already possible to draw several conclusions from the deterministic stationary solutions that we have given here.

In most cases, the value $k = k_1$ at which the living state becomes stable is much smaller than the value $k = k_2$ at which the dead state becomes unstable. This is particularly true if s_0 is small, as was probably the case for prebiotic synthesis. For example, in Figure 5.5, the two boundaries differ by several orders of magnitude when s_0 is small, and by a relatively small factor when s_0 is large. The gap between k_1 and k_2 is more pronounced when m is larger. Figure 5.5a shows the $\varepsilon = 0$ case with $m = 25$, which may be compared with the $\varepsilon = 0$, $m = 5$ case in Figure 5.3a. For the larger m, there is a wide separation of k_1 and k_2 across the full range of s_0. Thus, given that m may be quite long for functional ribozymes and f is likely to be very small, it would seem much more likely that a real-world situation would fall in the bistable region with k between k_1 and k_2 than in the living-only region with $k > k_2$. This means that a stochastic transition between dead and living states with parameter values in the bistable region is a probable scenario. In the case where $\varepsilon > 0$, a slight bias in the spontaneous synthesis is likely to be very relevant for the transition from the dead to the living state. In the dead state, when polymerization is random, the chance of forming homochiral polymers of the

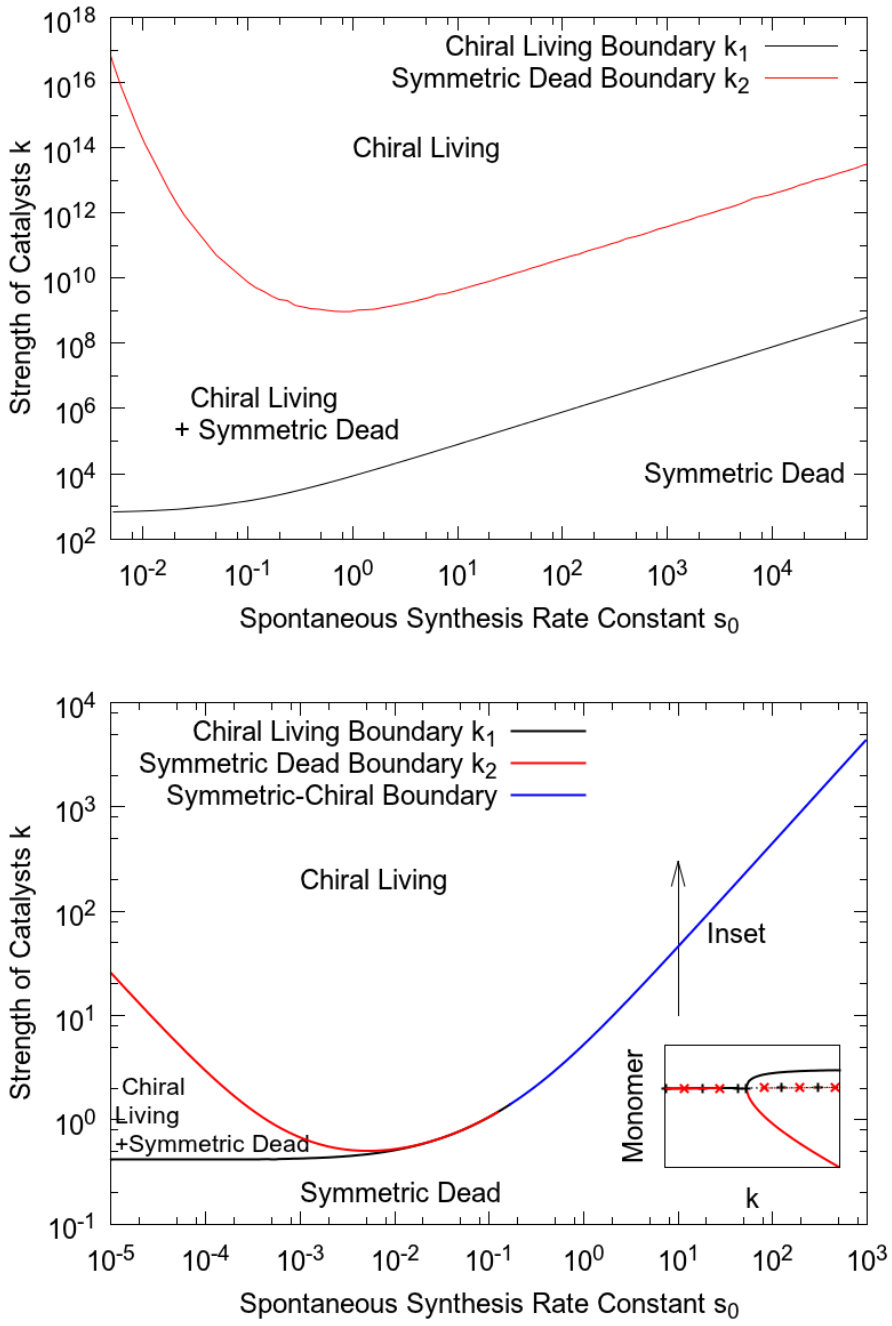

Figure 5.5: The effect of changing the minimum length m required for catalysis in the case where chemical synthesis is symmetric, $\varepsilon = 0$. (a) When $m = 25$, the gap between the two boundaries is much wider than for $m = 5$, which was shown in Figure 5.3(a). (b) When $m = 2$, there is a direct boundary between the symmetric dead state and the chiral living states (blue line). Moving across this boundary leads to a forward bifurcation in the monomer concentrations (see inset). The forward bifurcation only occurs when $m = 2$. For $m > 2$, the chiral living states originate via backward bifurcations, as shown in Figure 5.3(b) and 5.4(b).

dominant monomer may be much higher than for the rare monomer, even if the difference in the monomer concentrations is relatively small. The degree of chiral asymmetry of polymers will increase with increasing chain length (Bolli *et al.* 1997) due to differential rates of synthesis. It is much more likely that the system will jump to the prebiased living state the reverse biased state.

For completeness, and for comparison with previous models that deal with dimer catalysts, we will consider the case of $\varepsilon = 0$ and $m = 2$ in our model. The phase diagram is shown in Figure 5.5b. For small s_0 the boundaries k_1 and k_2 for the stability of the chiral living and symmetric dead states are separate, and there is an intermediate region where both types of solution are stable, as in the previous examples. However, for larger s_0 there is a single boundary between the symmetric and chiral states. The monomer concentrations as a function of k go through a forward bifurcation when this boundary is crossed, as shown in the inset to Figure 5.5b. Hence there is no region of bistability. This is qualitatively different from the case of $m = 5$ (Figure 5.3b), where a backward bifurcation occurs, and there is bistability for $k_1 < k < k_2$. As far as we are aware, this forward bifurcation occurs only when $m = 2$ in our model, and not for $m > 2$. As we are particularly interested in the origin of ribozymes, and as these are likely to have m considerably greater than 2, this case of $m = 2$ seems less relevant to scenarios for the origin of life.

The existence of a region of bistability of living and dead states is an important feature that emerges in all the variants of our model that we have

considered. The bistable region occurs in the models in our previous papers, which ignore chirality (Wu and Higgs, 2009; 2011), and in the fully homochiral case, $\varepsilon = 1$ (Figure 5.4), in which the origin of homochirality is a separate problem from the origin of life. The models for the prelife-life transition considered by Ohtsuki and Nowak (2009), also have this structure. In contrast, almost all previous models that consider the origin of homochirality have a simple forward bifurcation and no bistable region (Sandars, 2003; Brandenburg *et al.* 2005a; Ribo and Hochberg, 2008; Gleiser and Walker, 2008). The model of Saito and Hyuga (2005) is an exception in that it is a model of for homochirality that does show a bistable region for some parameter values. The origin of homochirality is a symmetry breaking transition, whereas the origin of life is a transition between dead and living states that differ in concentrations and reaction rates and it is not directly associated with symmetry breaking. In this chapter, we have considered the way these two transitions interact. When chirality is introduced into our origin of life models, the feature of bistability is retained from the non-chiral model and the instability in the chirality is induced by the transition from dead to living states. This leads to the novel feature of our models that the chiral states arise via a backward bifurcation rather than a forward bifurcation.

The idea of a stochastic transition between dead and living states occurs in the simple abstract model for the origin of life considered by Dyson (1999), and we expanded on this in the context of the RNA world in previous chapters. This picture has important consequences for the way that homochirality and life will

spread spatially across the surface of the Earth. Previous spatial treatments of chirality (Brandenburg and Multamaki, 2004; Gleiser and Walker, 2008; Gleiser *et al.* 2008) dealt with models that have a forward bifurcation. It was supposed that the system begins in a racemic state and that this becomes unstable if the parameters are suddenly quenched into a range where the chiral states are stable. This leads to simultaneous emergence of spatial domains of *L* and *D* with a length scale that grow slowly over time until one domain takes over the whole surface. According to the models in this chapter, however, the dynamics would be substantially different. If the system begins in a racemic dead state (with $\varepsilon = 0$) in a parameter range where the dead state is also stable, then the origin of life is initiated by a rare stochastic transition occurring in a localized region. Life would then spread rapidly and deterministically across the surface, because the living state synthesizes more catalysts that diffuse out into neighbouring regions and immediately trigger the transition to life in the neighbouring regions. The spread of life would take along whichever chirality happened to arise in the initial event. If there were a small pre-existing chemical bias ($\varepsilon > 0$), then the initial living state would be likely to follow the handedness of the pre-bias. However, as shown in chapter 4, when system size is so large that spreading time of homochiral state to the whole system is large compared with average transition time, there may be multiple transitions to different homochiral states if ε is small. Hence, there could be simultaneous competing forms of *L* and *D* life on the surface. The dynamics of

such competition may be different from previous models, hence it remains an interesting topic to be investigated.

5.9 Conclusions

The evidence from analysis of meteorite compositions now seems to indicate fairly conclusively that a modest enantiomeric excess of a few percent can arise in some kinds of organic molecules for non-biological reasons. Asymmetric photolysis seems to be the most plausible cause for this (as reviewed in the introduction of this chapter), although other mechanisms are also possible. Formation of biopolymer catalysts, such as RNAs, or some other nucleic acid analogue, is a key step in the origin of life, in our view. Life must have arisen in an environment in which the chemical synthesis of nucleotides was possible. If the chemical environment was chirally biased to some extent, then it is possible that prebiotic nucleotide synthesis was also chirally biased, *i.e.* there may have been a small but non-zero ε. However, the scarcity of examples of asymmetric autocatalytic systems based only on small molecules, suggests that it is unlikely that a fully homochiral system could have arisen by prebiotic chemistry at the monomer level. We argue that it is the biopolymers themselves that are the asymmetric autocatalysts. It is the origin of biopolymer catalysts that drives the transition to the living state. As these biopolymer catalysts are chiral, then the same transition drives the system to a homochiral state. If the chemical world were racemic ($\varepsilon = 0$), then the origin of life and the origin of homochirality would occur together. If there were a partial chiral bias before life ($\varepsilon > 0$), then the origin

of life would complete the transition to homochirality that was begun by chemical forces existing before life.

As discussed in the introduction, the possibility that homochirality emerges with or after the origin of life has largely been dismissed (Bonner1991, 1995), and a majority of research has focussed on abiotic theories where homochirality is required to emerge prior to the origin of life. Here we have shown that scenarios in which a homochirality emerged *with* life are serious possibilities. This has implications for astrobiological searches for life on other planets. If the abiotic hypothesis is correct, homochirality is not a valid biomarker, because non-living chemistries with a high chiral bias might exist that would be false positives for life. Alternatively, if homochirality arises only with life, homochirality may be one of the best biosignatures for detecting life on other planets, being both easily identifiable and characteristic only of living systems.

Chapter 6

Conclusion and Discussion

6.1 Importance of Stochasticity and Concentration Fluctuation for Origin of Life

I believe and have been trying to argue in this thesis that autocatalytic sets of biopolymers could exhibit life-like behaviour such as metabolism and reproduction. Hence the emergence of autocatalytic sets of biopolymers is the most important step from an organic molecular ensemble to primitive life. The activity level of autocatalysis of the reaction system is the criterion differentiating the living state with many catalytic polymers and high level of autocatalysis from the non-living state with very few catalytic polymers and low level of autocatalysis. The transition from non-living state to living state through concentration fluctuations is marked by the emergence of autocatalytic sets of biopolymers. No matter what effect the catalyst has, such as being a polymerase, a nucleotide synthase or even non-covalently linked polymer assemble catalyzing ligation, as long as it can shift equilibrium of the system to produce more of itself, it is possible that the system has a living and a dead state with different levels of autocatalysis.

It is known that magnitude of concentration fluctuations depends on the number of interacting molecules, which in turn depends on the size of the system. Due to the importance of concentration fluctuations, the effect of system size on average transition time from dead state to living state has been investigated in this thesis. It is shown that when the system size is too small to sustain any catalyst in the system, increasing the system size increases the chance to produce catalytic polymers, and therefore decreases the transition time. When the system size is smaller than the diffusion length but large enough to retain a stable concentration of catalytic polymers, the system is in the well mixed region in which increasing the system size reduces the concentration fluctuations and leads to a longer transition time. When the system size is larger than the diffusion length, the system behaves like many independent smaller regions with the size of the diffusion length. A transition could happen independently in any one region and spread out to neighbouring regions. The larger the system, the more such independent regions there will be, hence the shorter time it takes for the transition to happen in any one of them. When system size is small compared with spreading speed of the living state, the transition would only happen once. However, when the system is so large that the spreading time of the living state is longer than average transition time in a well mixed region, there could be multiple transitions in the whole system, which means that there would be multiple origins of life.

6.2 Metabolism and Replication

There is a long-standing debate in the origins of life field over whether metabolism preceded replication. The role of metabolism in the origin of life has been reviewed by Anet (2004). Several ideas for the energy source for metabolism have been proposed (Wächtershäuser, 1997; Russell and Hall, 1997; Morowitz *et al.* 2000; De Duve, 2003; Lindahl, 2004; Shapiro, 2006). Our model is related to that of Dyson (1999), who argues for metabolism first, however the aim of our model is to demonstrate how self-replicating biopolymers could have arisen, which is a key issue in replication-first theories. Therefore, to conclude this chapter, we wish to discuss where we stand on this issue.

Metabolism is typically defined as "the sum of the chemical reactions occurring in a cell, including the energy-releasing breakdown of molecules (catabolism) and the synthesis of new molecules (anabolism)". For discussion of the origin of life, we need something a little more precise. We will define metabolism as a chemical reaction system that has the following properties: (i) the system is driven by a free energy source, such as a supply of organic molecules, or an inorganic chemical system, or light; (ii) the free energy source is coupled to the synthesis of the component molecules of the system; (iii) the continued free energy input keeps the system in a non-equilibrium steady state rather than in thermodynamic equilibrium; (iv) the reaction system is autocatalytic, *i.e.* the component molecules catalyze synthesis of further component molecules. The first two properties capture the catabolism and anabolism aspects of the usual

definition. The third property follows from the first two, but it is worth emphasizing because large or complex component molecules may reach much higher concentrations than would occur if the system were in thermodynamic equilibrium, and the existence of large complex molecules is an important aspect of the chemistry of living systems. The fourth property, autocatalysis, is not mentioned in the standard definition of metabolism, but it seems crucial to us, so we will explicitly include it as part of our definition. Autocatalysis is always recognized as a requirement for life, but in discussions of metabolism, it is sometimes not clear whether autocatalysis is implied. This is part of the reason for the confusion over whether metabolism preceded replication.

Synthesis of nucleotides and RNA strands in the RNA world requires free energy input. These molecules would not exist in high concentration if they were allowed to come to thermodynamic equilibrium. The reaction system in chapter 2 is driven by input of F_1 and F_2. This captures the essential aspect, but in reality, there must have been many reaction steps involved in synthesis of nucleotides. Whatever these steps were, they needed to be in place before the RNA world could arise. It is clear that the first three properties preceded the RNA world; therefore if these three properties are sufficient as a definition of metabolism, we can say metabolism preceded the RNA world. However, above, we chose to incorporate autocatalysis into the definition of metabolism, and it is not immediately clear whether a fully autocatalytic metabolism preceded the RNA world. In our view, the question of whether metabolism preceded replication boils

down to the more precise question of whether autocatalysis preceded the origin of catalytic biopolymers.

Lindahl (2004) and Shapiro (2006) both very clearly state the view that autocatalytic cycles involving small molecules existed before RNA arose, *i.e.* they argue that all four properties of metabolism existed before RNA. Lindahl (2004) considered a reaction system with a quasi-stationary state, which would have properties (i)-(iii), but not (iv), and discussed how this could have been converted to a system with autocatalysis. In this picture, biopolymers arose only later. Shapiro (2006) pointed out all the difficulties associated with prebiotic RNA synthesis, and concluded that autocatalysis must have initially arisen with small molecules. However, he did not give a definite proposal of what the small molecule catalysts were or what were the reactions involved in the autocatalytic cycle. In contrast to this, currently known ribozymes are sufficient to give clear evidence that RNA sequences do catalyze polymerization and ligation reactions that would be necessary to form an autocatalytic cycle based on RNA. Thus, our model is based on the idea that it was the origin of the catalytic RNAs that closed the autocatalytic cycle. The dead state in our model is a non-equilibrium steady state with properties (i)-(iii) but no autocatalysis (because there are very few ribozymes in the dead state). However, in the living state, the RNA synthesis is principally catalyzed by the ribozymes, and the cycle is closed. In our model, autocatalysis and efficient biopolymer synthesis arise at the same time; hence if

autocatalysis is a requirement for metabolism, as in our definition, we may say that metabolism and replication arise at the same time.

For the mechanism discussed in this thesis to work, it is necessary for spontaneous nucleotide synthesis and polymerization to occur at some non-zero rate, but it is not necessary that these spontaneous reactions already be autocatalytic before the synthesis of ribozymes. To be fair, our model was not set up to look at the possibility of autocatalysis of small molecules, because nucleotide synthesis was simplified to a single reaction. It is possible that nucleotide synthesis occured as a product of another pre-existing autocatalytic cycle involving small molecules. In this case ribozymes could have introduced feedback into the system either by catalyzing the RNA polymerization, as in the model we considered, or by catalyzing any of the reactions in the small-molecule autocatalytic cycle. Something like this must eventually have occurred in the later stages of the RNA world, where we envisage RNA-based organisms with complex metabolisms involving many ribozyme-catalyzed reactions between small molecules.

In summary, we hope that our model bridges the gap between theories based on replication-first and metabolism-first ideas and helps to solve some of the problems in these two approaches. The extreme replication-first view is that life started with a single ribozyme acting as both catalyst and information carrier that was able to perfectly replicate its own sequence. However, the spontaneous appearance of such a perfect ribozyme may seem too miraculous to many. Our

model shows that the first ribozymes need not be perfect replicators. Any imperfect ribozyme that increases the polymerization rate to some extent will introduce feedback into the system and increase the rate at which further ribozymes are synthesized. The new ribozymes may include more efficient or more accurate ribozymes that will further increase the strength of the feedback, leading in a step-by-step manner to the origin of complex, highly efficient catalysts. On the other hand, a strict metabolism-first view would be that biopolymers such as RNA were not involved in the origin of life and that fully autocatalytic metabolic systems arose based on small molecules only. Such a metabolism would have had compositional information but no information stored in sequences. Although we agree that, in principle, a form of inheritance of compositional information is possible with small molecules only (see Wu and Higgs, 2008 and references therein), it is not clear how anything more than a minimal level of complexity could be achieved until biopolymer replication evolved. Furthermore, we have shown here that it is not necessary for an autocatalytic system based on small molecules to have existed before biopolymer catalysts arose. If RNA polymers can be synthesized at a small spontaneous rate, then small numbers of ribozyme catalysts will eventually arise. Small numbers are sufficient to have a large feedback effect in a finite volume and to cause the system to move to a state in which RNA synthesis is autocatalytic, *i.e.* the chance occurrence of a few spontaneously generated ribozymes may be sufficient to jump-start the RNA world.

6.3 Specificity and Generality of Catalysts

The polymerase ribozymes envisaged in this thesis are general, in the sense that they are assumed to increase the rate of polymerization irrespective of the sequence. The *Azoarcus* recombinase system considered in Chapter 3 and the ligase system of Lincoln and Joyce (2009) are specific, in the sense that they work with well defined building block strands. In one sense, specificity is good, because it insures the product of the reaction is the desired catalyst sequence. On the other hand, specificity is bad because it means that only a tiny fraction of strands in a mixture of random sequences can undergo the reaction. Neither the recombinase or the ligase in these two examples increase the rate of formation of the building blocks, and therefore they are limited by the supply of their building blocks. The general polymerase would not be limited in this way because it can act on any strand. The corresponding disadvantage is that a completely general polymerase still makes random sequences, and so only a tiny fraction of the product is useful. The model investigated here does not keep track of sequences or of the property that RNA polymerization is likely to be template-directed. In the protein world, RNA- and DNA polymerase enzymes are general, *i.e.* they can act on any sequence, but the sequence specificity arises because they are template directed and therefore they only act on the specific nucleotide sequences that are present. A template directed RNA-polymerase ribozyme in the RNA World could work in the same way if it could use any available strand as a template.

It is the generality of replication that allows evolution to occur. Once a mechanism has evolved that replicates any sequence, then the sequence can evolve without reinventing the replication mechanism. This is clearly what happened at some point in the history of life on Earth. On the other hand, specific ribozymes functioning with specific substrates might be simpler and more likely to arise initially, although they would be more constrained in terms of their structure and function and would probably be less likely to support evolution in the long term. Understanding the relationship between sequence specificity and generality in autocatalytic systems is an important unresolved issue that will be important for future experimental and theoretical work on ribozymes.

6.4 Intertwined Origin of Life and Homochirality

There are different scenarios in which homochirality could originate depending on chirality of prebiotically synthesized simple organic molecules and effect of autocatalysis on amplification of pre-existing bias or stochastic fluctuation as shown in Figure 5.1. The common focusing on simple organic molecules and long polymers makes origin of life could share the same stage as origin of homochirality. The importance of autocatalysis and stochastic fluctuations makes these two problems qualitatively similar to each other. Many different scenarios for origin of homochirality have been unified into a single framework as an extension of our basic polymerization model. In additional to previously hold views that origin of life is a different problem from origin of

homochirality, it is proposed in this thesis that origin of life may happen at the same time as origin of homochirality with emergence of autocatalytic sets of biopolymers.

6.5 Future Work

For the purpose of simplicity, sequence information has been discarded in all models of this thesis. Hence in all models with predefined type of catalytic ability, there are only two possible steady states: with many catalysts or with few catalysts. With sequence information, polymers with specific sequence, or even specific folded structure can have catalytic ability with different efficiency. Hence, there could be many different species of catalysts competing for resources. In this scenario, the system can have molecular level Darwinian evolution inventing catalysts with higher and higher efficiency.

Despite hugely different model details, it has been shown that the Two's Company model and the basic polymerization model behave very similarly to each other. I think the common features of these two models can also be found far outside the field origin of life. For example, the transition from dead to living state is similar to a nucleation processes, such as crystal nucleation or water droplet formation from vapour; spreading of the living state is similar to crystal growth process. When the system is small, the transition time is limited by the nucleation process, while when the system is large, the transition time would be

dominated by the growth process. Hence it may worth the effort to investigate an analytic explanation of such behaviour.

The error threshold problem has been mostly studied in models describing dynamics of a system after establishment of autocatalysis. A possibility for future work would be to incorporate the error threshold into the Two's company model to investigate its effect on origin of autocatalysis. In this way, parasites and competition between replicators can be investigated in such a simple system.

The origin of homochirality has been investigated in spatial models previously. However, in most previous models there is no region of parameter space where both racemic and homochiral steady states are stable. Thus, in simulations of the previous models, either the racemic state is stable forever, or homochiral patches of different handedness show up and disappear randomly across the whole system. Hence there is not a transition from a steady racemic to steady homochiral state. In our model, there is coexistence of racemic and homochiral states for the same set of parameters, and it is possible to show how a stable homochiral state could originate and spread out to replace the stable racemic state across the whole system.

6.6 Implication for Astrobiology

A major question for astrobiology is whether life in other planetary system is similar to that on earth. The wide availability of hydrogen, carbon, nitrogen, oxygen, phosphorus and sulfur in the universe implies that simple organic

molecules such as methane, formaldehyde, methanol, dimethyl ether, and hydrogen cyanide and amino acids, could form easily as discovered in meteorites and interstellar molecular clouds. There are already over 700 extrasolar planets discovered. Several of them have been found to reside in the habitable zone of their respective planetary systems, in which water remains in liquid state. On such extrasolar planets, biochemical reactions similar to those on earth could happen. Proteins and lipids are easy to form hence could be available on these extrasolar planets. However, due to difficulties to produce nucleotides prebiotically, different monomers could be used. Even if the same types of nucleotides are available, different linkages between monomers, such as 3'-5' or 2'-5' linkages could result in different types of polymers. Emergence of autocatalytic sets of biopolymers could still be the critical step to origin of life elsewhere, and we do not yet know whether similar polymers to those on Earth might be used by life elsewhere. However, the introduction of biopolymers opens up an almost infinitely large sequence space to explore, hence no reproducibility in the evolution process. To sum it up, on extrasolar planets in the habitable zone, if there is life, it should be carbon based, may have lipids and proteins, may use different polymer than RNA and DNA, and their evolutionary history could be totally different from that of life on earth. Hence to detect life on other planets, abundance of simple organic molecule such as amino acids may be a better biomarker than large biopolymers such as DNA, RNA.

It is known that the origin of life happened on Earth in the time interval between 4 billion years and 3.6 billion years ago. The Voyager 1 and 2 space probes have reached the edge of the Solar system now. Hence it has taken less than 4 billion years for development of a civilization with the capability to explore space. Even at the current speed of 20km/s of the Voyagers, it would take around 1 billion years for them to travel across the Milky Way. Hence with current technology, the transition time from non-life to space exploring civilization is of the same order of magnitude as the time required to explore the galaxy. It is conceivable that there would be another civilization in the Milky Way millions of years older than us, hence capable of travelling at much faster speed than us. Hence, it is possible that earth has been discovered long time ago or our human civilization is the lucky first space exploring civilization in the Milky Way.

The fact that terrestrial life is the only known form of life may make people feel lonely or lucky depending on one's perspective. However, the difficulties to explore other planets and reconstruct the exact scenario in which origin of life happened have forced scientists in the field of astrobiology to focus on theories and modelling. With few experimental facts to validate or invalidate all these theories and models, many hypotheses in astrobiology remain unproven. Hence what is the good of these models if there are so many unknown parameters that are difficult to verified experimentally? Is it better to design some novel experiments to discover concrete fact than to contemplate in one's armchair? I agree that experimental evidences are the most concrete advance of our

knowledge and they are the jury for the validity of theories and models. However, I believe that only through theories and models can people really put together all facts into a bigger picture to appreciate the natural laws governing all these facts. Biologists can tell us how organisms evolve from their ancestors, and genetic information of organisms can be obtained with molecular biology, while biochemistry techniques are available to investigate the interaction mechanisms of many organic molecules. However, even with all this information, it is difficult to define precisely what makes a living cell different from all its component molecules. The diversity of life forms on earth implies life should be a general dynamic behaviour not bound to specific set of molecules. I believe that through theories and models, it is possible to understand life as a special form of physical/chemical structure like a wave, which is not a special property of its medium, but a general dynamical structure of matter. And I believe that as a general dynamical structure, life could originate from different media in different environments. It is the Astrobiologist's role to understand instead of to describe what is life, and to determine the possible media and environments in which such a dynamic structure could occur.

BIBLIOGRAPHY

Abelson, P. H. (1966). Chemical events on the primitive Earth. *Proceedings of the National Academy of Sciences of the United States of America, 55*(6), 1365-1372.

Alfonsi A, Cances E, Turinici G, Ventura BD, Huisinga W (2005) Exact simulation of hybrid stochastic and deterministic models for biochemical systems. ESAIM Proceeding. 14: 1-13.

Anet FAL (2004) The place of metabolism in the origin of life. Curr. Opin. Chem. Biol. 8: 654-659.

Bader, G. and Deuflhard, P. (1983) A Semi-Implicit Mid-Point Rule for Stiff Systems of Ordinary Differential Equations. *Numer. Math.* 41, 373–398.

Balavoine, G., Moradpour, A., and Kagan, H. B.(1974) Preparation of chiral compounds of high optical purity by irradiation with circularly polarized light, a model reaction for the prebiotic generation of optical activity.*J. Am. Chem. Soc.* 96, 5152-5158.

Bagley, R. J., & Farmer, J. D. (1992, Feb). Spontaneous emergence of a metabolism. Paper presented at the 2nd Workshop on Artificial Life, Santa Fe, NM.

Bailey, J., Chrysostomou, A., Hough, J.H., Gledhill, T.M., McCall, A., Clark, S., Menard, F. and Tamura, M. (1998) Circular polarization in star-formation regions: implications for biomolecular homochirality. *Science* 281:672-674.

Bailey, J. (2001) Astronomical sources of circularly polarized light and the origin of homochirality. *Orig. Life Evol. Biosph.* 31:167-183.

Bartel, D. P., & Unrau, P. J. (1999). Constructing an RNA world (Reprinted from Trends in Biochemical Science, vol 12, Dec., 1999). *Trends in Cell Biology, 9*(12), M9-M13.

Bean HD, Anet FAL, Gould IR, Hud NV (2006) Glyoxylate as a backbone linkage for a prebiotic ancestor of RNA. Origins Life Evol. Biosph. 36: 39-63.

Benner, S.A., Carrigan, M.A., Ricardo, A. and Frye, F. (2006) Setting the stage: the history, chemistry, and geobiology behind RNA. In *The RNA World: Third Edition*, edited by R.F. Gesteland, T.R. Cech and J.F. Atkins, Cold Spring Harbor Laboratory Press, New York, pp 1-21.

Benner, S.A., Kim, H.J., Kim, M.J. and Ricardo, A. (2010) Planetary organic chemistry and the origins of biomolecules. *Cold Spring Harb. Perspect. Biol.* 2:a003467.

Briones C, Stich M, Manrubia SC (2009) The dawn of the RNA World: Toward functional complexity through ligation of random RNA oligomers. RNA 15: 743-749.

Bolli, M., Micura, R. and Eschenmoser, A. (1997) Pyranosyl RNA: chiroselective self-assembly of base sequences by ligative oligomerization of tetranucleotide-2',3' cyclophosphates (with a commentary concerning the origin of biomolecular homochirality). *Chemistry and Biology* 4:309-320.

Boerlijst, M. C., & Hogeweg, P. (1991). Spiral wave structure in pre-biotic evolution - Hypercycles stable against parasites. *Physica D, 48*(1), 17-28.

Boerlijst, M. C., & Hogeweg, P. (1995). Spatial gradients enhance persistence of hypercycles. *Physica D, 88*(1), 29-39.

Bonner, W.A. (1991) The origin and amplification of biomolecular chirality. *Orig. Life Evol. Biosph.* 21:59-111.

Bonner, W.A. (1995) Chirality and life. *Orig. Life Evol. Biosph.* 25:175-190.

Bonner, W.A. (2000) Parity violation and the evolution of biomolecular chirality. *Chirality* 12: 114-126.

Bonner, W.A. and Bean, B.D. (2000) Asymmetric photolysis with elliptically polarized light. *Orig. Life Evol. Biosph.* 30:513-517.

Bourbo, V., Matmor, M., Shtelman, E., Rubinov, B., Ashkenasy, N., & Ashkenasy, G. (2011). Self-assembly and Self-replication of Short Amphiphilic beta-sheet Peptides. *Origins of Life and Evolution of Biospheres, 41*(6), 563-567.

Blackmond, D. (2004) Asymmetric autocatalysis and its implications for the origin of homochirality *PNAS* 101:5732-5736

Brandenburg, A. amd Multamaki, T. (2004) How long can left and righ handed life forms coexist? *Int. J. Astrobiol.* 3:209-219.

Brandenburg, A., Andersen, A.C., Höfner, S. and Nilsson, M. (2005a) Homochiral growth through enantiomeric cross-inhibition. *Orig. Life Evol. Biosph.* 35: 225-241.

Brandenburg, A., Andersen, A.C. and Nilsson, M. (2005b) Dissociation in a polymerization model of homochirality. *Orig. Life Evol. Biosph.* 35: 507-521.

Cech, T. R., Zaug, A. J., & Grabowski, P. J. (1981). *In vitro* splicing of the ribosomal-RNA precursor of tetrahymena - involvement of a guanosine nucleotide in the excision of the intervening sequence. *Cell, 27*(3), 487-496.

Cech, T. R. (1986). A model for the rna-catalyzed replication of RNA. *Proceedings of the National Academy of Sciences of the United States of America, 83*(12), 4360-4363.

Cleaves, H. J., Chalmers, J. H., Lazcano, A., Miller, S. L., & Bada, J. L. (2008). A reassessment of prebiotic organic synthesis in neutral planetary atmospheres. *Origins of Life and Evolution of Biospheres, 38*(2), 105-115.

Costanzo, G., Pino, S., Ciciriello, F. and Di Mauro, E. (2009) Generation of long RNA chains in water. *J. Biol. Chem.* 284:33206-33216.

Crick, F. H. (1958). On protein synthesis. *Symposia of the Society for Experimental Biology, 12*, 138-163.

Cronin, J.R. and Pizzarello S (1997) Enantiomeric excesses in meteoritic amino acids. *Science* 275:951 – 955

De Duve C (2003) A research proposal on the origin of life. Orig. Life Evol. Biosph. 33: 559-574.

Derr, J., Manapat, M. L., Rajamani, S., Leu, K., Xulvi-Brunet, R., Joseph, I., et al. (2012). Prebiotically plausible mechanisms increase compositional diversity of nucleic acid sequences. *Nucleic Acids Research, 40*(10), 4711-4722.

Doudna, J. A., Couture, S., & Szostak, J. W. (1991). A multisubunit ribozyme that is a catalyst of and template for complementary strand RNA-synthesis. *Science, 251*(5001), 1605-1608.

Doudna, J. A., Usman, N., & Szostak, J. W. (1993). Ribozyme-catalyzed primer extension by trinucleotides - a model for the RNA-catalyzed replication of RNA. *Biochemistry, 32*(8), 2111-2115.

Doudna, J. A., & Cech, T. R. (2002). The chemical repertoire of natural ribozymes. *Nature, 418*(6894), 222-228.

Draper, W.E., Hayden, E.J. and Lehman, N. (2008) Mechanisms of covalent self-assembly of the *Azoarcus* ribozyme from four fragment oligonucleotides. *Nucleic Acids Res.* 36: 520-531.

Dyson, F. J. (1982). A model for the origin of life. *Journal of Molecular Evolution, 18*(5), 344-350.

Dyson, F.J. (1999) Origins of life.2nd ed. Cambridge University Press, New York.

Ehrenfreund, P., & Charnley, S. B. (2000). Organic molecules in the interstellar medium, comets, and meteorites: A voyage from dark clouds to the early earth. *Annual Review of Astronomy and Astrophysics, 38*, 427-+. Review database.

Eigen, M. (1971). Selforganization of matter and the evolution of biological macromolecules. *Naturwissenschaften, 58*(10), 465-523.

Eigen, M., & Schuster, P. (1977). Hypercycle - principle of natural self-

organization .a. emergence of hypercycle. *Naturwissenschaften, 64*(11), 541-565.

Eigen M, McCaskill J, Schuster P (1989) The molecular quasispecies. Adv. Chem. Phys. 79: 149-263.

Ekland, E. H., Szostak, J. W., & Bartel, D. P. (1995). Structurally complex and highly-active RNA ligases derived from random RNA sequences. *Science, 269*(5222), 364-370.

Ekland, E. H., & Bartel, D. P. (1996). RNA-catalysed RNA polymerization using nucleoside triphosphates. *Nature, 382*(6589), 373-376.

Ertem, G. (2004). Montmorillonite, oligonucleotides, RNA and origin of life. *Origins of Life and Evolution of the Biosphere, 34*(6), 549-570.

Farmer, J. D., Kauffman, S. A., & Packard, N. H. (1986). Autocatalytic replication of polymers. *Physica D, 22*(1-3), 50-67.

Ferris, J. P., Hill, A. R., Liu, R. H., & Orgel, L. E. (1996). Synthesis of long prebiotic oligomers on mineral surfaces. *Nature, 381*(6577), 59-61.

Ferris, J. P. (2002). Montmorillonite catalysis of 30-50 mer oligonucleotides: Laboratory demonstration of potential steps in the origin of the RNA world. *Origins of Life and Evolution of the Biosphere, 32*(4), 311-332.

Fox, S. W. (1980). Metabolic microspheres - origins and evolution. *Naturwissenschaften, 67*(8), 378-383.

Frank, F.C. (1953) On spontaneous asymmetric synthesis. *Biochim. Biophys. Acta* 11:459-463.

Fukue, T., Tamura, M., Kandori, Y., Kusakabe, N., Hough, J.H., Bailey, J., Whittet, D.C.B., Lucas, P.W., Nakajima, Y. and Hashimoto, J. (2009) Extended high circular polarization in the Orion massive star forming region: Implications for the origin of homochirality in the solar system. *Orig. Life. Evol. Biosph.* 40:335-346.

Ganti T (1979) A theory of biochemical supersystems and its application to problems of natural and artificial biogenesis. University Park Press, Baltimore, Maryland.

Gilbert, W. (1986). Origin of life - the RNA world. *Nature, 319*(6055), 618-618.

Giri, V., & Jain, S. (2012). The Origin of Large Molecules in Primordial Autocatalytic Reaction Networks. *Plos One, 7*(1), 18.

Gillespie DT (1976) A general method for numerically simulating the stochastic time evolution of coupled chemical reactions. J. Comput. Phys. 22: 403-434.

Glavin, D.P. and Dworkin, J.P. (2009) Enrichment of the amino acid l-isovaline by aqueous alteration on CI and CMmeteorite parent bodies. *Proc Natl Acad Sci USA* 106:5487 – 5492.

Gleiser, M. and Walker, S.I. (2008) An extended model for the evolution of prebiotic homochirality: a bottom-up approach to the origin of life. *Orig. Life Evol. Biosph.* 38:293-315.

Gleiser, M., Thorarinson, J. and Walker, S.I. (2008) Punctuated Chirality. *Orig. Life. Evol. Biosph.* 38:499-508.

Haldane, JBS(1929). The Origin of Life, *Rationalist Annual*, 148-69

Hanson, E. D. (1966). Evolution of the cell from primordial living systems. *The Quarterly review of biology, 41*(1), 1-12.

Hayakawa, T.; Fox, S. W. (1967). Copolymerization of the Leuchs anhydrides of the eighteen amino acids common to protein, *Arch. Biochem. Biophys.* 118: 441.

Hayden, E.J. and Lehman, N. (2006) Self-assembly of a Group I intron from inactive oligonucleotide fragments. *Chemistry and Biology* 13:909-918.

Hayden, E.J., von Kiedrowski, G. and Lehman, N. (2008) Systems chemsitry on ribozyme self-construction: Evidence for anabolic autocatalysis in a recombination network. *Angew. Chem. Int. Ed.* 47:8424-8428.

Hazen, R., Filley, G., and Goodfriend, G. (2001) Selective adsorption of L - and D -amino acids on calcite : Implications for biochemical homochirality. *PNAS* 98: 5487 – 5490.

Hein, J.E., Tse, E. and Blackmond, D. (2011) A route to enantiopure RNA precursors from nearly racemic starting materials. *Nature Chemistry* 3: 704 – 706.

Higgs, P.G. (2009) A Four-Column Theory for the Origin of the Genetic Code: Tracing the Evolutionary Pathways that Gave Rise to an Optimized Code. *Biology Direct* 4:16.

Higgs, P. G., & Pudritz, R. E. (2009). A Thermodynamic Basis for Prebiotic Amino Acid Synthesis and the Nature of the First Genetic Code. *Astrobiology, 9*(5), 483-490.

Hochberg, D. (2009) Mirror symmetry breaking and restoration: the role of noise and chiral bias. *Phys. Rev. Lett.* 102:248101

Hogeweg, P. (1994). Multilevel evolution - replicators and the evolution of diversity. *Physica D, 75*(1-3), 275-291.

Horowitz, N. H. (1945). On the Evolution of Biochemical Syntheses. *Proceedings of the National Academy of Sciences of the United States of America*. 31, 153-157

Inoue, T., Joyce, G. F., Grzeskowiak, K., Orgel, L. E., Brown, J. M., & Reese, C. B. (1984). Template-directed synthesis on the pentanucleotide CpCpGpCpC. *Journal of Molecular Biology, 178*(3), 669-676.

Islas, J.R., Lavabre, D., Grevy, J.M., Lamoneda, R.H., Cabrera, H.R., Micheau, J.C. and Buhse, T. (2005) Mirror symmetry breaking in the Soai reaction: a kinetic understanding. *PNAS* 102:13743-13748.

Jeffares, D. C., Poole, A. M., & Penny, D. (1998). Relics from the RNA world. *Journal of Molecular Evolution, 46*(1), 18-36.

Johnston, W.K., Unrau, P.J., Lawrence, M.S., Glasner, M.E. and Bartel DP (2001) RNA-catalyzed RNA polymerization: Accurate and general RNA-templated primer extension. *Science*. 292: 1319-1325.

Joshi, P.C., Aldersley, M.F. and Ferris, J.P. (2011) Homochiral selectivity in RNA synthesis: montmorillonite-catalyzed quaternary reactions of D, L-Purine with D, L- Pyrimidine nucleotides. *Orig. Life Evol.Biosph.*41: 213 – 236.

Joyce, G.F., Visser, G.M, van Boeckel, C.A.A., van Boom, J.H., Orgel, L.E. and van Westrenen, J. (1984) Chiral selection in poly(C)-directed synthesis of oligo(G). *Nature* 310: 602 –604.

Joyce, G.F. (1994) Forward in Book: *Origins of Life: The Central Concepts*, edited by Deamer, D. W. and Fleischaker, G. R.. Jones and Bartlett Publishers, Boston

Joyce, G. F. (2002). The antiquity of RNA-based evolution. *Nature, 418*(6894), 214-221.

Joyce, G.F. and Orgel, L.E. (2006) Progress towards understanding the origin of the RNA World. In *The RNA World: Third Edition*, edited by R.F. Gesteland, T.R. Cech and J.F. Atkins, Cold Spring Harbor Laboratory Press, New York, pp 23-56.

Kanavarioti, A., Bernasconi, C. F., & Baird, E. E. (1998). Effects of monomer and template concentration on the kinetics of nonenzymatic template-directed oligoguanylate synthesis. *Journal of the American Chemical Society, 120*(34), 8575-8581.

Kang TJ, Suga H (2007) In vitro selection of a 5'-purine ribonucleotide transferase ribozyme. Nucleic Acids Res. 35:4186-4194.

Kasting, J. F., & Catling, D. (2003). Evolution of a habitable planet. *Annual Review of Astronomy and Astrophysics, 41*, 429-463.

Kauffman, S. A. (1986). Autocatalytic sets of proteins. *Journal of Theoretical Biology, 119*(1), 1-24.

Kauffman SA (1993) The origins of order: Self organization and selection in evolution. Oxford University Press, Oxford.

Kawamura, K., & Ferris, J. P. (1999). Clay catalysis of oligonucleotide formation: Kinetics of the reaction of the 5 '-phosphorimidazolides of nucleotides with the non-basic heterocycles uracil and hypoxanthine. *Origins of Life and Evolution of the Biosphere, 29*(6), 563-591

Kawasaki, T., Sato, M., Ishiguro, S., Saito, T., Morishita, Y., Sato, I., Nishino, H., Inoue, Y. and Soai, K. (2004) Enantioselective synthesis of near enantiopure compound by asymmetric autocatalysis triggered by asymmetric photolysis with circularly polarized light. *J. Am. Chem. Soc.* 127:3274-3275.

Klabunovskii, E.I. (2001) Can enantiomorphic crystals like quartz play a role in the origin of homochirality on Earth? *Astrobiology* 1:127-131.

Klussmann, M., Iwamura, H., Mathew, S.P., Wells, D.H., Pandaya, U., Armstrong, A. and Blackmond, D.G. (2006) Thermodynamic control of asymmetric amplification in amino acid catalysis. *Nature* 441: 621-623.

Kuo, L.Y., Davidson, L.A. and Pico S. (1999) Characterization of the *Azoarcus* ribozyme: Tight binding to guanosine and gubstrate by an unusually small Group I intron. *Biochim. Biophys. Acta* 1489:281-292.

Kvenvolden, K., Lawless, J., Pering, K., Peterson, E., Flores, J., Ponnamperuma, C., et al. (1970). Evidence for extraterrestrial amino-acids and hydrocarbons in the Murchison meteorite. *Nature, 228*(5275), 923-926.

Lawrence, M.S. and Bartel, D.P. (2005) New ligase-derived RNA polymerases. *RNA* 11:1173-1180.

Lee, D. H., Granja, J. R., Martinez, J. A., Severin, K., & Ghadiri, M. R. (1996). A self-replicating peptide. *Nature, 382*(6591), 525-528.

Lehman, N. (2008) A recombination-based model for the origin and early evolution of genetic information. *Chemistry & Biodiversity* 5:1707-1717.

Lichtblau, D. (2000) Solving finite algebraic systems using numeric Gröbner bases and eigenvalues. Proceedings of the World Conference on Systemics, Cybernetics, and Informatics. 10: 555-560

Lifson, S. (1997). On the crucial stages in the origin of animate matter. *Journal of Molecular Evolution, 44*(1), 1-8.

Lincoln TA and Joyce GF (2009) Self-sustained replication of an RNA enzyme. *Science* 323:1229-1232.

Lindahl PA (2004) Stepwise evolution of nonliving to living chemical system. Orig. Life Evol. Biosph. 34: 371-389.

Lutay, A.V., Zenkova, M.A. and Vlassov, V.V. (2007) Nonenzymatic recombination of RNA: Possible mechanism for the formation of novel sequences. *Chemistry & Biodiversity* 4:762-767.

Ma, W. T., & Yu, C. W. (2006). Intramolecular RNA replicase: Possibly the first self-replicating molecule in the RNA world. *Origins of Life and Evolution of the Biosphere, 36*(4), 413-420.

Ma, W. T., Yu, C. W., & Zhang, W. T. (2007). Monte Carlo simulation of early molecular evolution in the RNA World. *Biosystems, 90*(1), 28-39.

Ma, W. T., Yu, C. W., Zhang, W. T., & Hu, J. M. (2010). A Simple Template-Dependent Ligase Ribozyme as the RNA Replicase Emerging First in the RNA World. *Astrobiology, 10*(4), 437-447.

Madison, K. M. (1953). The organism and its origin. *Evolution*, 7: 211-227.

Manapat, M.L., Chen, I.A. and Nowak, M.A. (2010) The basic reproductive ratio of life. *J. Theor. Biol.* 263:317-327.

Martins, Z., Botta, O., Fogel, M. L., Sephton, M. A., Glavin, D. P., Watson, J. S., et al. (2008). Extraterrestrial nucleobases in the Murchison meteorite. *Earth and Planetary Science Letters, 270*(1-2), 130-136.

McGinness, K. E., Wright, M. C., & Joyce, G. F. (2002). Continuous in vitro evolution of a ribozyme that catalyzes three successive nucleotidyl addition reactions. *Chemistry & Biology, 9*(5), 585-596.

Miller, S. L. (1953). A production of amino acids under possible primitive earth conditions. *Science (New York, N.Y.), 117*(3046), 528-529.

Monteiro, L. H. A., & Piqueira, J. R. C. (1998). A model for the early evolution of self-replicating polymers. *Journal of Theoretical Biology, 191*(3), 237-248.

Monteiro, L. H. A., & Piqueira, J. R. C. (1999). Modeling homopolymer self-replication: Implications for early competition. *Journal of Theoretical Biology, 196*(1), 51-60.

Morowitz, H. J., Kostelnik, J. D., Yang, J., & Cody, G. D. (2000). The origin of intermediary metabolism. *Proceedings of the National Academy of Sciences of the United States of America, 97*(14), 7704-7708.

Muller, H. J. (1929). The gene as the basis of life. *Proc. Int. Congr. Plant Sci*., 1: 897-921.

Nelson, K. E., Levy, M., & Miller, S. L. (2000). Peptide nucleic acids rather than RNA may have been the first genetic molecule. *Proceedings of the National Academy of Sciences of the United States of America, 97*(8), 3868-3871.

Nowak, M. A., & Ohtsuki, H. (2008). Prevolutionary dynamics and the origin of evolution. *Proceedings of the National Academy of Sciences of the United States of America, 105*(39), 14924-14927.

Ohtsuki, H. and Nowak, M.A. (2009) Prelife catalysts and replicators. *Proc. R. Soc. B* 276: 3783-3790.

Olasagasti, F., Kim, H.J., Pourmand, N., and Deamer, D.W. (2011) Non-enzymatic transfer of sequence information under plausible prebiotic conditions. *Biochimie* 93:556-561.

Oparin, A. I. (1924). Origin of Life, Moskovskiy Rabochiy, Moscow

Orgel, L. E. (1968). Evolution of the genetic apparatus. *Journal of molecular biology, 38*(3), 381-393.

Orgel, L. E. (1992). Molecular replication. *Nature, 358*(6383), 203-209.

Orgel, L. E. (2000). Self-organizing biochemical cycles. *Proceedings of the National Academy of Sciences of the United States of America, 97*(23),

12503-12507.

Orgel, L. E. (2004). Prebiotic chemistry and the origin of the RNA world. *Critical Reviews in Biochemistry and Molecular Biology, 39*(2), 99-123

Oro, J. (1961). Mechanism of synthesis of adenine from hydrogen cyanide under possible primitive earth conditions. *Nature, 191*, 1193-1194.

Paecht-Horowitz, M., Berger, J., & Katchalsky, A. (1970). Prebiotic synthesis of polypeptides by heterogeneous polycondensation of amino-acid adenylates. *Nature, 228*(5272), 636-639.

Pahle J (2009) Biochemical simulations: stochastic, approximate stochastic and hybrid approaches. Brief. Bioinform. 10: 53-64.

Pasek, M. and Lauretta, D. (2008) Extraterrestrial flux of potentially prebiotic C, N and P to the early Earth. *Orig. Life Evol. Biosph.* 38:5-21.

Pinheiro, V. B., Taylor, A. I., Cozens, C., Abramov, M., Renders, M., Zhang, S., et al. (2012). Synthetic Genetic Polymers Capable of Heredity and Evolution. *Science, 336*(6079), 341-344.

Pizzarello, S., Zolensky, M. and Turk, K.A. (2003) Nonracemic isovaline in the Murchison meteorite: chiraldistribution and mineral association. *Geochim Cosmochim Acta* 67:1589 – 1595

Pizzarello, S. and Weber, A.L. (2004) Prebiotic amino acids as asymmetric catalysts. *Science* 303:1151

Pizzarello, S., Huang, Y. and Alexandre, M.R. (2008) Molecular asymmetry in extraterrestrial chemistry: insightsfrom a pristine meteorite. *PNAS* 105:3700 – 3704.

Pizzarello, S. and Weber, A.L. (2010) Stereoselective syntheses of pentose sugars under realistic prebiotic conditions. *Orig. Life Evol. Biosph.* 40:3-10.

Plasson, R., Bersini, H. and Commeyras, A.(2007) Recycling Frank: spontaneous emergence of homochirality in noncatalytic systems. *PNAS* 101:16733-16738.

Plasson, R., Kondepudi, D.K., Bersini, H., Commeyras, A. and Asakura, K. (2007) Emergence of homochirality in far-from-equilibrium systems: Mechanisms and roles in prebiotic chemistry. *Chirality* 19:589-600.

Popa, R., Cimpoiasu, V.M. and Scorei, R.I. (2009) Rooting prebiotic chirality is spinomeric chemistry? *Astrobiology* 9:697-701.

Powner, M. W., & Sutherland, J. D. (2008). Potentially Prebiotic Synthesis of Pyrimidine beta-D-Ribonucleotides by Photoanomerization/Hydrolysis of alpha-D-Cytidine-2 '-Phosphate. *Chembiochem, 9*(15), 2386-2387.

Powner MW, Gerland B and Sutherland JD (2009). Synthesis of activated pyrimidine ribonucleotides in prebioticaly plausible conditions. Nature. 459:239-242.

Rajamani, S., Ichida, J. K., Antal, T., Treco, D. A., Leu, K., Nowak, M. A., et al. (2010). Effect of Stalling after Mismatches on the Error Catastrophe in Nonenzymatic Nucleic Acid Replication. *Journal of the American Chemical Society, 132*(16), 5880-5885.

Rajamani, S., Vlassov, A., Benner, S., Coombs, A., Olasagasti, F., & Deamer, D. (2008). Lipid-assisted synthesis of RNA-like polymers from mononucleotides. *Origins of Life and Evolution of Biospheres, 38*(1), 57-74.

Ribo, J.M. and Hochberg, D. (2008) Stability of racemic and chiral steady states in open and closed chemical systems. *Phys. Lett. A* 373:111-122.

Romero-Lopez, C., Diaz-Gonzalez, R., & Berzal-Herranz, A. (2007). RNA selection and evolution in vitro: Powerful techniques for the analysis and identification of new molecular tools. *Biotechnology & Biotechnological Equipment, 21*(3), 272-282.

Ruediger S, Shuai JW, Huisinga W, Nagaiah C, Warnecke G, Parker I, Falckey M (2007) Hybrid Stochastic and deterministic simulations of calcium blips. Biophys. J. 93: 1847-1857.

Ruiz-Mirazo, K., Pereto, J., & Moreno, A. (2004). A universal definition of life: Autonomy and open-ended evolution. *Origins of Life and Evolution of Biospheres, 34*(3), 323-346

Russell, M. J., & Hall, A. J. (1997). The emergence of life from iron monosulphide bubbles at a submarine hydrothermal redox and pH front. *Journal of the Geological Society, 154*, 377-402.

Russell, M. J. (2010). The Hazy Details of Early Earth's Atmosphere. *Science, 330*(6005), 754-754..

Saghatelian, A., Yokobayashi, Y., Soltani, K. and Ghadiri, M.R. (2001) A chiroselective peptide replicator. *Nature* 409: 797 - 801.

Saito, Y. and Hyuga, H. (2005) Chirality selection in open flow systems and in polymerization. *J. Phys. Soc. Japan* 74:1629-1635.

Sandars, P.G.H. (2003) A toy model for the generation of homochirality during polymerization. *Orig. Life Evol. Biosph.* 33:575-587.

Sato, I., Kadowaki, K., Ohgo, Y. and Soai, K. (2004) Highly enantioselective asymmetric autocatalysis induced by chiral ionic crystals of sodium chlorate and sodium bromate. *J. Molecular Catalysis A: Chemical* 216: 209-214.

Scott, W.G., Finch, J.T. and Klug, A. (1995) The crystal structure of an all-RNA hammerhead ribozyme: a proposed mechanism for RNA catalytic cleavage. *Cell* 81:991-1002.

Segre, D., Ben-Eli, D. and Lancet, D. (2000) Compositional genomes: Prebiotic information transfer in mutually catalytic noncovalent assemblies. *Proc. Nat. Acad. Sci. USA* 97: 4112-4117.

Segre, D., Ben-Eli, D., Deamer, D. W., & Lancet, D. (2001). The lipid world. *Origins of Life and Evolution of the Biosphere, 31*(1-2), 119-145.

Shapiro, R. (2006) Small molecule interactions were central to the origin of life. *Quarterly Rev. Biol.* 81: 105-125.

Soai, K., Shibata, T., Morioka, H. and Choji, K. (1995) Asymmetric autocatalysis and amplification of enantiomeric excess of a chiral molecule. *Nature* 378:767-768.

Soai, K., Sato, I. and Shibata, T. (2001) Asymmetric autocatalysis and the origin of chiral homogeneity in organic compounds. *The Chemical Record* 1:321-332.

Sulston, J., Lohrmann, R., Orgel, L. E., & Miles, H. T. (1968). Nonenzymatic synthesis of oligoadenylates on a polyuridylic acid template. *Proceedings of the National Academy of Sciences of the United States of America, 59*(3), 726-733.

Szabo, P., Scheuring, I., Czaran, T., & Szathmary, E. (2002). In silico simulations reveal that replicators with limited dispersal evolve towards higher efficiency and fidelity. *Nature, 420*(6913), 340-343.

Szathmary, E., & Demeter, L. (1987). Group selection of early replicators and the origin of life. *Journal of Theoretical Biology, 128*(4), 463-486.

Szathmary E (2000) The evolution of replicators. Philos. Trans. R. Soc. Lond. B. Biol. Sci. 355: 1669-1676.

Szostak J. W., Bartel D. P. and Luisi P. L. (2001) Synthesizing Life. Nature 409: 387-390.

Takeuchi, N., & Hogeweg, P. (2009). Multilevel Selection in Models of Prebiotic Evolution II: A Direct Comparison of Compartmentalization and Spatial Self-Organization. *Plos Computational Biology, 5*(10), 17.

Tian, F., Toon, O. B., Pavlov, A. A., & De Sterck, H. (2005). A hydrogen-rich early Earth atmosphere. *Science, 308*(5724), 1014-1017.

Unrau, P. J., & Bartel, D. P. (1998). RNA-catalysed nucleotide synthesis. *Nature, 395*(6699), 260-263.

Varela, F. G., Maturana, H. R., & Uribe, R. (1974). Autopoiesis: the organization of living systems, its characterization and a model. *Currents in modern biology, 5*(4), 187-196.

Vicens, Q., & Cech, T. R. (2009). A natural ribozyme with 3 ',5 ' RNA ligase activity. *Nature Chemical Biology, 5*(2), 97-99.

Visscher, J., Bakker, C. G., Vanderwoerd, R., & Schwartz, A. W. (1989). Template-directed oligomerization catalyzed by a polynucleotide analog. *Science, 244*(4902), 329-331.

Viedma, C. (2007) Chiral symmetry breaking and complete chiral purity by thermodynamic-kinetic feedback near equilibrium: Implications for the origin of biochirality. *Astrobiology* 7:312-319.

Wachtershauser, G. (1988). Before enzymes and templates - theory of surface metabolism. *Microbiological Reviews, 52*(4), 452-484.

Wachtershauser, G. (1997). The origin of life and its methodological challenge. *Journal of Theoretical Biology, 187*(4), 483-494.

Wattis, J. A. D., & Coveney, P. V. (1999). The origin of the RNA world: A kinetic model. *Journal of Physical Chemistry B, 103*(21), 4231-4250.

Weber, A.L. and Pizzarello, S. (2006) The peptide-catalyzed stereospecific synthesis of tetroses: a possible model for prebiotic molecular evolution. *Proc. Nat. Acad. Sci. USA*, 103:12713-12717.

Whittet, D.C.B. (1997) Is extraterrestrial organic matter relevant to the origin of life on Earth? *Orig. Life Evol. Biosph.* 27:249-262.

Wilson, D. S., & Szostak, J. W. (1999). In vitro selection of functional nucleic acids. *Annual Review of Biochemistry, 68*, 611-647.

Wochner, A., Attwater, J., Coulson, A., & Holliger, P. (2011). Ribozyme-Catalyzed Transcription of an Active Ribozyme. *Science, 332*(6026), 209-212.

Wu, M. and Higgs, P.G. (2008) Compositional Inheritance: Comparison of self-assembly and catalysis. *Orig. Life Evol. Biosph.* 38:399-418.

Wu, M. and Higgs, P.G. (2009) Origin of Self-replicating Biopolymers: Autocatalytic Feedback can Jump-start the RNA World. *J. Mol. Evol.* 69: 541-554.

Wu, M. and Higgs, P.G. (2011) Comparison of the roles of nucleotide synthesis, polymerization and recombination in the origin on autocatalytic sets of RNAs. *Astrobiology* 11: 895-906.

Zaher, H. S., & Unrau, P. J. (2007). Selection of an improved RNA polymerase ribozyme with superior extension and fidelity. *Rna-a Publication of the Rna Society, 13*(7), 1017-1026.